UNIVERSITY OF SOUTHAMPTON

School of Electronics and Computer Science

Human Mobility Models and Routing Protocols for Mobile Social Networks

by

Pitiphol Pholpabu

BEng, MSc

A doctoral thesis submitted in partial fulfilment of the requirements for the award of Doctor Philosophy at the University of Southampton

October 2016

SUPERVISOR: Professor Lie-Liang Yang

BEng, MEng, PhD, Fellow IEEE, Fellow IET

Professor of Communications, Southampton Wireless Group

School of Electronics and Computer Science University of Southampton

Southampton SO17 1BJ

United Kingdom

Dedicated to my family

UNIVERSITY OF SOUTHAMPTON

ABSTRACT

School of Electronics and Computer Science
Faculty of Physical Science and Engineering

Doctor of Philosophy

Human Mobility Models and Routing Protocols for Mobile Social Networks

by Pitiphol Pholpabu

In mobile social networks (MSNs), there are a number of challenges to face, which include the design of well-performed routing protocols. Since performance evaluation of a routing protocol in real world is costly and time consuming, it is usually more practical to evaluate the performance relying on the syn-thetic data generated by simulations. Accordingly, a number of mobility models have been proposed to provide the real-trace-like scenarios that can be used in development and performance evaluation of routing protocols. In this thesis, we concern the problem of dynamic routing in MSNs. First, two mobility models are proposed, which are the Preferred-Community-Aware Mobility (PCAM) and Role Playing Mobility (RPM) models. While designed based on the simplicity and randomness of the Random WayPoint (RWP) mobility model, the PCAM model enhances it by exploiting the fact that people often have their favorite places to visit, resulting in the so-called human social behavior of mutual preferred communities. On the other hand, the RPM model further improves the PCAM model by jointly considering people's behaviour of mutual-preferred-communities and their daily schedules. Then, based on the mobility models proposed, we design some routing protocols and investigate the effect of human social behavior on the routing performance in MSNs. Firstly, a Social Contact Probability assisted Routing (SCPR) protocol is proposed, which is capable of exploiting the properties of encounters between mobile nodes (MNs) and the relationship strength between MNs and communities. Secondly, considering that the energy-efficiency issues have not been addressed in the existing routing protocols for MSNs, we propose two types of energy-concerned routing protocols, which are the Energy-Concerned Routing (EnCoR) and Energy-efficient Social Distance Routing (ESDR) protocols. It can be shown that these two types of routing protocols are capable of achieving the trade-off among Energy Consumption (EC), Delivery Ratio (DR), and Delay (D), shortened as the EC/DR/D trade-off. Specifically, the EnCoR protocol controls the EC/DR/D trade-off by a threshold introduced to the route selection process, while the ESDR protocol achieves the EC/DR/D trade-off by taking into account of the length of messages and the estimation of the number of hops. Furthermore, we show that, by invoking our EnCoR or ESDR scheme, most existing routing protocols can be readily extended to their corresponding versions that are flexible to achieve the EC/DR/D trade-off. In this thesis, the

performance of the proposed routing protocols are investigated with the aid of simulations, which are compared with a range of existing routing protocols for MSNs. Our studies and performance results show that the proposed protocols are capable of efficiently integrating the merits of high delivery ratio, low delivery latency and low resource consumption of the existing protocols, while simultaneously circumventing their respective shortcomings. Our proposed protocols are capable of attaining a good trade-off among the delivery ratio, average delivery delay, and the cost of resources (including energy) for operation of the protocols.

Declaration of Authorship

I, **Pitiphol Pholpabu**, declare that the thesis entitled **Human Mobility Models and Routing Protocols for Mobile Social Networks** and the work presented in it are my own and has been generated by me as the result of my own original research. I confirm that:

- This work was done wholly or mainly while in candidature for a research degree at this University;
- Where any part of this thesis has previously been submitted for a degree or any other qualification at this University or any other institution, this has been clearly stated;
- Where I have consulted the published work of others, this is always clearly attributed;
- Where I have quoted from the work of others, the source is always given. With the exception of such quotations, this thesis is entirely my own work;
- I have acknowledged all main sources of help;
- Where the thesis is based on work done by myself jointly with others, I have made clear exactly what was done by others and what I have contributed myself;
- Parts of this work have been published.

Signed: ..... Date: .....

Acknowledgements

First of all, I would like to give my sincere gratitude to my supervisor Prof. Lie-Liang Yang for his excellent and careful supervision and support. His guidance and inspiration have greatly benefited me in the past four years of my PhD study.

Secondly, I wish to express my appreciation to Prof. Sheng Chen for his encouragement and engagement for my research. Furthermore, it is really my pleasure to work with everyone in our warming and generous Southampton Wireless group.

Last but not the least, I would like to express my heartfelt appreciation to my parents for their endless love and support.

List of Publications

[1] **P. Pholpabu** and L. Yang, "Social Contact Probability Assisted Routing Protocol for Mobile Social Networks," *IEEE 79th Vehicular Technology Conference (VTC Spring) 2014*, pp.1-5, 18-21 May 2014, published.

[2] **P. Pholpabu** and L. Yang, "A Mutual-Community-Aware Routing Protocol for Mobile Social Networks," *IEEE Global Communications Conference (GLOBECOM) 2014*, pp.2917-2922, 8-12 December 2014, published.

[3] **P. Pholpabu** and L. Yang, "Role Playing Mobility Model for Mobile Social Networks," *IEEE/ICC International Conference on Communications in China (ICCC) 2015*, pp.1-6, 2-4 November 2015, published.

[4] **P. Pholpabu** and L. Yang, "Routing Protocols for Mobile Social Networks Achieving Trade-off Among Energy Consumption, Delivery Ratio and Delay," *IEEE/ICC International Conference on Communications in China (ICCC) 2015*, pp.2917-2922, 2-4 November 2015, published.

[5] **P. Pholpabu** and L. Yang, "Social Contact Probability Assisted Routing Protocol for Mobile Social Networks," *IEEE Access*, submitted.

[6] **P. Pholpabu** and L. Yang, "Energy-Concerned Routing Protocols for Mobile Social Networks," *IEEE Transactions on Vehicular Technology*, submitted.

Contents

Summary of Acronyms and Abbreviations

AODV:	Ad-hoc On-demand Distance Vector.
BS:	Base Station.
C-SCP:	Community-linked Social Contact Probability.
CAOR:	Community-Aware Opportunistic Routing.
CCDF:	Complementary Cumulative Distribution Function.
CL:	Community-Linked.
DN:	Destination Node.
DSDV:	Destination-Sequenced Distance-Vector.
DSR:	Dynamic Source Routing.
DTN:	Delay Tolerant Network.
EC/DR/D:	Energy Consumption/Delivery Ratio/Delay.
ECF:	Energy Cost Factor.
ECSNR:	Ego-Centric Social Network Routing.
EnCoR:	Energy-Concerned Routing.
ESDR:	Energy-efficient Social Distance Routing.
FN:	Forwarding Node.

HiBOp: History-based Routing Protocol for Opportunistic Networks.

LATP: Least Action Trip Planing.

MANET: Mobile Ad-hoc Network.

MN: Mobile Node.

MPR: Multiple Relay.

MSN: Mobile Social Network.

N-SCP: Node-linked Social Contact Probability.

NL: Node-Linked.

OLSR: Optimized Link State Routing.

OPNET: Opportunistic Network.

PRoPHET: Probability Routing Protocol using History of Encounters and Transitivity.

PC: Preferred Community.

PCAM: Preferred-Community-Aware Mobility.

RPG: Reference Point Group.

RPM: Role Playing Mobility.

RWP: Random WayPoint.

SCP: Social Contact Probability.

SCPR: Social Contact Probability assisted Routing.

SLAW: Self-Similar Least-Action Walk.

SN: Source Node.

SOSIM: Social-Similarity-based.

SREP: Social Relationship Enhanced Predicable.

SWIM: Small World in Motion.

TC: Topology Control.

Chapter 1

Introduction

This chapter discusses motivation of the research, challenges of the existing technology, and contributions given by this research. The thesis overview is also given at the end of this chapter.

1.1 Motivation

In recent years, mobile devices that have short-range radio functionality, such as smart phones and tablets, are increasingly popular. With these mobile devices, a type of networks that do not rely on a mobile network infrastructure, referred to as mobile ad-hoc network (MANET), has been proposed. In the conventional fixed infrastructure networks, an end-to-end connection is composed of a connection from a source node (SN) to a base station (BS), a number of connections between BSs, and a connection from the last BS nearby a destination node (DN) to the DN. Since it is a centralized approach, the system collapses when a problem is occurred on those core devices or when there are some disconnections between BSs. In addition, the communication may be interrupted, when a MN moves from a BS coverage area to another. Instead, MANET is an infrastructureless network which requires no fixed BSs, such as access points. In MANET, an end-to-end connection is created from a number of connections between mobile nodes (MNs). MNs play both roles of a client, such as SNs and DNs, and a message forwarder, which is sometimes referred to as forwarding nodes (FNs). Data transfer in MANETs consisting of moving MNs is one of the main challenges for routing protocol development. Message transfer may be done by sending messages directly from a SN to a DN or sending the messages via a number of FNs until they reach the DN. Accordingly, the main requirement for a routing protocol operated in MANETs is the ability to compare and choose the best possible route from a SN to a DN among all the possible routes. Another concern in MANETs is power consumption, since mobile devices have limited battery power. In MANETs, MNs have

to contribute some of their battery power in order to relay messages. Moreover, the high number of involved MNs results in an increased resource consumption, including transactions between MNs, memory usage, computational power and battery power. As a result, the best scenario for a routing algorithm is to find the best route, which consists of the least number of FNs, but still yields a high delivery ratio and a low end-to-end delay.

In MANETs, there are some scenarios resulting in that the communications between MNs becomes interrupted. A connection between two MNs may be disconnected and take long time to build another connection. This is because some MANETs cover a vast area by a small number of MNs (e.g. vehicles, animals, humans, etc.), which are often out of each other's communication range. Such scenarios include rural areas with no mobile network coverage, vihecular networks which have high dynamic network topology, or disaster relief networks that the BSs have been damaged. In this case, there are no end-to-end path connection at any time. In literature, this type of MANETs is referred to as the Delay Tolerant Network (DTN) (or Disruption Tolerant Network) [1, 2]. The same as MANET, the network topology of DTN is dynamic and MN's mobility is unpredictable. However, the added characteristics of frequent and long disconnection may significantly degrade the performance of the DTN, if the existing routing protocols in MANETs are employed. In other words, the routing techniques in MANETs, which rely on the end-to-end paths, are not suitable for DTNs. Therefore, a new approach, referred to as the store-carry-forward model [2], has been proposed to provide communications in DTNs. With this approach, whenever the next hop of the route towards a DN is unavailable, the MN stores and carries the message until it contacts the DN or finds a new suitable message carrier. Along with the DTNs, there are different routing techniques having been developed based on the store-carry-forward model, including, e.g., the multiple-copy and single-copy approaches. Specifically, the multiple-copy approach or the flooding algorithm aims at the highest message delivery rate. Epidemic routing [3] is one of the examples in this catagory. In the Epidemic routing, a message carrier, which may be a SN or a FN, distributes multiple copies of messages to the encountered FNs until the message reaches the designated DN. The main drawback of the multicopy routing is the tremendous resources required for message transfer operations, which include bandwidth, memory space, battery power, etc. By contrast, in the single-copy approach, a single copy of message is either forwarded from a SN through FNs to the DN, or is rather kept to the SN and forwarded directly to the DN. Comparing to the multiple-copy approach based routing algorithms, the single-copy based routing protocols significantly decrease the resource consumption. However, they may result in longer end-to-end delay and lower delivery ratio. In addition, they usually require more computational power, in order to estimate the performance of the encountered MNs so as to make the decision whether a message should be given to a FN.

Focusing on the networks where MNs are humans, a sub-class of DTNs referred to as the

Opportunistic Network (OPNET) has been defined [4]. OPNETs in general have the same characteristics as the DTNs. Specifically, OPNETs are proposed based on the assumption that humans' mobilities are unpredictable and humans' moving ranges can be many times of the operational coverage of short-range radio devices. As a result, connections between two MNs are often disrupted and it is hard to establish a fully connected path from a SN to its DN at any time. Consequently, a data transfer process can only be completed by the opportunity, when two MNs happen to be in a nearby area within their communication range. Similar to DTNs, because of this partially-connected behavior, the existing routing techniques for MANETs may fail to operate in OPNETs. On the other hand, in contrast to DTNs, OPNETs focus on the mobility of humans, which is suggested not totally random, but instead, to move in certain patterns. Based on these facts, routing techniques for OPNETs, such as the PRoPHET [5], have been developed to improve the performance of message transmission.

Mobile Social Network (MSN) is a sub-class of DTNs and OPNETs which inherit the characteristics of frequent and long disconnection of the DTNs. MSNs is also a type of OPNETs, in which humans move in patterns. However, MSNs exploit the social relationship between humans, which is referred to as the human social behaviors, in order to increase the efficiency of message delivery. In MSNs, there are generally three factors affecting humans' mobility behaviors. First, people often meet and spend time with acquaintances. Milgram's experiment [6] has demonstrated the benefit of using the acquaintance chains in order to pass a document from one MN to another. It is demonstrated that, although a SN does not know its DN, usually only a small number of FNs are involved for the document delivery from the SN to the DN. Furthermore, the experiment has proved the hypothesis that people share mutual acquaintances and the acquaintance chains can be regarded as partially connected routes from SNs to their corresponding DNs. Another factor of MSNs is that each person has a list of favorite places, or preferred communities, which they prefer to visit. For instances, company employees are likely to spend most of their time at their companies, students have scheduled classes to attend, housewives often have their preferred shops to do shopping, people have their favorite places to visit for the purpose of exercises, relax, or entertainment, etc. Due to the above-mentioned, people with the same preference are likely to meet more often than those not having similar preference. The last factor is that people have their routines. Repeated mobility patterns exist, which can be found from observing their schedules. The repeating patterns may happen daily, weekly, or longer period. For examples, employees and students usually go to their companies and schools, respectively, in the morning and go back home in the evening, people who do not work or study in their home towns tend to travel on Monday, Friday, weekends, etc. Accordingly, by observing individuals or groups of people who have similar acquaintances, community preferences, and schedules, their movement patterns may be predicted.

Relying on the single-copy routing, the routing protocols in MSNs make use of human social

behaviors in order to reduce resource consumption and computational complexity, while simultaneously reserving a high delivery ratio and a low end-to-end delivery latency. In literature [7–14], most of the routing protocols in MSNs have been developped by exploiting the mutual acquaintances of people. However, people's social relationship can be very complicated, and it is often impossible to capture all of them and store in mobile devices. In order to predict the next meeting and find out a route for message delivery, researchers usually consider two other facts in addition to the acquaintance chains. First, it is more likely that two MNs know each other, if they often contact. The examples of the routing protocols exploiting this fact are PRoPHET and SimBet [7]. In these protocols, delivery possibilities are evaluated from MNs' encounter history. The more often meeting between two MNs means that there is a higher possibility for their next meeting. By observing the delivery probabilities of the neighbor MNs with the DN, it is possible for a message to reach the DN through a number of FNs, although the message holder does not have direct contact with the DN. Another fact is that two people with similar interests are likely to meet often. This information can also be exploited to improve the routing performance in MSNs. However, this method generally requires direct information from MNs. For examples, the LABEL [15] and BUBBLE [16] protocols use the basic interests of mobile clients, the HiBOp protocol [9] compares a person's information to another, the Social-Greedy protocol [10] qualifies the common interest by asking a set of questions and finding the similarity of the answers.

In the development of routing protocols for MSNs, near realistic simulation is required, since it costs a lot of resources and time for carrying out experiments in real-life scenario. In MSN studies, the simulation of a routing protocol has two main parts, including message generation, and mobility model, apart from the routing protocol itself. The message generation part is responsible for generating the messages with given characteristics. For the sake of simplicity, some parameters which are irrelevant to the purpose of the simulation may be ignored. By contrast, the mobility model controls the movements of the MNs in a considered MSN. According to Bai and Helmi [17], the existing mobility models can be divided into four categories. First, MNs in random-based mobility models move randomly in terms of their directions or positions. Although this is the easiest to implement, it is however not suitable for the development of routing protocols for MSNs, because the movements of each MN are unpredictable. The other three types of mobility models are the models with temporal dependency, the models with spatial dependency and the models with geographic restriction, respectively. These models are more realistic, owing to more realistic factors being considered. Specifically, these protocols combine the characteristics of real mobility scenarios, including smooth changes of speed and direction, movements depended on a group instead of individual, obstacle and path restrictions, etc. Furthermore, there are another group of mobility models considered in [18], which is referred to as the mobility models based on human behavior. We should note that, as a trade-off of considering more realistic issues, the mobility

models often become more difficult for implementation.

1.2 Research Challenges

As in MANETs, DTNs, and OPNETs, mobile devices in MSNs have limited energy, as their power is provided by batteries. Due to this, mobile devices have many other resultant limitations of, such as, memory usage, computational power, and radio signal transmission power. Therefore, in the development of the routing protocols for MSNs, it is essential to design the energy-efficient algorithms, which consume the least possible battery power, but are capable of maintaining a high delivery ratio and a low end-to-end delay. In literature, the routing protocols are mainly either multiple-copy or single-copy based. In general, the multiple-copy routing protocols are capable of choosing a short route, to achieve a high delivery ratio and a low end-to-end delay. However, the multiple-copy protocols involve a lot of FNs and, hence, consume a big amount of resources, including network capacity, MNs' memory space, energy, etc. By contrast, the single-copy routing protocols result in a relatively low delivery ratio and a relatively long end-to-end delay. Even worse, they are often unable to find the shortest route from a SN to a DN, but instead, choose some other less optimum routes. However, in comparison to the multiple-copy routing protocols, the single-copy routing protocols may consume much less resources for message transmission. For this sake, most of the routing protocols in MSNs are based on the single-copy approach. Therefore, in MSNs, it is highly challenging to design the routing protocols, which are capable of achieving the best trade-off among the delivery ratio, end-to-end delay, average number of hops per delivered message, and resource consumption.

In this thesis, we will motivate to design the routing protocols that are capable of attaining the trade-off among these factors in Chapters 4 and 5. In MSNs, the routing protocols exploit the social behaviors of mobile device carriers, in order to enhance the networking performance, while aiming at the lowest energy consumption. Since the single-copy protocols are preferred over the miltiple-copy protocols due to the above-mentioned consideration, an effective prediction of MNs' mobility is critical, for determining the best possible route from a SN to its DN. Therefore, the main challenge here is to find the effective methods to measure the strength of the social relationship among MNs. In literature, different social factors have been considered and the measurement of the social relationship strength has been investigated in different dispectives [19–26]. In this thesis, we will also address the social relationship measurement issues in Chapter 4.

In addition, in terms of the human mobility, as above-mentioned, random mobility models are simple, but unrealistic. On the other hand, the more realistic mobility models are harder to implement and a given model is often likely to be suitable for only one scenario, but not in general.

Furthermore, most existing mobility models cannot capture the human social behaviors, such as mutual acquaintances, mutual communities, and routine similarity, that have direct effects on their mobility. Therefore, it is still challenging to integrate the human social behaviors into the mobility models, in order to use them more efficiently to design the high-efficiency routing algorithms. In this thesis, we will propose the mobility models reflecting the human social behaviors in Chapter 3.

1.3 Research Contributions in This Thesis

Against the background and challenges, in this thesis, we propose new human mobility models and routing protocols by taking into account of human social behaviors. The main contributions of this report are summarized as follows:

- First, a Preferred-Community-Aware Mobility (PCAM) model is proposed. This mobility model exploits the human social behavior of preferred communities to make it close to practice. Simultaneously, it is capable of maintaining the simplicity and random movement characteristics of the Random WayPoint (RWP) mobility model [27].

- Second, a Role-Playing Mobility (RPM) model is designed to reflect the behavior of humans' daily schedules, in terms of the roles played by individuals. In our model, one MN may play multiple roles and carry out multiple activities in different scenarios.

- Third, we propose and investigate a Social Contact Probability assisted Routing (SCPR) protocol. Our SCPR protocol is capable of taking the advantages of two types of the relationships, which are MN-to-MN relationship, referred to as the node-linked relationship, and MN-to-community relationship, called as the community-linked relationship. We measure the node-linked relationship based on the human social behavior of mutual acquaintances while the community-linked relationship is measured based on how often a MN visits a community. Through these two types of relationship, our SCPR protocol exploits the characteristics of encounter history, including frequency, regularity, freshness, and transitivity, to find the best possible route for message delivery. Furthermore, the SCPR protocol can either exploit alone the strength of community-link relationship or alone the node-linked relationship to find the best route for message delivery.

- Finally, in order to achieve the best possible trade-off among delivery ratio, end-to-end delivery delay and energy consumption, we propose two types of energy concern of routing protocols for MSNs, which are the EnCoR and ESDR protocols. Their performance is studied and compared by considering different operational scenarios. Our studies show that these

routing protocols are highly flexible for achieving the trade-off among energy consumption, delivery ratio, end-to-end delivery delay, i.e., the DC/DR/D trade-off.

1.4 Thesis Overview

The rest chapters are summarized as follows.

Chapter 2 provides the background review of the factors affecting human mobility behaviors, existing mobility models, and the routing protocols for various types of mobile networks, including MANETs, DTNs, and MSNs. In more detail, the chapter begins with an introduction for the human social behaviors that affect human mobility behaviors associated with providing a number of statistical features of human mobility. Then, we continue to discuss the existing mobility models in wireless moblie networks. In our discussion, mobility models are categorized into five groups. The first group are purely random models where MNs move randomly. In the second group, the current movement of a MN is temperally depended on its previous state. The third group are the models with spatial dependency, which allow MNs to move in groups. Then, in the fourth group of models with geographic restriction, the scenarios with boundaries are considered, where MNs' movements are limited by obstacles. Lastly, the fifth group of models are based on the human social behaviors imitated human mobility that taking into account of personal preferences. Furthermore, in this chapter, we review a number of well-known routing techniques for the MANETs, DTNs, and MSNs networks.

In Chapter 3, we propose two mobility models for simulation of human mobilities as well as studying the performance of the different routing protocols developed in the following chapters. First, the PCAM model is proposed by joint of the RWP model [27] and the community-based mobility model [5, 28]. In addition to the randomness provided by the RWP model, the PCAM model also exploits the human behaviors that people tend to have some preferable places to visit. The second mobility model proposed is the RPM model, which is designed based on the intuition that every person usually has several roles to play. Typically, a person may have a primary role and several secondary roles. Here, a primary role represents the main role of a person to play, which reflects his/her daily schedule, while secondary roles are mainly reflected by a person's behaviors in his/her leisure time.

In Chapter 4, we propose a routing protocol, namely, the SCPR protocol. In brief, the SCPR protocol exploits two types of relationship, including node-link and community-link relationships, in order to attain good performance in terms of delivery ratio, end-to-end message delay, and the number of hop counts. Specifically, in the SCPR protocol, a message is forwarded from a message carrier to an encountered MN, when the encountered MN has a higher delivery probability than the

former one to the DN. Here, the delivery probability is evaluated from the strength of node-link and community-link relationships. By taking into account of encounter properties, including frequency, regularity, freshness, and transitivity, the strength of node-link relationship can be measured. Furthermore, the SCPR protocol considers community-link relationship by measuring the preference levels of preferred communities (PCs). The results of the experiments and its performance in comparison to the existing well-known techniques show that the proposed SCPR protocol is capable of efficiently integrating the merits of high delivery ratio, low delivery latency and low resource consumption of the existing protocols, while circumventing their respective shortcomings.

Chapter 5 introduces two types of energy-concerned routing techniques, which are the EnCoR protocol and the ESDR protocol, which are capable of achieving the trade-off among energy consumption (EC), delivery ratio (DR), and delay (D), i.e., the EC/DR/D trade-off. In our EnCoR protocol, the EC/DR/D trade-off is controlled by introducing a threshold for the route selection. Specifically, when a message carrying MN encounters another MN, it forwards the message to the encountered MN, only when the delivery probability from the encountered MN to the DN is higher than that from itself to the DN by at least the threshold. In this way, the EnCoR protocol can effectively control the trade-off among the consumed energy, delivery ratio and average delay. In terms of the ESDR protocol, we first analyze the effect of message length on the energy consumption during message transmission. Then, we propose a hop estimation method for finding the shortest delivery route based on the social relationship among the MNs. Then, the ESDR protocol makes the routing decisions based on these two metrics as well as the delivery probabilities. By controlling the contribution of these factors, the ESDR can also control the EC/DR/D trade-off. With the aid of the EnCoR and ESDR protocols, in this chapter, we then extend some existing routing protocols for MSNs, including, our proposed SCPR, PRoPHET, and the BUBBLE protocols, to their corresponding energy-concerned ESCPR, EPRoPHET and EBUBBLE protocols. Finally, the performance of these routing protocols is investigated by simulations based on our PCAM mobility model. Our studies and performance results show that all these protocols are capable of attaining the EC/DR/D trade-off.

Finally, Chapter 6 concludes this thesis and explains some possible future research areas in terms of modelling of mobility and routing protocols for MSNs.

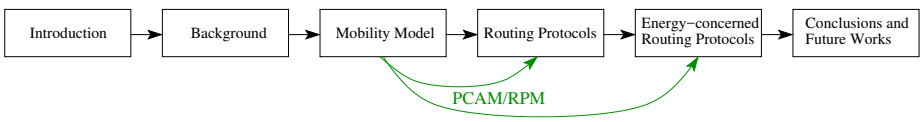

Figure 1.1: A chart explaining the flow of the thesis.

In brief, Fig. 1.1 explains the flow of the thesis where PCAM and RPM models are proposed in Chapter 3 and are used in Chapter 4 and Chapter 5 for performance measurement of routing protocols.

Chapter 2

Literature Review

This chapter provides a background overview for Mobile Ad-hoc Networks (MANETs), Delay Tolerant Networks (DTNs), Opportunistic Networks (OPNETs) and Mobile Social Networks (MSNs). A number of representative routing algorithms developed for these networks are specifically discussed. In addition, different mobility models widely used for investigation of the routing algorithms in these networks are discussed.

2.1 Introduction

In some harsh communication environments, such as rural areas and during disasters, that infrastructure networks are unable to provide their service coverage or fail to operate, there are possibly no connection available between mobile nodes (MNs) for building a connection from a source node (SN) to a destination node (DN). In these scenarios, the independent networks that do not depend on any fixed access points are required. With the aid of relays, which are also referred to as forwarding nodes (FNs), it is possible to set a communication link between a SN and its DN. However, there are a range of limitations that the existing networking technologies may not overcome, including, for examples, frequent and long partitions of MNs, large area with a small number of MNs, etc. Recently, researches have been carried out to make use of human social behaviors, in order to increase the connectivity of MNs and to improve the performance of such networks. In this chapter, we discuss the effects of human social behaviors on human's mobility. Based on this, we review a number of existing mobility models as well as the routing protocols for MANET, DTN, OPNET, and MSN.

2.2 Human Social Behavior

Recent researches, such as [23–25], have demonstrated that human mobility has repeating patterns. In people's daily life, there are several factors affecting their mobility patterns, including people who they know, which is referred to as acquaintances, popularity of the places they may choose to visit, which is referred to as preferred communities (PCs), and time of the day. In [6], it is showed that a collection of relationships among human beings may form an acquaintance chain. According to this research, the length of chains typically varies from two to ten intermediate acquaintances. However, there are some obstacles for applying the acquaintance chain, including the difference of classes in social structure and genders, since people usually prefer to communicating with the other people from the same social classes and the people of the same genders. These observations suggest that people with similar social features usually have more chances to become acquaintances and, hence, have more chances to meet. For this reason, later, there are some researches having been conducted, which include the Social Relationship Enhanced Predicable (SREP) routing protocol [29], Social feature enhanced group-based routing [30], Social-similarity-based (SOSIM) routing protocol [31], Ego-Centric Social Network Routing (ECSNR) protocol [32], and M-Dimension [33]. Specifically, in terms of the PCs, people usually have a number of places where they prefer to visit more than the other places. Apart from personal preferences, the popularity of places also play an important role on people's decision. Specifically, in [34, 35], the authors have suggested that people often go to the places that are not very far away from their homes, as well as the places where they may have more chances to meet people. Furthermore, it is suggested that people usually have repeating mobility patterns, which start and end in a day. Corresponding to this observation, for examples, in [34–37], mobility models have been proposed by assuming that a MN daily starts and ends at a specific location, which is referred to as its home.

Recently, there are several researches [19–26] having studied the human mobility behaviors, and discovered several statistical elements from the real traces of human mobility. Specifically, in [36], the authors have summarized these elements into four main features, namely, the truncated power-law flights and pause-times, heterogeneously bounded mobility areas, dichotomy of inter-contact times, and the fractal waypoints, which are further detailed as follows.

2.2.1 Truncated Power-Law Flights and Pause-Times

By exploiting the traces of bank-note circulation in the United States, Brockmann et al. [19] have observed that the distribution of human traveling distances truncates as a power-law distribution. Furthermore, there are several human-trace-based experiments supporting Brockmann's observation, including [20, 21] which capture human traces by recording the locations of mobile phone

users. Apart from the human mobility flights, [21, 22] have found that the complementary cumulative distribution function (CCDF) of the periods of time that people spend within each place, referred to as pause time, follows a truncated power-law distribution.

2.2.2 Heterogeneously Bounded Mobility Areas

In [20], the authors have studied some people's trajectories, and identified that human mobilities have simple repeatable patterns within their own territories. The traces of mobile phone users demonstrate a high degree of temporal and spatial characteristics, while each individual travels and stops at the same location frequently. The traces also show that individual mobile phone users have different mobility areas and travelling distances.

2.2.3 Dichotomy of Inter-Contact Times

In [23], [24], the authors have investigated the empirical distribution of the inter-contact times obtained from a number of real traces. It is suggested that the CCDF of the inter-contact times fits a power-law distribution truncated on a log-log scale. For the sake of comparison, the power-law is normalized to fit the granularity of $t = 120$ seconds, giving the CCDF in the form of

$$P[X \geq x] = \left(\frac{x}{120}\right)^{-\alpha} \tag{2.1}$$

Furthermore, the authors have introduced an estimator for the slope of the power-law graph, which is referred to as the heavy tail index α. Specifically, let m be the sample's median. Then, α can be estimated as

$$\alpha = \frac{\ln(2)}{\ln(m) - \ln(120)} \tag{2.2}$$

Later, in [25], the authors have shown that the CCDF of the inter-contact times follows a power-law distribution for approximately half a day, and then, decays exponentially. Correspondingly, the authors described this property as the dichotomy of inter-contact times. According to a number of experiments carried out in association with [38, 39], Fig.2.1 shows the distribution characteristics of inter-contact times, which are best described by the dichotomy of inter-contact times. Specifically, during the first period, the Intel2006 and Cambridge2005 traces are best fit with the power-law distribution with a heavy tail index of 0.6, while the Cambridge2006 and INFOCOM2005 traces are best described by the power-law with the slopes of 0.2 and 0.35, respectively. After then, all four traces are truncated by a exponential distribution.

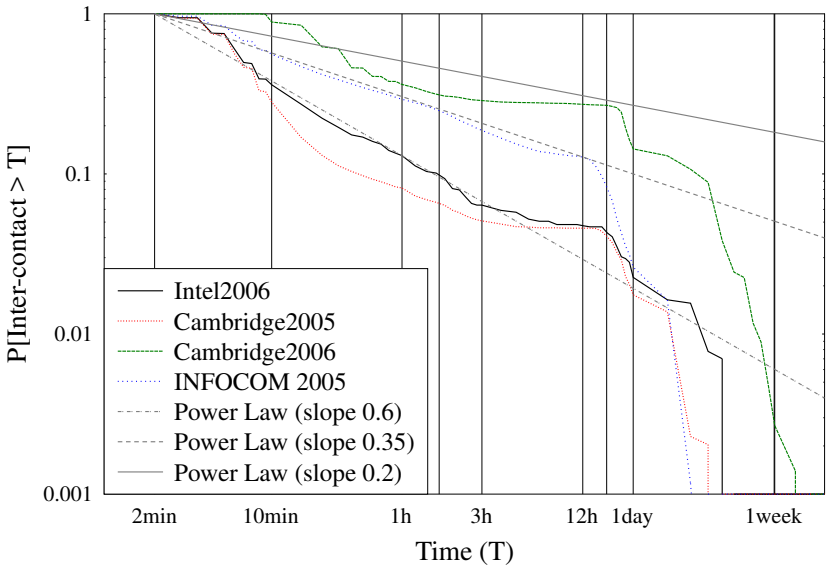

Figure 2.1: A graph shows the CCDF of inter-contact times on a log-log scale for four real traces.

2.2.4 Fractal Waypoints

In [26], the authors have analyzed the GPS traces of human walks and claimed that the waypoints, where people stop by, can be modeled by fractal points. The bursty-manner distribution of gaps between fractal points, on either a one-dimension or a multi-dimension, has the characteristic of a power-law distribution. This observation implies that people prefer to visit the places where other people also like to visit. Similarly, some other researches, including [36], [34], [35] have also shown that people are often attracted to the more popular places.

2.3 Mobility Models in Wireless Adhoc Networks

In the study of wireless communication systems, it is usually more practical to rely on the synthetic data generated by models derived from practice, since performance evaluation of communication schemes and protocols in real environments are costy and time consuming. Specifically, the simulation of routing algorithms consists of moving MNs and message delivery in a virtual environment with pre-defined settings. While the routing algorithms control how messages are delivered from SNs to their DNs, mobility models determine the mobility patterns of MNs. In this type of simulations, the movement patterns are considered to be crucial and have a high impact on the performance of a routing algorithm operated in real world. Researchers have developed varieties of mobility models, in order to represent the mobility characteristics of mobile users in the real world. For example, Bai and Helmy in [17] have divided mobility models into four main groups,

namely, the random-based mobility models, models with temporal dependency, models with spatial dependency, and the models with geographic restriction. When MSNs are considered, there is in fact another group of mobility models, as mentioned in [18], which is referred to as the mobility models based on human behavior. Below we provide a brief overview for these mobility models.

2.3.1 Random-Based Mobility Models

The models in this group are based on the assumption that every MN moves freely and randomly without any restriction. Each MN independently chooses its direction, destination, and speed. These models have been widely used in simulation studies, as they are relatively easy to implement and analyze in comparison to the other approaches. However, this type of mibility models lack of reflecting the realistic scenario factors, including, such as, temporal dependency, spacial dependency, geographic restriction [17].

2.3.1.1 Random Waypoint Model

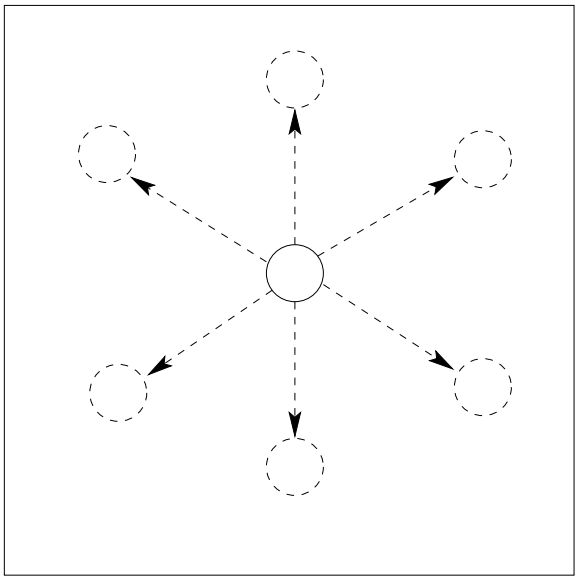

Figure 2.2: An example illustrating the mobility behavior of a MN in the RWP model which moves towards a new position.

The random waypoint (RWP) model [27] has been first developed and used in order to compare the performance of the routing protocols for mobile ad-hoc networks. As shown in Fig.2.2, in the context of the mobility model, the movement pattern of a MN starts by remaining at the original position for a *pause time*. Then, it moves to a random-selected destination with a speed uniformly chosen between zero and a predefined maximum speed. After arrival at the destination, the MN

pauses for a *pause time*. Then, it chooses a new destination, and moves toward its new destination with another randomly chosen speed. The above procedure repeats until the completion of simulation. Later, there are some researches improving the mobility characteristics of the RWP model, including node distribution [40] and stochastic properties [41].

2.3.1.2 Random Walk Model

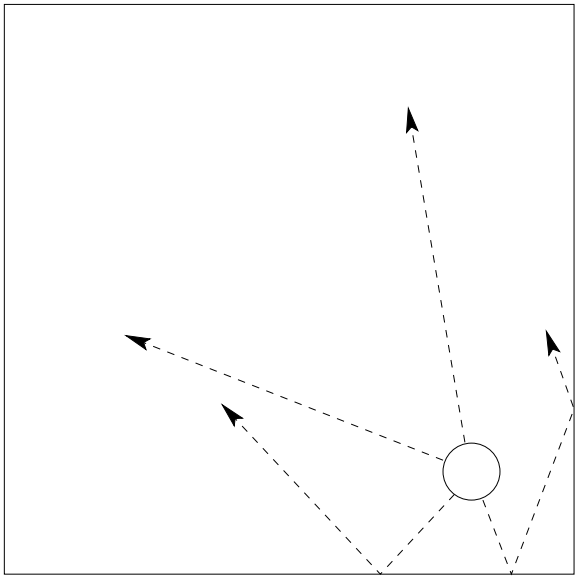

Figure 2.3: An example illustrating the mobility behavior of a MN in the random walk model which moves towards a new direction.

The random walk mobility model [42] has been developed and been widely used to reflect individual movements related to cells [43, 44]. Random walk models are often used to simulate the Brownian motion and the unpredictable movements of natural objects, such as, molecules. With this mobility model, as shown in Fig.2.3, at the beginning of the simulation, each MN randomly selects a direction and a speed from the sets of [0,2π] and [*speedmin*, *speedmax*], respectively. Then, it moves in the chosen direction with the selected speed for a fixed time or distance. At the end of each movement, the MN chooses a new direction and a new speed, and moves again. In the case of reaching a boundary of a predefined simulated area, the MN bounces back in the direction determined by the angle of the incoming direction. This model is similar to the random waypoint model without pause time, and it models higher randomness than the random waypoint model [17].

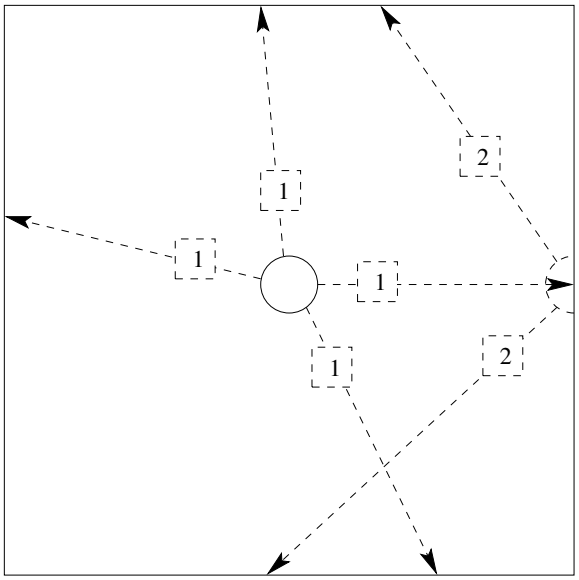

Figure 2.4: An example illustrating the mobility behavior of a MN in the random direction model which moves towards a new direction until reaching the boundary.

2.3.1.3 Random Direction Model

In [45], the authors observed the mobility behaviors of MNs under the RWP model, and found that the density of MNs in the middle of a simulated area is relatively higher than that in the other areas, especially, in the areas near borders. This is because MNs moving to their destinations often need to cross the middle area. Accordingly, a new mobility model has been proposed, which is referred to as the random direction model. In this mobility model, as shown in Fig.2.4, each MN chooses a direction randomly and uniformly in [0,2π) degree, instead of choosing a destination under the random waypoint model. Then, the MN travels in the selected direction with a random speed until it reaches the boundary. Then, the MN moves again after a pause time with a new speed in a new direction chosen from $[0, \Pi]$ degree against the boundary. This process continues, until the end of the simulation. It has been observed that, when the random direction model is employed, data transmission usually requires in average a higher number of hops, in comparison to the other mobility models, due to the short pause at boundary [44].

2.3.2 Models with Temporal Dependency

In random mobility models, the changing rate of velocity, i.e., acceleration, and the direction of MNs are independent of each other. Moreover, the changes are usually not related to their previous states [17]. This means that the memoryless movement may suddenly stops and sharply turns towards a new direction [44]. However, in practice, objects usually change their speeds and di-

rections depending on their previous states, presenting the characteristics of temporal dependency. Therefore, in [46–48], the authors have developed the mobility models, where MNs' movements are temporally correlated, as detailed below.

2.3.2.1 Gauss-Markov Model

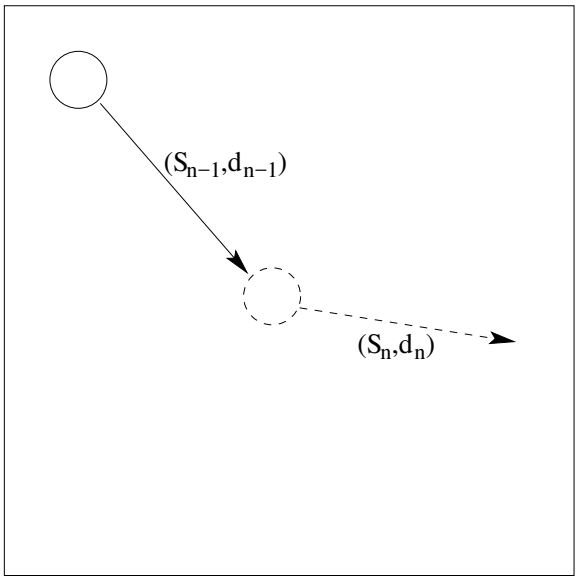

Figure 2.5: An example illustrating the mobility behavior of a MN in the Gauss-Markov model which moves with a new speed and a new direction explicitly depended on the previous state.

In [46], Liang and Hass have proposed to use the Guass-Markov model for MNs' mobility modelling. Furthermore, the constant velocity fluid-flow model and the random walk mobility model are introduced as the extreme cases. Specifically, the MNs in the constant velocity fluid-flow model have strong memory, which creates smooth movement patterns. This model is hence suitable for vehicular mobility simulations. By contrast, the high randomness and memoryless characteristics of the random walk mobility model are suitable for describing pedestrian movements, as in this case, stop-and-go interruptions of MNs frequently occur. The Gauss-Markov model provides a trade-off between the above two extreme scenarios. The equations (2.3) and (2.4) shown below are used to generate the current speed and direction, which are explicitly dependent on the previous states [17, 49].

$$S_n = \alpha S_{n-1} + (1-\alpha)\overline{S} + (1-\alpha^2)\sqrt{S_{x_{n-1}}} \tag{2.3}$$

$$d_n = \alpha d_{n-1} + (1-\alpha)\overline{d} + (1-\alpha^2)\sqrt{d_{x_{n-1}}} \tag{2.4}$$

where S_n and d_n denote speed and direction in the time period n, $\overline{S}$ and $\overline{d}$ represent average speed

and average direction, $S_{x_{n-1}}$ and $d_{x_{n-1}}$ are variables from a Gaussian distribution. Finally, $\alpha \in [0, 1]$ is a constant value.

From (2.3) and (2.4), we can see that by adjusting the memory level α, a wide range of mobility patterns can be created. Specifically, when the memory level is high or close to one, the movements of MNs become fluid-flow-like. On the other hand, the memoryless random walk patterns can be created by letting the memory level α close to zero.

2.3.2.2 Smooth Random Mobility Model

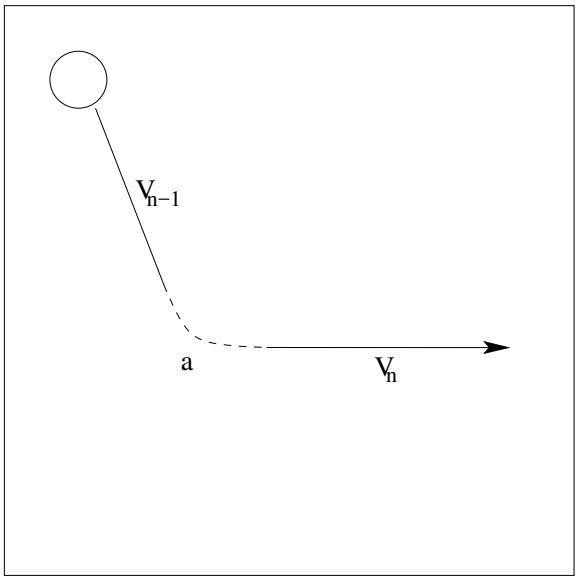

Figure 2.6: An example illustrating the mobility behavior of a MN in the smooth random model which avoids sharp turns and smoothly changes to a new speed with an acceleration a.

In order to enhance the random mobility model in terms of the temporal dependency, the authors in [47, 48] have proposed the smooth random mobility model. For the MNs operated under this model, each of the MNs chooses its initial speed randomly based on the random mobility model. It then moves with the initial speed until a new speed is generated from a random process. Then, it changes to the new speed smoothly with a linear acceleration chosen uniformly in $[a_{min}, a_{max}]$, until reaching the new speed. Moreover, considering the practice, that speed is not necessary constant, the speed distribution of MNs is also considered. Specifically, the velocities of MNs are chosen from an interval $[0, V_{max}]$. However, they are not uniformly distributed in this interval. Instead, individual MNs have their specific speed distribution for choosing their speed in $[0, V_{max}]$. Similarly, the direction of a MN changes over time by following an exponential distribution. Furthermore, in the smooth random mobility model, the direction is assumed to be uniformly

distributed in $[0, 2\pi]$.

2.3.3 Models with Spatial Dependency

In the above described mobility models, one MN moves freely without affecting the others in terms of their velocities, locations and directions [17]. In practice, however, collision between two MNs may occur. Furthermore, there are wireless communication applications requiring team collaboration, with a team leader as the center of the group, while the other group members move following the leader. In these types of scenarios, the movements of MNs are correlated in space, called as the spatial dependency. Correspondingly, in MSNs, there are mobility models proposed to take the spatial dependency into account, which are specified in more detail as follows.

2.3.3.1 Reference Point Group Mobility Model

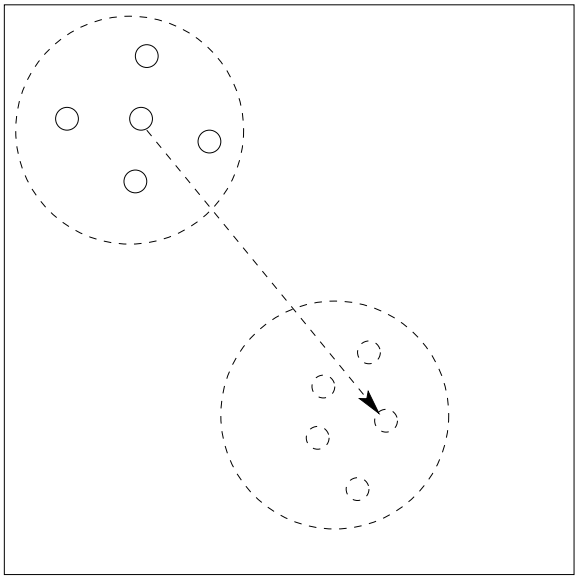

Figure 2.7: An example illustrating the mobility behavior of MNs in the RPG model which move in group following the group leader.

The reference point group (RPG) mobility model has been first introduced by [50] in order to reflect the relationship between MNs. Under this mobility model, a logical center is first identified, MNs within the same group then follow the center's motion in terms of their locations, speeds, directions, accelerations and so on. Specifically, for each step of movement, the movement of the group leader is first defined. Then, all the member MNs are randomly placed in the neighborhood of the reference point. Let the velocity of the group leader be expressed as V^t_{group}, and the random vector of the ith MN from its reference point be expressed as RM^t_i. Then, the velocity of the ith

MN is determined by the formula of [17, 50, 51]

$$V_i^t = V_{group}^t + RM_i^t \tag{2.5}$$

In the study of MNs, the simulate scenarios generated by the RPG model are usually closer to the reality, as in practice there are situations, such as, military operations, where MNs move in groups.

2.3.3.2 Other Spatial Dependant Models

Based on the behaviors of random orbit, Sánchez and Manzoni [52] have proposed three correlated mobility models, namely, the column mobility model, pursue model, the nomadic community mobility model. In the column mobility model, MNs in a group use a reference position as the center

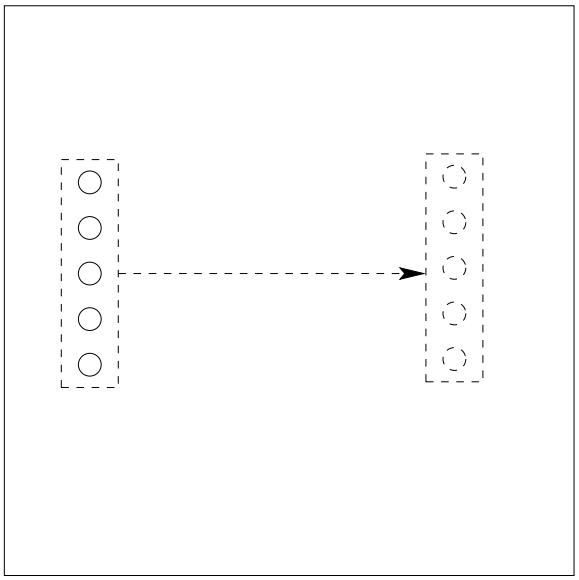

Figure 2.8: An example illustrating the mobility behavior of MNs in the column model which form a line and move along with their neighbors.

of the group, while the MNs form a line similar to a row of soldiers. Then, the MN group move in a certain direction towards a new defined reference position, with every MN uniformly matches its movement with its neighbors, as shown in Fig.2.8. In terms of the pursue mobility model, similar to the RPG model, a group of members follow their group leader which freely and randomly moves, as shown in Fig.2.9. However, there is a speed limit on the followers and, furthermore, certain randomness is added, when the leading MN stops. Finally, as shown in Fig.2.10, the nomadic community mobility model provides the mobility patterns of moving communities. When a community is settled, each of MNs defines its own private area and moves randomly around its reference position. When the community moves, all MN members move following the community's

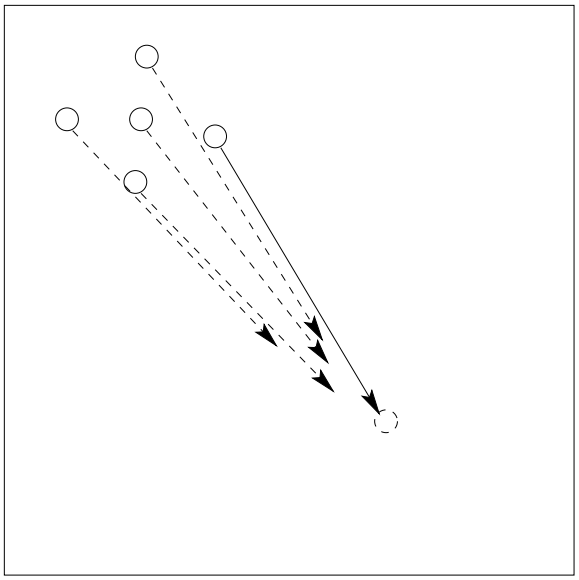

Figure 2.9: An example illustrating the mobility behavior of MNs in the pursue model which move in group following the group leader.

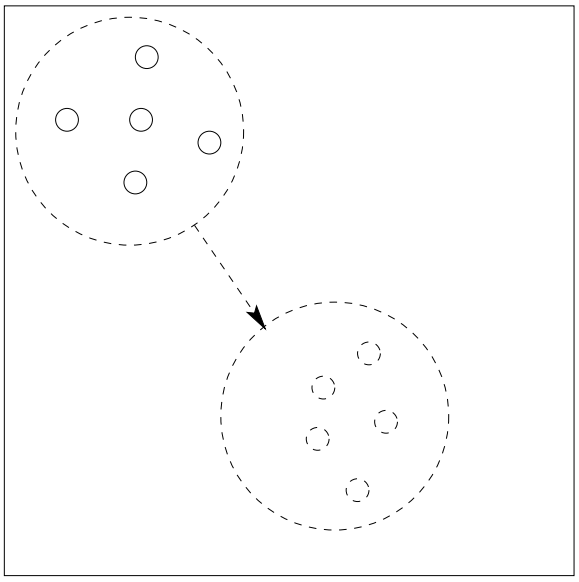

Figure 2.10: An example illustrating the mobility behavior of MNs in the nomadic model which move in group following the moving community.

movement.

2.3.4 Mobility Models with Geographic Restriction

The lack of environment consideration is another limitation of the random-based mobility models, since in practice MNs cannot move fully freely and randomly. Instead, the movement of a MN is

constrained by its surroundings. For example, vehicles only move on roads and streets, pedestrians may be blocked by objects like buildings. In order to simulate the scenarios in real life, geographic restrictions may be needed to be imposed. Hence, a few of mobility models have been proposed by taking into account of the geographic constraints, which are described below.

2.3.4.1 Obstacle Mobility Model

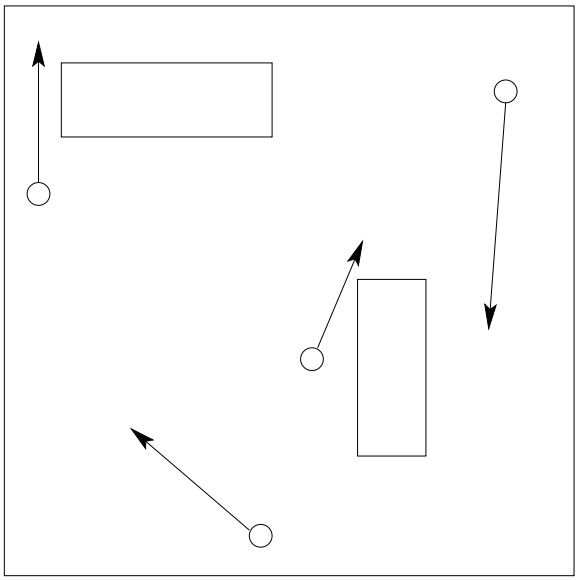

Figure 2.11: An example illustrating the mobility behavior of MNs in the obstacle model which move around avoiding obstacles.

In order to model more realistic mobility behavior, the authors in [53] have proposed a mobility model by considering three realistic scenarios: conference, event coverage and disaster area, each of which has different obstacles and MNs' movement patterns. In the first scenario, MNs are mostly static with only little moving. Walls and doors act as the obstacles reflecting radio signals in the area. In the event coverage scenario, it is assumed that there are a group of highly mobile people and vehicles, and many obstacles are placed randomly in the area. In the last scenario of modelling the situations during the disaster, a small number of vehicles moving at high speed and some people of slowly moving are assumed.

In [54], the authors have further improved the model by introducing the activity types and areas, which are used to set the initial locations and destinations. Specifically, the simulation area is divided into some activity sites, which are grouped into a number clusters. MNs are then randomly assigned to the clusters. Then, each area in a cluster is given a rank. Specifically, the activity areas within the same cluster are given the highest rank, while that having the highest count of the shortest hops are given the lowest rank. Based on the modelling, a new ranking-assisted routing algorithm

has been proposed. With this ranking-assisted routing algorithm, MNs have a high possibility to move towards the areas having the same activity type.

2.3.4.2 Pathway Mobility Model

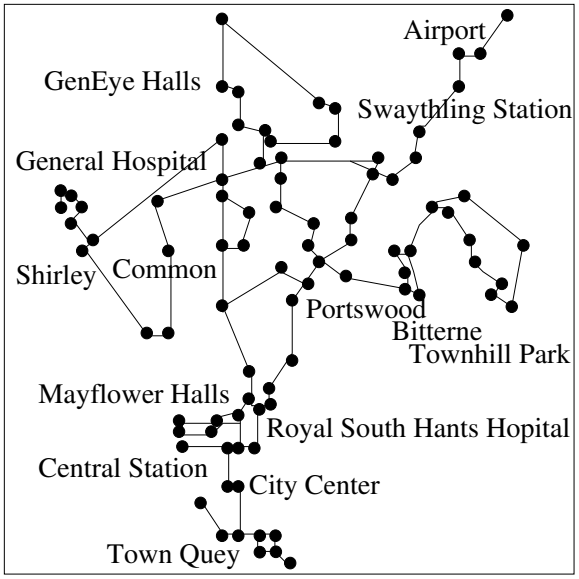

Figure 2.12: An example graph modelling bus routes in Southampton for the graph-based model.

The pathway mobility model constrains MNs' movements by some paths on a generated map [17]. The pathways can be predefined on the map using either a random algorithm or the real map of a considered city. For example, in the graph-based mobility model proposed by [55], as shown in Fig.2.12, a graph is used to connect pathways and locations, and vertices and edges are used to represent places and pathways connecting the places, respectively. With the settings, initially, each of MNs is randomly placed on a vertex of the graph. Then, it finds the shortest path to its next chosen destination and moves towards this destination. Upon reaching a new destination, the MN pauses for a random period of time and then moves towards a next destination.

2.3.5 Models Based on Human Behaviors

In order to model human's mobility, several mobility models have been proposed based on the studies of human mobility behavior [18]. Below, we discuss four popular mobility models, which are designed by considering human's mobility behaviors.

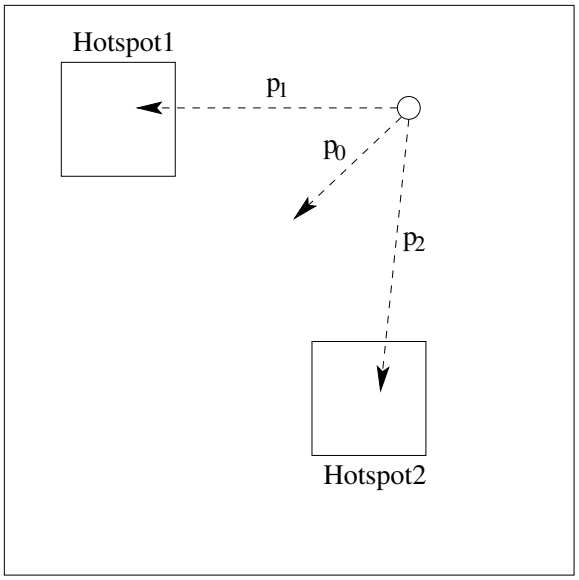

Figure 2.13: An example illustrating the mobility behavior of a MN in the RWP model with hotspots which usually visits hotspots with probability p_i and sometimes moves to other locations with probability p_0.

2.3.5.1 Random Waypoint Mobility Model with Hotspots

In [56], Abdulla and Simon have shown that the MNs' inter-contact times in the RWP and random direction mobility models are best described by exponential distributions. However, the studies in [23–25] show that the distribution of inter-contact times of human mobilities can be approximated by a power-law distribution for a period of time, beyond of which, it truncates exponentially. Later in [57], the authors have proposed a modified RWP mobility model, referred to as the random waypoint mobility model with hotspots. In this mobility model, a MN is assigned to one or several hotspots of the square areas within a simulation area. A MN moves towards each of the hotspots according to a predefined probability. Specifically, let us consider an example of a system with N hotspots. Assume that MN A is assigned to M hotspots, namely $H_1, H_2, \ldots, H_M$. Then, MN A randomly chooses a hotspot H_i with a probability p_i, and then moves towards a random point within the hotspot H_i. In order to address the randomness, MN A also has a probability of $p_0 = 1 - \sum_{i=1}^{M} p_i$ to move to the other locations other than the assigned hotspots.

2.3.5.2 Working Day Movement Model

The working day movement model proposed in [37] is designed based on the daily activities of people, who go to work in the morning, spend their day time at work, have some activities with friends, and travel back homes at the end of the day, as shown in Fig.2.14. The model is developed by combining a number of submodels, which consist of four major activities, including staying at

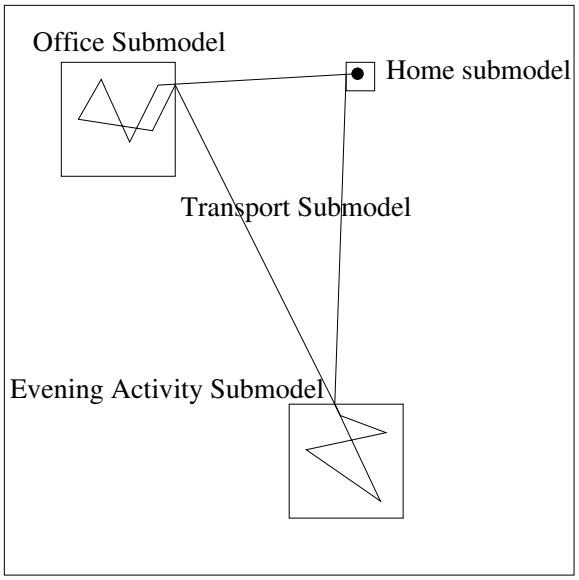

Figure 2.14: An example illustrating the overview mobility behavior of a MN in the working day model which goes to work in the morning, visit a favorite place in the evening, and go back home at the end of the day.

home, activities at office, activities in the evening, and transportation. By considering that people often leave their mobile devices somewhere, such as tables, while they are at home, the home activity submodel simply assume static MNs. By contrast, in the context of the office activity submodel, a MN is allowed to travel within the office's area. Specifically, a MN enters the office area from a specific location, referred to as a door. Then, it moves with a walking speed towards a destination, such as a desk, where it pauses for an amount of time following a Pareto distribution [37]. When the MN wakes up, it finds a new destination. The MN repeats walking, pausing, and finding a new destination, until the work time is over. Furthermore, the authors suggest that people may participate group-based activities at the end of a working day, which might be shopping, walking around, and going to favorite spots. Accordingly, the evening activity submodel is designed by assigning a favorite meeting spot to each of MNs, and grouping MNs based on the favorite spots. Given a favorite spot, MNs do not move until all the group members arrive. Then, the group of MNs move on streets following the random walk mobility model, as discussed in Section 2.3.1.2. Finally, the transportation submodel is divided into three types of transportation ways, including walking, car, and bus. Using a real map, as shown in Fig.2.15, walking corresponds to low speed MN movements along the shortest path to a destination, while car and bus move relatively fast. Furthermore, buses travel following fixed routes.

Figure 2.15: An example illustrating three routes, including walking (green), car (red), and bus (blue), for the transportation submodel.

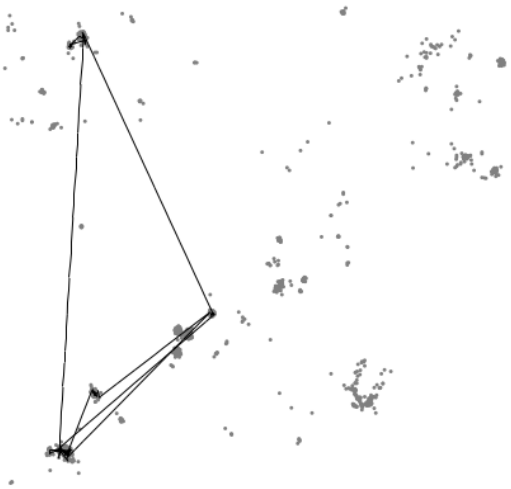

Figure 2.16: An example movement trace of a MN and waypoints generated by the SLAW model [36].

2.3.5.3 Self-Similar Least-Action Walk Mobility Model

In [36], the authors have proposed a mobility model specifically for modelling of human walks, referred to as the self-similar least-action walk (SLAW) mobility model. The model is designed based on the statistical studies of human mobility behaviors, including the truncated power-law flights and pause-times, heterogeneously bounded mobility areas, truncated power-law inter-contact times and the fractal waypoints. In the SLAW mobility model, a number of waypoints are created with the point-to-point gaps following a power-law distribution. Then, based on the least-action princi-

ple that a MN travels to its destinations with minimum discomfort, the authors have developed a trip planing algorithm, which is referred to as the least action trip planing (LATP) algorithm. In order to implement the heterogeneously bounded mobility areas, an individual walker model has been developed to restrict the traces generated by LATP algorithm. Furthermore, the authors have considered the randomness of human mobility by allowing MNs to move out of their predefined walking areas. As an example, Fig.2.16 shows a mobility trace of a MN and waypoints generated by the SLAW model.

2.3.5.4 Small World in Motion Mobility Model

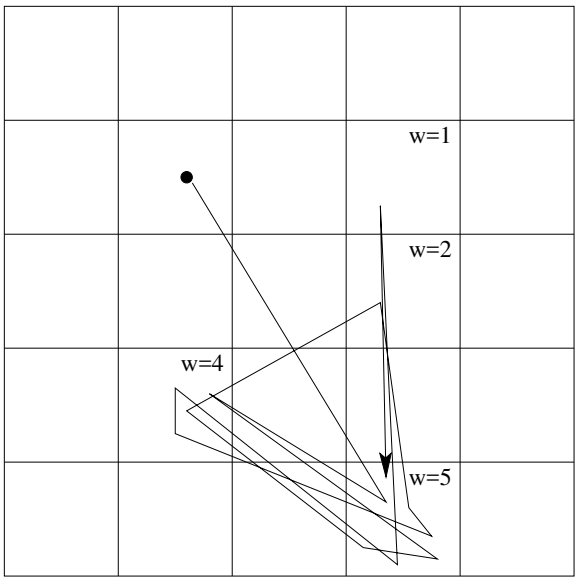

Figure 2.17: An example illustrating the mobility behavior of a MN in the SWiM model which usually visits the cells that have high weight.

The small world in motion (SWiM) mobility model [34, 35] has been developed with considering the model's simplicity and its ability to predict the performance of networking protocols. Based on the fact that people usually prefer to choose the best and the most popular places, which are also not far away from where they live, in the SWIM mobility model, a MN selects its destination based on a weight. This weight changes according to the popularity of the place, as well as to the distance between the place and its home. Specifically, at the beginning of a simulation, a square simulation area is divided into a number of small square cells. Each MN is then assigned to a cell, referred to as its home. Then, it selects the next destination randomly, as the result that it does not have the a priori knowledge of any popular places. Therefore, at first, the number of MNs seen by any destination is set to zero, which is updated during the simulation, whenever a MN arrives at a destination. Specifically, let A be one of the MNs and h_A be A's home. Let C be a destination cell.

Table 2.1: Summary of existing mobility models.

Year	Author	Contribution
1997	Rubin *et al.* [42]	Random walk mobility model for wireless cellular networks based on Brownian motions.
1998	Broch *et al.* [27]	Random waypoint mobility model based on random-based mobility scheme.
1999	Liang *et al.* [46]	Guass-Markov mobility model based on Guass-Markov random process.
	Hong *et al.* [50]	Reference point group mobility model based on group mobility.
	Johansson *et al.* [53]	Obstacle mobility model based on reality that obstacles can be found.
2001	Royer *et al.* [45]	Random direction mobility model to reduce the population density in the central area.
	Bettstetter [47, 48]	Smooth random mobility model to improve the smoothness of changing MNs' velocity.
	Sánchez *et al.* [52]	Three mobility models based on group mobility, including the column mobility model, pursue model, the nomadic community mobility model.
2002	Tain *et al.* [55]	Graph-based mobility model based on a real map.
2005	Hui *et al.* [23]	Distribution of inter-contact times of human mobilities.
2007	Abdulla *et al.* [56]	Distribution of inter-contact times in the RWP and random direction mobility models.
2008	Abdulla *et al.* [57]	RWP mobility model with hotspots to improve the realistic mobility patterns of RWP model.
	Ekman *et al.* [37]	Working day movement model based on people's daily schedule.
2009	Lee *et al.* [36]	Self-similar least-action walk mobility model focusing on the statistical studies of human mobility behaviors.
	Mei *et al.* [34]	Small world in motion mobility model based on people's daily schedule and some statistical features of human mobility behaviors.

Then, a weight for the destination cell C in the context of MN A is evaluated as

$$w(C) = \alpha \cdot d(h_A, C) + (1 - \alpha) \cdot s(C) \tag{2.6}$$

where $d(h_A, C)$ is a decreasing function in terms of the power of the distance between MN A's home and the destination cell C, while $s(C)$ is the number of MNs that MN A meets in the destination cell C, since MN A arrives at cell C last time, $0 \leq \alpha \leq 1$ is an adjustable constant. Once a MN chooses its next destination, it moves towards the destination in a straight line with a speed depended on the distance between the starting point and the destination. For examples, as shown in Fig.2.17, assume all other cells have $w = 0$, the MN is likely to frequently visit the cells with $w = 4$ and $w = 5$. In summary, the mobility models considered so far in this section are listed in Table 2.1

2.4 Routing in Mobile Ad-hoc Networks (MANETs)

MANET is a distributed mobile network without central control, where MNs move and network structures are dynamic [58, 59]. Therefore, instead of routing through a central base station in cellular networks, or by some signal processing center, such as servers, in wired networks, in MANETs, individual MNs are responsible for routing and delivering messages through multiple hops. Since the topology of MANET is dynamic, the conventional routing protocols developed for wired networks cannot perform well. For this sake, a range of routing protocols have been proposed. In MANETs, the routing protocols can be categorized into two types [58, 59]: reactive routing protocols and proactive routing protocols. Reactive routing protocols perform route discovery only when there is a request. Hence, the routing process results in relatively lower network traffic and lower routing overhead but usually longer delay, than the proactive routing protocols. By contrast, proactive routing protocols actively find routes and store the routing information at all MNs in the same network. Therefore, they usually result in shorter delay, while consume more resources for routing tables, than the reactive routing protocols. Below we discuss several routing protocols introduced for MANETs, which include the destination-sequenced distance-vector routing protocol, dynamic source routing protocol, ad-hoc on-demand distance vector routing protocol, and optimized link state routing protocol.

2.4.1 Destination-Sequenced Distance-Vector Routing Protocol

In [60], Perkins and Bhagwat have proposed a routing protocol, namely, the destination-sequenced distance-vector (DSDV) routing protocol, for MANET. It represents a modified routing protocol of the conventional distance vector routing algorithm. However, in order to overcome the partial connectivity problem, the routing tables in the DSDV routing protocol is regularly updated. Specifically, each MN creates and maintains a routing table, which is updated in two ways: periodic updating and immediate updating. While the former is carried out regularly after a period of time, the latter updating is performed whenever there is a significant change of routing information. In this routing protocol, each MN has a routing table containing the entries of preferred neighbors acting as relays, which are the neighboring MNs having the lowest numbers of hops towards the DNs. Each entry in the routing table is tagged with a sequence number generated by the DN for a purpose of routing information updating. Since updating is frequently carried out, a large of overhead for routing is required [59]. Moreover, the DSDV routing algorithm has been developed on the basis of bidirectional links. Hence, routing loops may exist in the networks.

2.4.2 Dynamic Source Routing Protocol

The dynamic source routing (DSR) algorithm [61] is another routing protocol for MANETs, which do not require periodic routing table updating. In DSR protocol, each MN has a route cache containing a number of route records, where a route record provides the hop-by-hop route information from the MN to a DN, and a route discovery is performed when there are no matched route records in its cache. For the route descovery, a SN broadcasts a route request packet to its neighbor MNs. If one of the MNs matches its address with the DN or there is a route from the MN to the DN within its cache, a route reply packet containing the list of hops to the DN is created and returned to the SN. Otherwise, the MN adds its address to the route record and rebroadcasts the packet. In the DSR protocol, route discovery is also performed during route maintenance. Specifically, when an error occurs during a packet transmission using a cached route, the forward node (FN) found a broken link sends a route error message back to the original sender, i.e., the SN. Then, the SN activates the route discovery process, and replaces the damaged route with the new one. Then, the packet is re-transmitted using the new route.

The DSR protocol is efficient for operation in static topologies and networks containing low mobility MNs. However, it has not been designed for the networks having high topology dynamic [59]. In this case, route discovery and route maintenance may demand huge overhead. Moreover, the route discovery increases significantly the latency of packet transmission, and the maintenance in highly dynamic MANET, due to the time required to find new routes for the failed existing ones.

2.4.3 Ad-hoc On-demand Distance Vector Routing Protocol

The ad-hoc on-demand distance vector (AODV) routing protocol [62] has been developed based on a combination of the DSDV routing and DSR protocols. The same as the DSDV routing protocol, in AODV routing protocol, each MN stores only the next hop towards a DN. However, the on-demand concept used in the DSR protocol has been taken into account by the AODV routing protocol. In the AODV routing protocol, a route discovery is performed only when the MN has a packet to transmit. Similar to the DSR protocol, the sender broadcasts a route request packet to discover a route to the desired DN. Along the route, each MN also set up a reverse route for sending a feedback message. When a message sent by the SN reaches the DN or a MN containing a route record to the DN, a route reply message is generated and sent back to the SN using the same route. In order to maintain the symmetric links, a source sequence number is added to the header of the route request packet. In terms of the route maintenance, only the MNs taking the roles of senders, FNs and DNs along the active routes are considered. Whenever the sender moves, a route discovery procedure is re-initiated. If a MN in an active route changs its position, a special route reply packet is created to

inform the affected SNs. Furthermore, Hello message is introduced for route failure detection. The AODV routing protocol can have a quicker response to a link failure and consumes less resources for routing discovery and maintenance, in comparison to the DSDV routing protocol. However, the introduction of periodic link-status-update messages causes an increased network overhead [59]. Moreover, the same as the DSR protocol, the initial route discovery of the AODV routing protocol results in extra delay of message delivery.

2.4.4 Optimized Link State Routing Protocol

The above three routing protocols considered so far are all reactive routing protocols. By contrast, the optimized link state routing (OLSR) protocol [63] is a proactive routing protocol designed based on the link state algorithm. As the link state requires link reliability information, the OLSR algorithm performs flooding periodically in order to discover the network topology. The OLSR protocol minimizes the overhead introduced by the flooding processes by allowing only a number of selected MNs to operate the flooding procedures. Specifically, the so-called multipoint relays (MPRs) are selected to act as the gateways for broadcasting topology control (TC) messages to the entire network. In this way, the number of retransmissions in the same region of the network can be reduced. In terms of neighbor sensing, each MN periodically broadcasts a 'Hello' message. Relying on the employment of MPRs, the OLSR protocol is suitable for the large and dense networks, where communication traffic exists between a set of MNs in the same region. As it is a proactive routing protocol, routes are always available for data transmission, which minimizes the delay due to route discovery. However, the specifications of the OLSR protocol is not clear about how MPRs should be selected.

2.5 Routing in Delay Tolerant Networks (DTNs)

Delay tolerant networks (DTNs) belong to a sub-type of networks of MANETs, where MNs are likely to experience frequent and long disconnection and there might not be end-to-end connections between senders and their corresponding receivers [1, 2]. Hence, the traffic delivered should tolerate certain delay. As a subcategory of the MANET, DTNs inherit all the challenges of MANET, including for instances, dynamic network topology and unpredictable movement of MNs, energy consumption limitation, low and asymmetric bandwidth, high bit-error rate, and limited hardware resources [2]. Since the routing protocols designed in the context of MANETs are based on the assumption that there is a possible route from any SN to its DN, these routing algorithms are usually not efficient for operation in DTNs. Therefore, a number of routing protocols have been designed specifically for DTNs. In general, routing in DTNs may make use of the mobility of MNs, such

as, vehicles, animals, humans, etc., to act as relay for message delivery between a SN and its DN. However, different DTNs have different characteristics and experience different constraints, which are required to be dealt with correspondingly. In this section, we consider only the DTNs with humans as message carriers, which are classified as the opportunistic networks (OPNETs), in line with our investigation of mobile social networks (MSNs).

According to [4], OPNETs belong to a sub-class of the DTNs, where human beings are message carriers. In OPNETs, data transfer is depended on the movements of MNs, which occurs at the moments, when two MNs move into each other's signal transmission range. Since in OPNETs there are usually no fully connected paths from a SN to its DN, these moments of meetings between MNs are called connection opportunities. Explicitly, the routing algorithms designed for general MANETs and DTNs are not well suitable for delivering messages in OPNETs. Therefore, in literature [3, 5, 64], a number of routing algorithms have been developed specifically for the OPNETs. Generally, the routing algorithms for OPNETs are based on two approaches [2]: flooding and wait-and-forward. For the approach of flooding, a MN copies all its received messages to any MNs that it encounters. This approach is capable of maximizing the successful delivery ratio and minimizing the delivery delay. However, it may consume a huge amount of resources of the system, including bandwidth, storage, and energy. By contrast, the wait-and-forward approach only performs data transfer, when a SN encounters the DN. In this case, the data transfer process has the lowest resource usage, but may yield a very low delivery ratio and a very long delay. In order to improve the delivery performance of the above two approaches, recent routing techniques try to make a good trade-off among the resource usage, delay and delivery probability. Below, we discuss two representative routing algorithms for OPNETs, which are the Epidemic and the PRoPHET. These two algorithms have been addresses in many references [24, 65–73], and also extended for MSNs [7, 9, 10, 15, 16].

2.5.1 Epidemic Routing

Vahdat and Becker [3] have introduced the epidemic routing, in order to maximize the message delivery ratio and to minimize the message latency. Based on the assumption that a MN periodically and randomly encounters with other MNs, messages are distributed to any encountered MNs, until they reach their DNs. Since multiple copies of a message are used and scattered in the network, the probability of successful delivery of the epidemic routing is high and the delivery delay is low. In order to reduce the resource consumption, the number of messages that a MN carries on behalf of others can be limited by a maximum number. Moreover, the limit on the maximum number of hops may be used, and a message will be dropped, when the allowed maximum number of hops is reached, no matter whether it is delivered or not. Upon reaching the DN, a message

acknowledgement is returned. At this point, a MN is able to free its buffer, when it knows that the message has received by the DN.

2.5.2 Probability Routing Protocol using History of Encounters and Transitivity (PRoPHET)

The PRoPHET protocol [5] has been proposed based on the observation that, in reality, MNs do not move randomly, but instead, they move in patterns. By capturing the mobility behaviors of MNs, an encounter history can be built for aiding further calculations and routing decisions. The PRoPHET algorithm requires an initial phase called *warm up* to collect encounter history to build a database, which is updated whenever an encounter occurs. Then, based on the database, the delivery probabilities of different routes are determined. Specifically, computing the delivery probabilities can be divided into three cases. Firstly, when any two MNs meet, their summary vectors containing the probability information are exchanged. The MNs use this information to update their own delivery probability vectors as

$$P_{(a,b)} = P_{(a,b)_{old}} + (1 - P_{(a,b)_{old}}) \times P_{init} \tag{2.7}$$

where $P_{init} \in [0,1)$ is a constant for initialization, $P_{(a,b)_{old}}$ represents the old delivery probability from MN a to MN b, while $P_{(a,b)}$ represents the new one. Secondly, if a pair of MNs have not met each other for a while, the corresponding probability value is decreased in the form of

$$P_{(a,b)} = P_{(a,b)_{old}} \times \gamma^k \tag{2.8}$$

where γ^k is an *age constant* with $\gamma \in [0,1)$ and k is called the number of elapsed time units.

Finally, if MN b often meets MN a and MN c, it assumes that MN c is a potential FN between MN a and MN b. This means that there is a transitivity effect towards the probability value between MN a and MN b. With the aid of the transitivity, the probability value between MN a and MN c can be updated according to the formula

$$P_{(a,c)} = P_{(a,c)_{old}} + (1 - P_{(a,c)_{old}}) \times P_{a,b} \times P_{b,c} \times \beta \tag{2.9}$$

where the *scaling constant* $\beta \in [0,1]$ controls the scale of the transitivity impact.

In [64], the authors have made some changes to the above equations. Specifically, a small positive constant δ is added to the equation of Eq.(2.7), while Eq.(2.9) has also been changed to the value given by the largest one between an old delivery probability and a transitive probability.

After the modification, we have the formulas

$$P_{(a,b)} = P_{(a,b)_{old}} + (1 - \delta - P_{(a,b)_{old}}) \times P_{init} \tag{2.10}$$

$$P_{(a,c)} = \max(P_{(a,c)_{old}}, P_{a,b} \times P_{b,c} \times \beta) \tag{2.11}$$

where δ is small positive value, such as, 0.01.

In terms of message forwarding, when MN a meets a FN b, the PRoPHET makes the decision simply by comparing the pre-calculated probability of the two MNs to the DN. If MN a finds that MN b has a higher probability than itself to the DN, the message is then forwarded to MN b for further delivery. The PRoPHET protocol has the advantages of greatly reducing resource consumption, when comparing with the epidemic routing protocol. However, the PRoPHET protocol may yields lower delivery ratio and longer delivery delay than the epidemic routing protocol.

2.6 Routing in Mobile Social Networks (MSNs)

Mobile social networks (MSNs) belong to the family of the opportunistic networks of DTNs. They process routing by exploiting both the social behaviors of humans and the mobility patterns of MNs [74]. In reality, the movements of MNs in MSNs may be predicted, as people's mobility is controlled by many factors, such as, daily schedules, roles acted, communities joined as well as their hobbies. The research of Milgram [6] has demonstrated that the world is small in terms of people's social networks, and in this small world, people share mutual acquaintance with each other. In these social networks, messages can be delivered with the aid of FNs to the desired DNs though the acquaintance chains. Therefore, the theory of MSNs has been developed, in order to improve the successful delivery rate, decrease the latency of message delivery and reduce MNs' resource consumption for message delivery. Correspondingly, a range of routing algorithms have been proposed for MSNs. In this section, we review a number of routing algorithms for MSNs, including the LABEL, BUBBLE, SimBet, HiBop and the Social-Greedy algorithms.

2.6.1 LABEL Routing Protocol

On the top of the multiple-copy-multiple-hop flooding schemes, the LABEL [15] routing protocol has been proposed based on the fact that the mobilities of humans appear in patterns and are bound to affiliations, groups or communities. The main idea behind the LABEL is the fact that people usually stay inside their communities and occasionally visit the other communities. Therefore, people from the same community have more chances to meet each other than those from different communities. Many later works, including the SREP [29], social feature enhanced group-based

routing [30], SOSIM [31], ECSNR [32], and the M-dimension routing protocol [33], have also been implemented based on these observations. Specifically in the LABEL, MNs are divided into groups according to their labels (affiliations), and messages are finally delivered by the MNs having the same affiliations as the corresponding DNs. In the LABEL, routing requires a small amount of overhead in the process of group matching, and the algorithm is easy to implement. However, each MN needs to decide which group it belongs to. The performance of the LABEL protocol is a trade-off between the delivery ratio and the resource consumption. In contrast to the Epidemic algorithm of using multiple copies, the LABEL protocol is a single-copy transmission protocol. Hence, it demands significantly less resource consumption, but yields a smaller successful delivery ratio and a higher message latency than the epidemic algorithm.

2.6.2 BUBBLE Routing Protocol

The BUBBLE [16] routing protocol has been proposed by combining the affiliation concept of the LABEL protocol with the knowledge of MNs' centrality. Similar to the LABEL protocol, when operated under the BUBBLE protocol, individual MNs are assigned to the different groups of different affiliations, which are ranked according to their popularity. In the BUBBLE protocol, there are two ranking systems, namely global ranking and local ranking. A MN's global rank tells how many other MNs that the MN has seen, while a MN's local rank shows the number of the MNs met by the MN, which have the same affiliation as the MN. Apart from using the labeling principles as done in the LABEL protocol, in the BUBBLE protocol, a message sender also prefers to sending messages via higher rank (or more popular) MNs, since they have higher chances to meet other MNs. In detail, when operating under the BUBBLE protocol, a message is forwarded from the message sender, which is not necessary the SN generating the message, to another MN, if one of the following conditions is met.

1. Condition 1: The encountered MN is the DN that the message is destined to;
2. Condition 2: The message sender has an affiliation different from the DN but the encountered MN has the same affiliation as the DN;
3. Condition 3: Both message sender and encounter MN have an affiliation different from the DN, while the encountered MN has a higher global rank than the message sender;
4. Condition 4: Both message sender and encounter MN have the same affiliation as the DN, while the encountered MN has a higher local rank than the message sender.

From above we can see that a message is forwarded through a number of MNs, in which a later MN has a higher global rank than a previous one, until to a MN with the same affiliation as the

DN. Then, the local ranking system is activated, in the same manner, to deliver the message to its DN. Similar to the LABEL protocol, in the BUBBLE protocol, the information about the MNs' affiliations is assumed to be known by all the MNs. Furthermore, similar to PRoPHET, BUBBLE protocol requires initial period, in order to find and exchange the information about the surrounding MNs and to build the hierarchy ranking tree.

2.6.3 SimBet Routing Protocol

The SimBet routing protocol proposed in [7] uses MNs' centralities and social similarities, in order to reduce the resource consumption overhead of the Epidemic protocol, and to increase the delivery ratio of the PRoPHET protocol. In the SimBet protocol, the calculation of betweenness centrality can be explained with the aid of an $n \times n$ symmetric matrix, for example, shown as

$$A_{n_1} = \begin{array}{c} \\ n_1 \\ n_2 \\ n_3 \\ n_4 \\ n_5 \end{array} \begin{array}{c} \begin{array}{ccccc} n_1 & n_2 & n_3 & n_4 & n_5 \end{array} \\ \begin{bmatrix} 0 & 1 & 1 & 1 & 0 \\ 1 & 0 & 1 & 0 & 1 \\ 1 & 1 & 0 & 1 & 0 \\ 1 & 0 & 1 & 0 & 1 \\ 0 & 1 & 0 & 1 & 0 \end{bmatrix} \end{array} \tag{2.12}$$

which is called the adjacent matrix of MN 1. In Eq.(2.12), A_{ij} equals 1, if there is a contact between MN i and MN j, otherwise, it equals 0. Then, $A^2_{n_1} \cdot [A_1 - A_{n_1}]$ is calculated, here $A^2_{n_1} = A_{n_1} \cdot A_{n_1}$, A_1 is a matrix with the same size as A_{n_1} and all its entries are one, and $A^2_{n_1} \cdot [A_1 - A_{n_1}]$ denotes the element wise multiplication between the matrix $A^2_{n_1}$ and the matrix $A_1 - A_{n_1}$. Eq.(2.13) is the result of the above calculation, where we only concern the values that are non-zero and located above the diagonal. Based on Eq.(2.13), the betweenness of MN 1 is evaluated by the sum of reciprocols of the non-zero entries shown in Eq.(2.13), which is $\frac{1}{2} + \frac{1}{3} + \frac{1}{2} \approx 1.33$.

$$A^2_{n_1} \cdot [A_1 - A_{n_1}] = \begin{array}{c} \\ n_1 \\ n_2 \\ n_3 \\ n_4 \\ n_5 \end{array} \begin{array}{c} \begin{array}{ccccc} n_1 & n_2 & n_3 & n_4 & n_5 \end{array} \\ \begin{bmatrix} * & * & * & * & 2 \\ * & * & * & 3 & * \\ * & * & * & * & 2 \\ * & * & * & * & * \\ * & * & * & * & * \end{bmatrix} \end{array} \tag{2.13}$$

With the SimBet protocol, the similarity of a MN is determined by the number of common neighbours, which is simply given by the number of non-zero entries of the column in the matrix

A_{n_1} corresponding to the MN after ignoring the row of the target MN. For example, from Eq.(2.12), MN 1 has the similarity of two with MN 2, 3, 4 and 5, since all of them have the same number of non-zero entries of two, when ignoring the row n_1 in Eq.(2.12). The similarity value of two MNs can also be defined by the indirect contact through another MN. For example, let us assume that MN 1 and MN 6 share only one neighbor of MN 3. Then, the similarlity between MN 1 and MN 6 via indirect contact can be obtained by the number of non-zero entries in the column n_6, by ignoring the row n_1 in Eq.(2.14), which is equal to one.

$$A_{n_1} \begin{array}{c} \begin{matrix} n_6 \end{matrix} \\ \begin{bmatrix} 0 \\ 0 \\ 1 \\ 0 \\ 0 \end{bmatrix} \end{array} = \begin{array}{c} \\ \begin{matrix} n_1 \\ n_2 \\ n_3 \\ n_4 \\ n_5 \end{matrix} \end{array} \begin{array}{c} \begin{matrix} n_1 & n_2 & n_3 & n_4 & n_5 & n_6 \end{matrix} \\ \begin{bmatrix} 0 & 1 & 1 & 1 & 0 & 0 \\ 1 & 0 & 1 & 0 & 1 & 0 \\ 1 & 1 & 0 & 1 & 0 & 1 \\ 1 & 0 & 1 & 0 & 1 & 0 \\ 0 & 1 & 0 & 1 & 0 & 0 \end{bmatrix} \end{array} \tag{2.14}$$

Having obtained the similarity values of the MNs, then we can calculate the SimBet utility, which is a numeric indicator whether a message should be forwarded, from the formula

$$SimUtil_n(d) = \frac{Sim_n(d)}{Sim_n(d) + Sim_m(d)} \tag{2.15}$$

$$BetUtil_n = \frac{Bet_n}{Bet_n + Bet_m} \tag{2.16}$$

$$SimBetUtil_n(d) = \alpha SimUtil_n(d) + \beta BetUtil_n \tag{2.17}$$

where MN n is a sender attempting to forward messages to the DN d via FN m, $Sim_n(d)$ is the similarity between MN n and destination MN d calculated from Eq.(2.14), $SimUtil_n(d)$ is the SimBet's similarlity utility of MN n towards MN d, Bet_n is the betweeness of MN n computed from Eq.(2.13), $BetUtil_n$ is the SimBet's betweeness utility of MN n, α and β are controllable parameters satisfying $\alpha + \beta = 1$, and, finally, $SimBetUtil_n(d)$ is the SimBet utility of MN n towards MN d.

Routing in the SimBet protocol is operated as follows. Assume that MN A holding a message meets MN B, a 'Hello' message is first sent to MN B to verify if MN B is a new neighbour to MN A. Then, MN A transmits all the messages destined to MN B to MN B, while receiving from MN B a list of MNs that MN B has encountered. After MN A updates its adjacent matrix, the similarity and betweeness are calculated from the matrices in Eq.(2.14) and Eq.(2.13). Then, using the similarity and betweeness from both MN A and MN B, the similarity, betweeness, and SimBet utilities are updated based on Eq.(2.15), Eq.(2.16), and Eq.(2.17). Finally, MN A forwards the

messages destined to the DNs that MN B has higher SimBetUtil values to than MN A does.

In order to take the encounter history into account, in [8], the authors have improved the SimBet protocol to the SimBetAge protocol by introducing a parameter of 'freshness'. In this protocol, a weighted time-dependent graph is used to calculate the similarity and betweenness of each of the MNs. During the time between the encounters of two MNs, the freshness decreases exponentially, but it is dramatically enhanced upon their encounter again.

2.6.4 History-based Routing Protocol for Opportunistic Networks (HiBOp)

The HiBOp protocol [9] has been proposed by considering the behaviors when people meet. In general, during the first meeting of people, they usually introduce each other by exchanging their personal information, mutual acquaintance, personal interest, etc. The HiBOp protocol mimics these behaviors by exchanging the data stored as classes in the Identity Table (IT) for MNs, for example, as shown in Table 2.2, when they encounter during the neighbour discovery phases. The MNs' IT during the data exchange phase is defined as the current context (CC). Then, a history table is created for the delivery probability calculation. Based on these information, messages are forwarded to the MNs having higher delivery probabilities or having more similar information as the DN.

Table 2.2: Example of an Identity Table (IT)

Personal information	
Name	Pitiphol
Surname	Pholpabu
Email	pp1c12@ecs.soton.ac.uk
Phone	xxxxxxxxxxx
NID	xxxxxxxxxxxxx
Residence	
Street	Salisbury Street
City	Southampton
Work	
Street	University Road
City	Southampton
Organization	University of Southampton
Hobies	
Address	Building 18
City	Southampton
Association	University of Southampton
System information	
MAC-Bluetooth	xx:xx:xx:xx:xx:xx
MAC-802.11	xx:xx:xx:xx:xx:xx
IP-Address	xxx.xxx.xxx.xxx

Table 2.3: Example of a Repository Table

Aggr	Class	Carriers	C_C	C_H	C_R
Southampton	City	X, Y, Z	...	...	...

In the HiBOp protocol, the delivery probability of MNs is calculated in three main steps: 1) recording the counters to the repository tables; 2) calculating the attribute profile; and 3) calculating the delivery probability. Specifically, for the repository table, three counters are used, as shown in Table 2.3, which are named the continuity counter (C_C), heterogeneity counter (C_H), and redundancy counter (C_R). During an encounter, for each attribute of an encountered MN, the counter of C_C of the attribute is increased by one, if the encountered MN is found in the history table. By contrast, if the attribute is new to the history table, the attribute is then added to the history table along with an increment of the counter C_H. Finally, the counter C_R contains the number of times that the new attribute appears in the IT. Based on the contents of these counters, the delivery probability are calculated, as detailed in [9].

2.6.5 Social-Greedy Routing Protocol

Based on a number of social-related questions, in [10], the authors have proposed a so-called social-greedy routing algorithm based on the social distances between MNs measured by the Jaccard index described in [10]. Specifically, the social distance between MN u and MN v is calculated as

$$\sigma^i_{jaccard}(u,v) = \frac{\mid \Gamma^i_u \cap \Gamma^i_v \mid}{\mid \Gamma^i_u \cup \Gamma^i_v \mid} \tag{2.18}$$

$$dist(u,v) = \left(\sum_{i=1}^{d} \frac{\sigma^i_{jaccard}(u,v)}{d} \right)^{-1} \tag{2.19}$$

where Γ^i_u is the answer set of MN u for question i, and $\mid X \mid$ is the cardinality of a set X, while d is the total number of questions.

In literature, there are three versions of social-greedy algorithms proposed [10]. In the first version, a SN duplicates the message to three FNs, if the FNs are socially closer to the DN. The SN keeps the message until it encounters the DN or when the time-to-live (TTL) is expired. The second version is similar as the first one. A SN forwards a message to its first encountered FN, provided that the FN is closer to the DN than the SN. Then, when the SN further encounters FNs, the message is only sent to those that are socially closer to the DN than the previous ones. Finally, for the third version, the message is forwarded from one MN to another, provided that the latter one is socially closer to the former, until it arrives at the DN. Whenever a message is forwarded to a new MN, it is deleted from the old MN.

Table 2.4: Summary of routing protocols for MANETs, DTNs, and MSNs.

Year	Author	Contribution
1994	Perkins *et al.* [60]	MANETs: Destination-sequenced distance-vector (DSDV) routing protocol based on the distance-vector algorithm.
1996	Johnson *et al.* [61]	MANETs: Dynamic source routing (DSR) protocol purely based on the reactive routing approach.
1999	Perkins *et al.* [62]	MANETs: Ad-hoc on-demand distance vector (AODV) routing protocol based on the distance-vector algorithm and on-demand feature similar to the DSR protocol.
2000	Vahdat *et al.* [3]	DTNs: Epidemic routing protocol, for DTNs, based on the multiple-copy approach for maximizing delivery ratio and minimizing delay.
2003	Clausen *et al.* [63]	DTNs: Optimized link state routing (OLSR) protocol, which is a proactive routing protocol designed based on the link state algorithm.
	Lindgren *et al.* [5]	DTNs: Probability routing protocol using history of encounters and transitivity (PRoPHET), designed based on the single-copy approach to reduce resource consumption in comparison to the multiple-copy approaches.
2007	Hui *et al.* [15]	MSNs: LABEL routing protocol, using affliation for MN grouping.
	Daly *et al.* [7]	MSNs: SimBet routing protocol, with similarity and betweeness measured using matrix multiplication.
2008	Hui *et al.* [16]	MSNs: BUBBLE routing protocol, based on affliation feature of LABEL and ranking system for both global and local groups.
	Boldrin *et al.* [9]	MSNs: History-based routing protocol for opportunistic networks (HiBOp) exploiting personal information for closeness among MNs.
2009	BitschLink *et al.* [8]	MSNs: SimBetAge routing protocol, by intorducing an aging system to the SimBet routing protocol.
2010	Jahanbakhsh *et al.* [10]	Social-greedy routing protocol designed based on social distance measured by Jaccard index.

So far, a range of routing protocols have been overviewed in the content of the MANETs, DTNs, and MSNs. The routing protocols considered in this chapter are listed in Table 2.4 associated with their main characteristics.

2.7 Chapter Summary

In this chapter, we have first discussed the human's social behaviors that may affect human's mobility patterns. Then, a range of mobility models and routing protocols have been overviewed in the context of the MANETs, DTNs, OPNETs and MSNs. Then, advantages, disadvantages, as well as their main characteristics have been briefly discussed. In the following chapters, the per-

formance of some of the mobility models and routing protocols reviewed in this chapter will be studied and compared with the proposed ones. Specifically, in Chapter 3, we will propose mobility models based on the simplicity of the random waypoint (RWP) model. In later chapters, we will show the performance comparison between the proposed routing protocols and a number of existing protocols, including, Epidemic, PRoPHET, SimBet, LABEL, BUBBLE protocols. Since the Epidemic protocol is operated based on the multiple-copy approach, we will refer the Epidemic protocol as a benchmark, in terms of delivery ratio, end-to-end delay, and number of hops. While PRoPHET and SimBet protocols represent the routing protocols exploiting direct relationship between MNs, LABEL and BUBBLE represent those developed based on human social behavior of mutual community.

Chapter 3

Mobility Models for Mobile Social Networks

In chapter 2, we have reviewed a few of mobility models, which show that the mobility models in MSNs are scenario dependent. In the study of wireless communication systems, it is usually more practical to rely on the synthetic data generated by models derived from practice, since performance evaluation of communication schemes and protocols in real environments are costy and time consuming. However, the traditional mobility models are not capable of reflecting human mobility patterns and the generated traces do not allow for sensitivity analysis of the performance of the routing algorithm [35, 75]. In this chapter, we propose two new mobility models, namely the preferred-community-aware mobility (PCAM) model and the role playing mobility (RPM) model. Our performance study of the different routing protocols proposed in the following chapters will be mainly based on these mobility models. Specifically, our PCAM model is designed by taking into account of the simplicity and randomness of the random waypoint (RWP) mobility model, as well as the human social behavior of mutual preferred communities (PCs). By exploiting the fact that people usually have favorite places to visit, the PCAM model reflects more closely the humans social behaviors than the RWP mobility model, while still reserves the nature of randomness and simplicity of the RWP model. By contrast, our RPM model is designed by exploiting the fact that people's daily lives have community preference and depend on repeating daily schedules. The proposed mobility model can integrate people's roles, daily activities as well as occasional activities. Our studies demonstrate that PCAM model is capable of generating the mobility patterns that are closer to the real traces than the RWP model. In terms of the RPM model, it is capable of generating the mobility patterns that best fit the real traces recorded, when compared with the other two mobility models.

3.1 Introduction

In the study of MSNs, there are a number of challenges, including the design of well-performed routing protocols. Since the performance evaluation of routing protocols using real traces is costy and time consuming, it is more practical to rely on the synthetic data, generated by simulations based on the certain models abstracted from practice. Accordingly, a number of mobility models have been proposed, which can be used in development and performance evaluation of the routing protocols in MSNs. Until recent years, random waypoint (RWP) mobility model [27] has been the one of the most favorable mobility models used in academic researches, due to its simplicity in terms of implementation and optimization. However, the mobility traces generated from the RWP model is too random to reflect human's mobility behaviors. Furthermore, the RWP model makes MNs meet in the central areas with a higher probability than their meeting in the border areas [48, 76–78].

The researches in recent years show that human mobility has repeating patterns [23–25]. Furthermore, some researchers suggest that there are several factors affecting the mobility patterns, which include people who they know, popularity of the places they may choose to visit, and time of the day. Specifically, in human based MSNs, an acquaintance chain can be observed from human relationships [6]. People who know each other tend to meet more often. Accordingly, people may have connections through their mutual acquaintances. Furthermore, in [34, 35], it is suggested that people usually visit the places or communities which are close to their homes and where they have high chance to meet other people. When two or more people prefer to go to the same communities, it is likely that they often meet each other within their preferred communities. Finally, it is suggested that humans usually have repeating mobility patterns, which start and end in a day. During a day, if two or more people have a similar schedule, they are likely to meet often.

Recently, there are a number of mobility models having been proposed based on the above-mentioned observations. As some examples, the RWP model with hotspots [56] has been proposed as a simple community-based mobility model, in order to reflect the reality that MNs have a higher chance to visit the locations within communities than the locations outside of communities. The working day movement model [37] tries to mimic the mobility pattern of the humans with daily routines. Usually, in the morning, a MN moves from a starting location which is referred to as its home. Then, it moves and pauses within the areas of its workplace and favorite places. Finally, the MN travels back home in the evening. The self-similar-least-action walk (SLAW) mobility model [36] has been designed based on a number of statistical features of human mobilities. Based on the MNs' travel distances, data obtained from researches, it has been found that pause times, inter-contact times, and the distances between communities follow truncated power-law distributions. Furthermore, the small world in motion (SWIM) mobility model [34, 35] has been proposed

based on the human behaviors of PCs and daily routines.

In order to recreate the traces closely reflecting human's mobility patterns, in this chapter, we propose two mobility models for MSNs by exploiting human's preference factors, including human's social behaviors of mutual PCs and routine similarity. Our mobility models are referred to as the preferred-community-aware mobility (PCAM) model and role playing mobility (RPM) model. Specifically, the PCAM model is designed based on the simplicity of the RWP mobility model and the human social behaviors of mutual preferred communities. On the other hand, the RPM model is developed based on a more complicated approach, which is based on the human's social behaviors of mutual preferred communities, routine similarity, multiple roles and multiple daily activities by each of MNs, etc.

The rest of the chapter is organized as follows. Section 3.2 briefly review the existing works on human's social behaviors and human mobility behaviors. In Section 3.3, we describe the PCAM model, while the RPM model is addressed in Section 3.4. Finally, in Section 3.5, the comparison among the PCAM, RPM, RWP, and a number of real traces are provided.

3.2 Human Social Behaviors

In general, humans' mobilities are dependent on their duties, responsibilities, roles, preferences, etc. As some examples, teachers and students go to their schools on weekdays during term-time, a person usually has a number of preferred places for shopping foods and clothes. Humans' mobilities are also influenced by other factors, such as, preferences or behaviors of other humans and geographic restriction. For example, some people tend to go to the places where they are popular among others, some people may prefer to traveling in groups of well organized, while some others may prefer more independence when on traveling, cars and pedestrians have to move along streets and walking trails. In mobile ad-hoc networks (MANETs), various mobility models have been proposed in order to reflect the above-mentioned factors [34–37, 56, 79].

In order to understand human's mobility behavior, researchers have now focused more on the human's social behaviors. Recently, the research results, such as [23–25], demonstrate that human's mobilities present repeating patterns. Normally, in people's daily lives, there are a number of factors affecting their mobility patterns, which include the people who they know, referred to as acquaintances, popularity of the places they may choose to visit, time of day or year, etc. Firstly, in terms of the acquaintances, Milgram [6] has shown that an acquaintance chain can be formed from the relationships in a group of people who may not know everyone in the group. The research reveals that an acquaintance chain can be created with the length between any two people spanning two to ten intermediate acquaintances. Secondly, considering the influence of places' popularity

on human's mobility, a person usually has a collection of places, where she or he refers to visit. These kind of places are called as the preferred communities (PCs). For examples, most people mainly stay at home or their working places, people usually have their favorite places to hang out alone or enjoy with friends. In [80], the studies have demonstrated that people have their favorite communities and usually visit their favorite communities, in addition to staying at home. Furthermore, the research results show that up to 90 percent of the participants' mobilities can be grouped into seventeen patterns, and one participant usually moves back and forth between one to six communities. Apart from an individual's preferences, the popularity of a community also has strong influence on the individual's decision to visit the community. In [34, 35], the authors have suggested that people often visit the places where they have higher chances to meet people. Moreover, the distances between the places and people's homes also affect people's decisions about whether they are going to visit the places. In general, people prefer to visit the places close to their homes. Finally, the studies show that human's mobilities usually have the repeating patterns that start and end in a day. The places to start and end their daily patterns are usually their homes. In references, there are a number of mobility models designed based on these observations, including those proposed in [34–37].

Furthermore, recent researches have identified several statistical elements reflecting the characteristics of human's mobility behaviors. The authors in [36] have claimed that there are four main features in human mobilities, which include the truncated power-law flights and pause-times, heterogeneously bounded mobility areas, dichotomy of inter-contact times, and the fractal waypoints. Firstly, human traces show that both the flights and pause times obey the truncated power-law distribution. More specifically, in [19–21], the authors have found that human's traveling distances, referred to as flights, are best described by a truncated power-law distribution. Later in [21, 22], the authors have demonstrated that the periods of time that people spend within individual places, referred to as pause times, follow a decayed power-law distribution. Secondly, human's mobilities are bounded to some areas. In [20], human's trajectories have been investigated based on the real traces obtained via tracking of mobile phone users. The traces reveal a high degree of temporal and spatial characteristics that people repeatedly move and stop within the same areas. This implies that individual mobile phone users have different mobility areas of different sizes. Furthermore, the complementary cumulative distribution function (CCDF) of the time between two consecutive meetings of a pair of MNs, which is referred to as the inter-contact time, is similar to a truncated power-law distribution during the first half of a day and, afterwards, to an exponential distribution [23–25]. The authors in [25] have referred to these characteristic as the dichotomy of inter-contact times. Finally, the authors in [26] have suggested that the gaps between the waypoints where people often stop by follow a power-law distribution, which is similar to the concept of the fractal points, as defined in [81].

3.3 Preferred-Community-Aware Mobility Model

Until recent years, the RWP model [27] has been one of the most common used in routing protocol development due to its simplicity in terms of implementation and configuration. However, the traces generated by RWP model is too random and do not well reflect humans' repeating mobility patterns, as discussed in the previous section. In this section, we propose a mobility model, namely the preferred-community-aware mobility (PCAM) model, for modeling the social behaviors of MNs. By considering people's movement behaviors, our mobility model is designed by exploiting the advantages of the random mobility model, RWP mobility model [27], and the community-based mobility model [5, 28]. On top of the simplicity inherited from the RWP model, the PCAM model is also capable of reflecting the human social behavior of preferred communities (PCs), where people usually have different preference for the places they would like to go.

In PCAM model, we assume that the mobility model is operated in an area of $w \times l$ square units. Within this area, reflecting MNs' potential PCs, N communities of each covering an area of $w_c \times l_c$ square units are created where $w_c << w$ and $l_c << l$. Some communities may overlap with each other. Then, a number of MNs randomly distributed inside the areas covered by the communities, and each MN is assigned a number of PCs, as the result of the fact that one MN may belong to one or several communities with certain probabilities. Furthermore, from each MN to its PCs, corresponding probabilities are assigned, which represent the levels of preference towards the PCs.

As an example, Fig.3.1 shows the mobility behavior of MN 1. In this MSN, there are N communities, expressed as $C_1, C_2, \ldots, C_N$, respectively. We assume that MN 1 is initially assigned to community C_1 and it travels to its PCs C_1, C_2 and C_3 with the probabilities of P_1, P_2 and P_3, respectively. According to the experiments carried out in [80], we assume that MN 1 has only a probability of 0.1 traveling to the other unpredictable communities, $C_4, C_5, \ldots, C_N$. Therefore, MN 1 has a total probability of $P_1 + P_2 + P_3 = 0.9$ to be associated with the communities C_1, C_2 and C_3.

In addition to the randomness as above-described, our mobility model also inherits the characteristics of the RWP mobility model [27]. In our MSN, a MN first randomly chooses a point within a selected community, which represents its next destination. It then travels towards that point with a speed randomly chosen between 0 and V_{max}. After arrival at the destination, the MN pauses for a fixed time t_{pause}. Then, the above process is repeated until one simulation session is completed.

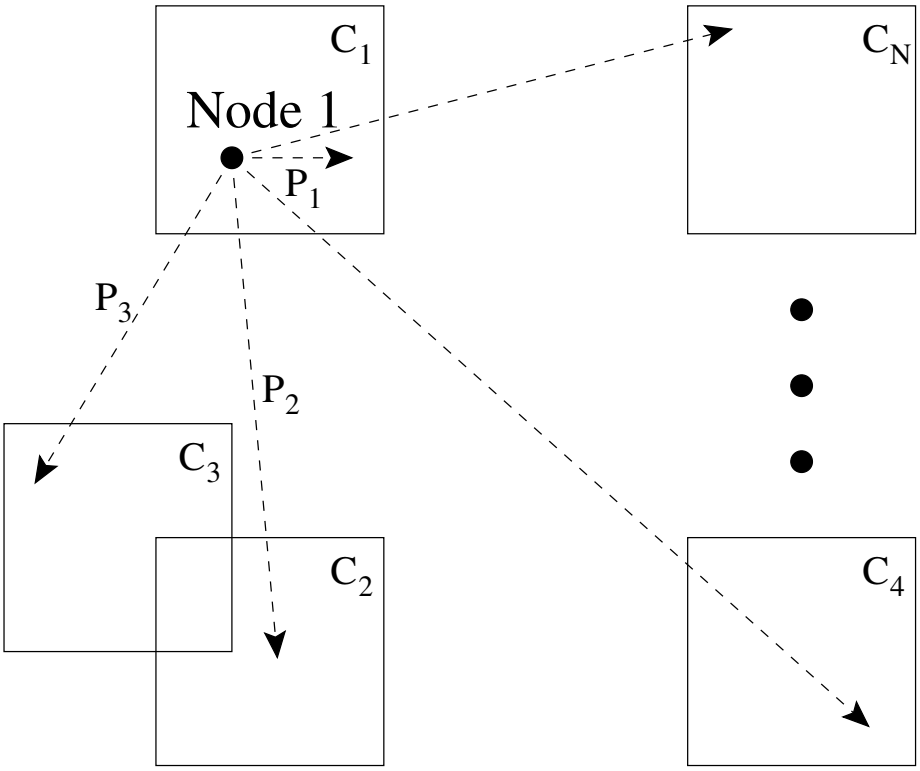

Figure 3.1: An example illustrating the mobility behavior of a MN in our PCAM model.

3.4 Role Playing Mobility Model

In this section, we describe the RWP model, which shares some similarity with the working day movement model [37] for delay tolerant networks (DTNs). Our mobility model is designed based on the intuition that every person usually has several roles in her or his social life. Typically, an individual person has one primary role and several secondary roles. Here, the primary roles are the ones of each containing one or more primary activities that the person usually does on the daily basis. For example, the duty or role of a student is going school on weekdays. On the contrary, the secondary roles of a person are usually referred to those secondly activities that the person prefer to do in her or his leisure time. For example, some people like to go shopping after their jobs, some students like to hang out together at their favorite clubs during evening, while some others prefer watching movies, playing games, doing sports, etc. Therefore, mobilities in MSNs are dependent on people's roles.

Although it is not a requirement, similar to the PCAM mobility model, we assume that our RPM is operated within a rectangular area of $w \times l$ square units. Within the considered area, there are N communities of each covering an area of $w_c \times l_c$ square units, and some communities may overlap with each other. At first, we assume that there are N_{MN} MNs distributed inside the areas

covered by the N communities. The starting location of every MN is registered as the MN's home. In the RPM model, each MN is assigned a number of roles, which may include one primary role and several secondary roles. Furthermore, each role contains a number of activities, and each activity is characterized by a community, where the activity occurs and a time period that the activity lasts. However, the time periods of primary and secondary activities have some different characteristics. In primary activities, a time period is defined by the arrival time, t_{arrive}, and departure time, t_{depart}. This is because the fact that people usually start and end their primary activities, such as, of work or having schools, at nearly the same times every day. By contrast, the occurrences of secondary activities may be very random during people's free times. Furthermore, people may have different levels of preference towards the secondary activities. For example, it is unlikely that a person always goes to the same restaurant. Considering all the above mentioned, in our RPM model, a secondary activity is characterized by the following two factors, a preference level, L_{prefer}, and a pause time, t_{pause}. Here, the preference level is reflected by the activity's occurrence frequency, while the pause time represents the time spent on the activity.

In addition to the above-described role-dependent social behavior, our RPM model also takes into account the point-to-point mobility characteristics as that considered in the RWP mobility model [27] and the working day movement model [37]. Specifically, in the RPM, there are two types of mobilities, which are the high-speed mobilities, generated by people traveling, such as, by cars, buses, bikes, etc., and the low-speed mobilities, generated by people on walking for example. Typically, high-speed mobilities represent the cross-community mobilities occurring when people travel between communities. By contrast, low-speed mobilities are usually the inside-community mobilities occurring when people walk within the same communities.

In our RPM model, the mobility characteristics of MNs are divided into three phases. In the first phase, at the start, a MN is stationary at its starting location within its home community, until a time when it is allowed to travel to its next destination. Then, it randomly chooses a position within the community where it carries out its primary activity, which gives its next destination and is referred to as the 'workplace' for convenience of description. Then, a speed is chosen between V_{min} and V_{max} uniformly, which represents the speed of its cross-community traveling from its home to its workplace. With the above information, the traveling distance between its home and its workplace as well as the traveling time required can be calculated. From these, the MN knows its primary activity's arrival time t_{arrive}. Furthermore, based on the traveling time and the activity's arrival time, the MN also knows when it should start its traveling, in order to arrive at its workplace at the primary activity's arrival time. The second phase starts, when the MN arrives at its workplace and, in this phase, the MN is characterized by the inside-community mobilities. Specifically, after arrival at the workplace, the MN pauses for a random period of time. Then, another position within the same community is chosen, which represents the MN's next destination. Then, the MN moves

to the next location with a walking speed V_{walk}. The above inside-community mobility process is repeated, until the departure time t_{depart}, as stated in the context of the primary activity. In the third phase, the secondary roles may be activated at the end of the primary activities. In detail, at the departure time t_{depart} of the primary activities, a MN may choose to go home with a probability of P_{home}, or activate a secondary role with a probability of $1 - P_{home}$. If a secondary role is activated, the MN randomly selects an activity from a set of them, based on the occurrence probabilities reflected by the preference levels L_{prefer} of the secondary activities. Then, the MN randomly chooses a location within the community where the secondary activity to be carried out, and travels toward the chosen location following the cross-community mobility by a speed randomly chosen between V_{min} and V_{max}. After arriving at the destination, the MN pauses for t_{pause}. Then, it may randomly choose to go home or activate another secondary activity. Note that, in our model, a MN is only allowed to carry out at most N_{act} secondary activities before it goes home. Finally, when the MN chooses to go home or after it has participated in N_{act} activities, the MN travels back home by following the cross-community mobility with a speed randomly chosen between V_{min} and V_{max}. After the arrival, it stays at home until the departure time on the next day. Then, the above-described mobility process is repeated until one simulation session is completed. Note that, the next destination of a MN may be within the current community or in a new community. In other words, a MN has a chance to move within its current community, which is depended on the probabilities of the PCs.

As an example, Fig.3.2 demonstrates a one-day mobilities of MN 1. In this MSN, we assume that there are N communities, expressed as C_1, C_2, ..., C_n, ..., C_N. MN 1 is initially at community C_1, representing its home community. We assume that MN 1 has the primary activity, which occurs within the community C_2. Hence, when it arrives at the first destination at t_{arrive} in C_2, it wanders around the community C_2 until t_{depart}. Then, it chooses either to go home or move to another community according to certain probabilities. Let us assume that the maximum number of secondary activities that can be carried out before going home is $N_{act} = 2$. Then, MN 1 may have three possible actions, resulting in the following three possible routes:

1. Route 1: MN 1 goes home directly from C_2;
2. Route 2: MN 1 first travels to another community and, then, goes home;
3. Route 3: MN 1 first travels to two other communities and, then, goes home.

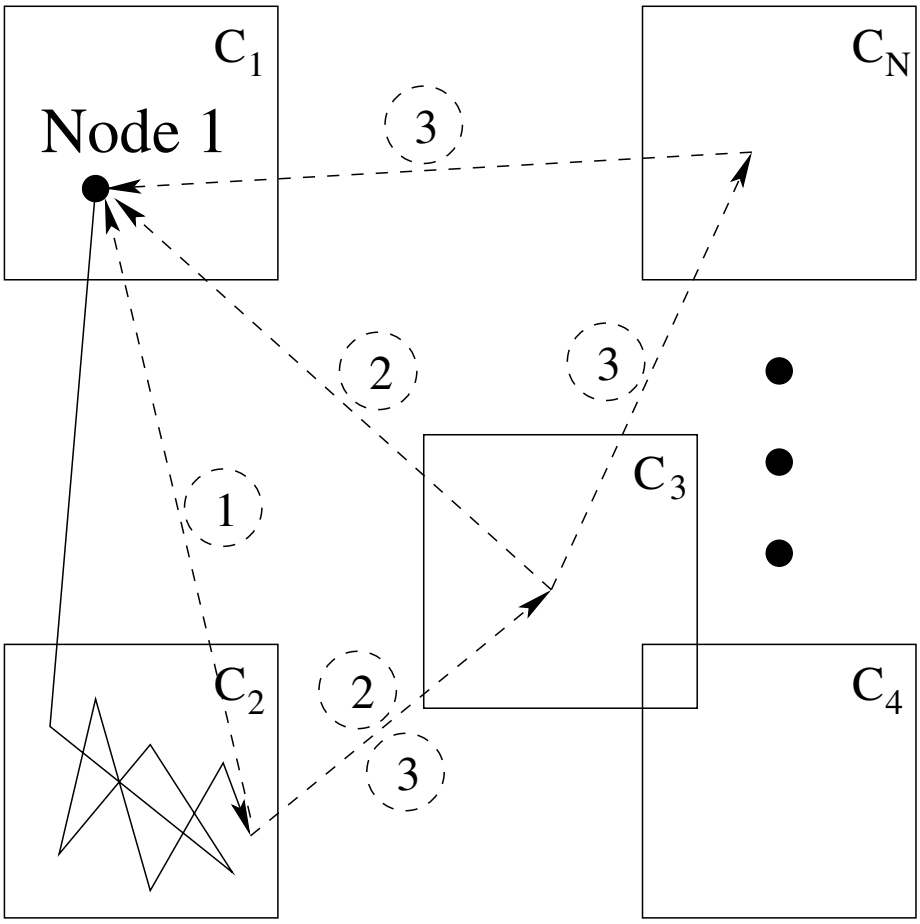

Figure 3.2: An example illustrating the mobility behavior of a MN in our RPM model.

3.5 Comparison of the PCAM, RPM, and RWP Models

In this section, we compare the mobility traces generated by our RPM mobility model with that generated by the RWP and PCAM models, and four real traces. In the following chapters, we will investigate the performance of the SCPR, PRoPHET, SimBet, LABEL, BUBBLE, and Epidemic routing protocols, when they are operated with the PCAM or RPM model.

In our simulations, we consider a MSN with the coverage of 1000×1000 square meters (m^2). Within this area, there are 15 communities of each covering an area of 100×100 m^2. At the beginning of simulation, we assume that these 15 communities are randomly distributed in the considered area, and some communities may overlap with each other. In the considered MSN, we assume that there are 50 MNs, which are firstly randomly distributed inside the areas covered by the 15 communities. The original location of each MN is registered as its home. Then, each MN is assigned a primary role and a random number of secondary roles. In this experiment, we assign for each primary role one primary activity, which contains a random community ID, random

arrival time $t_{arrive} \in [7,9]$ AM, and random departure time $t_{depart} \in [4,6]$ PM. By contrast, a secondary role contains a random number of activities. Each secondary activity consists of a random community ID, a random preference level $L_{prefer} \in [1-10]$, and random pause time $t_{pause} \in [0.5,3]$ hours. In terms of the point-to-point mobility, we set the maximum and minimum speeds for the cross-community mobilities to $V_{max} = 20\ m/s$ and $V_{min} = 1\ m/s$, respectively, while the speed for the inside-community mobilities is set to $V_{walk} = 1.4\ m/s$, which is people's average walking speed. Furthermore, we set the probability of going home at the end of the primary activity to $P_{home} = 0.5$. The maximum number of secondary activities per MN per day is set to $N_{act} = 2$.

For operations of the routing protocols, we assume that MNs repeatedly check their neighbors within a range of $r = 30$ meters, and an interval for update is $t_{interval} = 60$ seconds. The simulation session lasts $T = 15$ days. Furthermore, for the RWP and PCAM models, we use the same settings as that described in [27] and [79], respectively. In detail, the parameters for the RPM model are summarized in Table 3.1.

Table 3.1: Summary of the parameters used for simulations.

Parameter	Value	Unit
Simulation area	1000×1000	m^2
Community area	100×100	m^2
No of communities	15	*communities*
No of MNs	50	*MNs*
V_{max}	20	m/s
V_{min}	1	m/s
V_{walk}	1.4	m/s
t_{arrive}	7-9 AM	-
t_{depart}	4-6 PM	-
L_{prefer}	1-10	-
t_{pause}	30-180	*minutes*
P_{home}	0.5	-
N_{act}	2	*activities*
r	30	m
$t_{interval}$	60	s
T	15	*days*

Figs. 3.3, 3.4, and 3.5 show the mobility traces generated by the RWP, PCAM and the RPM models. While, in the RWP model, a MN moves over the entire area, a MN in the PCAM and RPM models only moves between and inside communities. The traces generated by the RWP model are usually unrealistic, as traces cover the whole area and MNs move towards the central area. As shown in Fig. 3.3, MNs have a much higher probability to stay in the central area than that to move around the edges. By contrast, the PCAM model generates traces based on the preferred community approach, which assumes that a MN normally travels towards communities or popular areas, such as

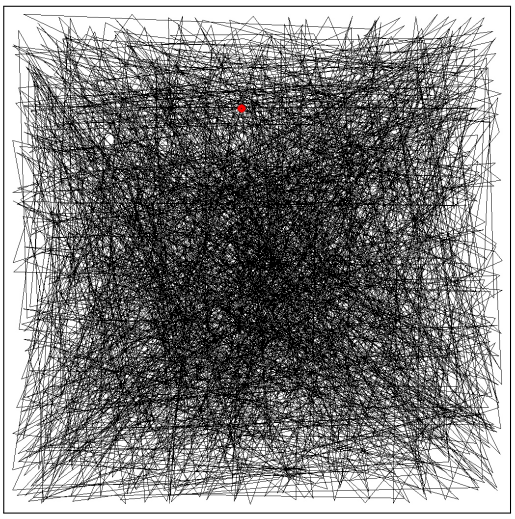

Figure 3.3: Mobility traces generated by the RWP model for one MN in 15 days.

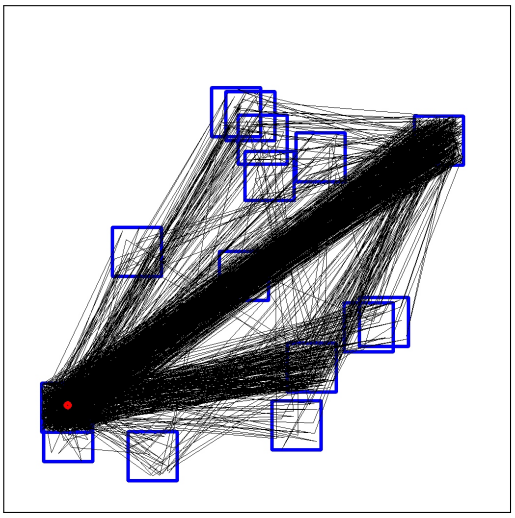

Figure 3.4: Mobility traces generated by the PCAM model for one MN in 15 days.

schools, workplaces, shopping centers, etc. As a result, as shown in Fig. 3.4, there are very dense traces between communities, especially, between those popular communities. Therefore, under the PCAM model, two MNs usually have a high chance to meet, when they prefer to the same communities. In terms of the RPM model, as shown in Fig. 3.5, the traces show the characteristic of preferred communities, similar to the PCAM model. However, for the same length of simulation time, the trace density between two communities is dramatically lower than that shown in Fig. 3.4 for the PCAM model. This is because, according to their roles in the RPM model, people usually carry out their primary activities in the morning and travel back homes in the evening. Hence, the probability of traveling between communities is low, when in comparison to that happened under the PCAM model.

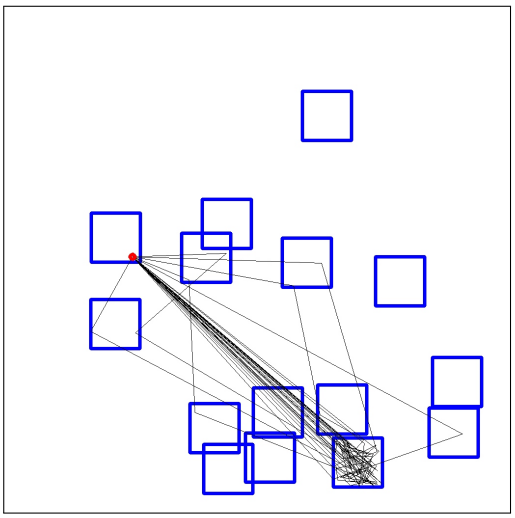

Figure 3.5: Mobility traces generated by the RPM model for one MN in 15 days.

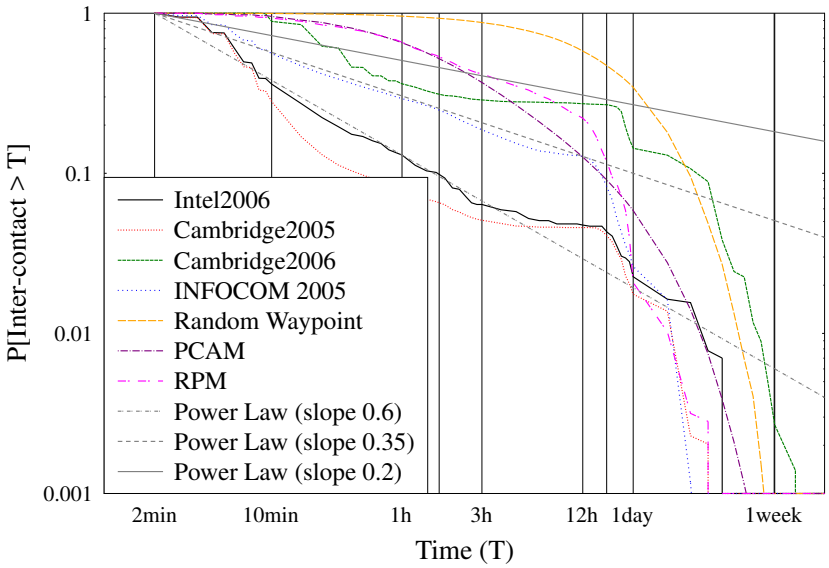

Figure 3.6: CCDF of the inter-contact time in the RPM, RWP and PCAM models, as well as that of four real traces.

Fig. 3.6 shows the CCDFs of the inter-contact time (P[Inter-contact ¿ T]) of the MNs operated in the PCAM, RPM and RWP models. Also in the same figure, the CCDFs of four real traces are provided, which are the traces of Intel 2006, Cambridge 2005 and InfoCom 2005 from Cambridge Huggle project [38] and Cambridge 2006 from UPMC Data project [39] on a log-log scale. As seen in the figure, the real traces during the first twelve hours can be best fitted by the power law distributions associated with the corresponding slopes. Specifically, the Intel 2006 and Cambridge 2005 data sets fit the power law distribution with a slope of 0.6, while the data sets of InfoCom 2005 and Cambridge 2006 are best fitted by the power law distributions with the slopes of 0.35

and 0.2, respectively. After the first twelve hours, all the CCDFs have an exponential cut-off, which follow the observations in [23–25]. As shown in Fig. 3.6, the CCDFs of the inter-contact time in the PCAM and RWP models lack of the power law distribution characteristic, but follow the exponential distributions on the same log-log scales over all the time period. By contrast, for the RPM model, the CCDF of the inter-contact time first appears in a power law distribution with a slope of 0.2 and, then, changes to appear like an exponential distribution. From the above comparison, we are implied that the RPM mobility model is capable of providing the mobility patterns that are close to that in practice.

3.6 Chapter Summary and Conclusions

In this chapter, we have proposed the PCAM and RPM mobility models for MSNs, in order to jointly reflect people's social characteristics, including randomness, waypoint effect, mutual-community-based relationship, repeated daily routines, as so on. The PCAM model is designed based on the RWP model by taking into account the mutual-community-based relationship, while the RPM model are designed by considering individuals' roles and activities, both daily activities and occasional activities are integrated into the mobility model. Our studies and simulation results demonstrate that the mobility patterns generated by the PCAM model are closer to the real traces when comparing to the RWP mobility model, while the RPM mobility model fits the best with the real traces than the RWP and PCAM mobility models. In the RPM mobility model, the CCDF of the inter-contact time shows the power law distribution characteristic during the first 12 hours before truncating, which is similar to the characteristics of real mobility traces. In chapters 4 and 5, the performance of a range of routing algorithms for MSNs will be investigates in the content of the PCAM or RPM models.

Chapter 4

Social Contact Probability Assisted Routing Protocol

In Section 2.4, 2.5, and 2.6 of Chapter 2, we have reviewed a range of routing protocols for MSNs, including the Epidemic, PRoPHET, SimBet, LABEL, and BUBBLE protocols. A typical characteristic of these protocols is that they are mainly motivated to maximize the delivery ratio without much concern about the resource consumption. In this chapter, we concern the problem of dynamic routing in mobile social networks (MSNs). By exploiting the social characteristics of mobile nodes (MNs) in MSNs along with the fact that people's daily lives have community preferences, a routing protocol, referred to as the social contact probability assisted routing (SCPR) protocol, is proposed. The proposed protocol is capable of efficiently integrating the merits of high delivery ratio, low delivery latency and low resource consumption of the Epidemic, PRoPHET, SimBet, LABEL and BUBBLE protocols for MSNs, while circumventing their respective shortcomings. In our routing protocol, approaches for measuring encounter probability and people's community preference are proposed, both direct meetings in one community and indirect contacts via different communities are considered. The performance of the proposed protocol and that of the five other routing protocols as above-mentioned are investigated and compared in the context of the more realistic PCAM mobility model, which as mentioned in Chapter 3, jointly considers people's social characteristics, including randomness, Waypoint effect and mutual-community-based relationship. Our studies and performance results show that the proposed protocol is capable of attaining a good trade-off between the average delay of information delivery and the cost of resources for operation of the protocol.

4.1 Introduction

Nowadays, mobile devices with short-range wireless functionalities, such as, IEEE 802.11, Bluetooth, or/and other radio-based solutions, have been integrated into people's daily lives. These devices provide the cheap infrastructureless networks that may provide connectivities among mobile users or mobile nodes (MNs). In these networks, a typical scenario is that there are sometimes insufficient MNs that can be discovered to form the physically connected paths from some source nodes (SNs) to their required destination nodes (DNs). In this case, the existing routing protocols depending on physically connected paths fail to work. As a result, some sub-category networks have been identified, which include, such as, delay tolerant networks (DTNs), opportunistic networks (OPNETs) and mobile social networks (MSNs). Specifically, MSNs inherit the characteristics of long communication delay and short opportunistic data transmission, respectively, from DTNs and OPNETs. However, MSNs employ the capability to make use of the mobility behaviors of mobile device carriers as well as of their relationship, in order to improve routing performance. In literature, there are a range of routing protocols specifically dedicated to MSNs, which include the LABEL [15], BUBBLE [16], SimBet [7], HiBop [9], Social-Greedy Routing [10], etc.

In the context of the route discovery in MSNs, while direct connections between SNs and their respective DNs are the straightforward routes, there are indirect multi-hop routes which connect SNs and their DNs via other MNs. With the aid of this type of indirect routes, a higher information delivery ratio and a shorter message delivery time than that achieved by using only direct contacts can usually be attained. Against the background, in this chapter, we first analyze the mobility behaviors of humans and quantify some of the important social aspects, including acquaintances, favorite places and time periods, etc., that we believe have strong impact on route discovery in MSNs. Similar to [30, 82, 83], we first detect MNs' mobility patterns based on their encounter history. Then, the lists of favorite communities of individual MNs are identified. In terms of the encounter history of MNs, three social factors affecting the social contact probability (SCP) of MNs are introduced and investigated, so as to make use of them to explain the possible acquaintance relationship between MNs. In detail, first, we consider the encounter frequency of any two MNs. Then, the regularity of encounters of MNs is analyzed and quantified. Finally, the aging effect of encounters is addressed. Moreover, we investigate the relationship between MNs in terms of the social behaviors presented via favorite places, referred to as the preferred communities (PCs), as well as the time spent with individual communities. Specifically, by investigating the characteristics of the mobility patterns considering people's community preferences, the lists of individual's PCs are collected and their degrees of preference are quantified. Upon considering the impacts of the above-mentioned social factors, in this chapter, we then propose a routing protocol, namely, the Social Contact Probability assisted Routing (SCPR) protocol. Furthermore, we investigate the

performance of our SCPR protocol and compare it with some well-known routing protocols for MSNs, such as, the Epidemic [3], PRoPHET [5], SimBet [7], LABEL [15], BUBBLE [16], etc., protocols, when assuming that they are operated in association with the PCAM mobility model proposed in Chapter 3. Our studies and performance results in this chapter show that the SCPR protocol is capable of integrating the merits of the Epidemic, PRoPHET, SimBet, LABEL and the BUBBLE protocols, while simultaneously circumventing their shortcomings. It is able to attain a good trade-off between the successful delivery ratio, the average delay of information delivery, and the cost of resources for operation of the protocol.

The remainder of this chapter is organized as follows. In Section 4.2, we analyze the social characteristics and quantify the encounter probability and people's community preferences. Section 4.3 states the operation details of the SCPR. Finally, Section 4.4 demonstrates and explains the performance results.

4.2 Analysis of Social Characteristics of Mobile Nodes

In this section, we analyze and quantify the social effects of MNs in MSNs, in order to exploit them in the routing algorithm to be addressed in Section 4.3. We measure the strength of the social relationship between two MNs by the SCP. This section discusses two types of social relationships, including the explicit relationship between two MNs, which is called as the node-linked (NL) relationship, and the implicit relationship between two MNs obtained through their mutual PCs, which we refer to as the community-linked (CL) relationship for convenience.

4.2.1 Node-Linked Relationship

The NL relationship describes the social relationship of two MNs via their direct meeting behavior. Depending on the encounter history, a number of social aspects, including the number of contacts, transitivity property of contacts and inter-contact time, are considered. First, let us consider the scenario where two MNs directly meet.

4.2.1.1 Direct Connection

In order to exploit the social relationship between any two meeting MNs without invoking too much extra computation, we focus on the egocentric encounter history, which does not depend on the global knowledge of the entire system. As a result, we can identify three social factors, which substantially affect the probability of information delivery. These social factors are the *frequency of encounters*, *regularity of encounters*, and the *duration between two adjacent encounters*, which is

also the inter-contact time. In principle, while a higher encounter frequency implies a better chance of future meeting, a higher regularity of encounters makes the prediction about future meetings more accurate. Below we explore the first two factors and explain how to invoke them in our routing algorithm to be addressed in Section 4.3. The third factor will be considered in association with the aging process in Section 4.2.1.3.

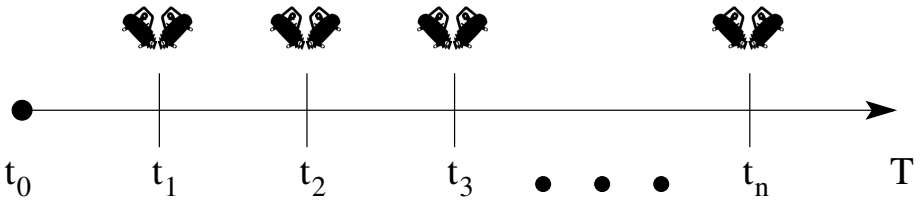

Figure 4.1: A time line demonstrating the encounter history of two MNs.

Based on the fact that mobile devices have the neighbor discovery mechanism, we use the intervals between two consecutive activations of the mechanism to measure the encounter probability. As shown in Fig.4.1, let two reference MNs are observed from $t = 0$ until $t = T$ (now). Let n denote the number of encounters between the two reference MNs within $(0, T)$. Let N_{max} be the number of times that the discovery mechanism is activated within $(0, T)$, which represents the maximum number of encounters of two MNs. Then, the encounter probability can be measured as

$$P_F \approx \frac{n}{N_{max}} \tag{4.1}$$

which becomes more declared as T increases. Let $t_{interval}$ represent the period that the neighbor discovery processes activate. Then, we have $N_{max} = T/t_{interval}$ and, hence,

$$P_F = \frac{n \times t_{interval}}{T} \tag{4.2}$$

In terms of the regularity of encounters, explicitly, the frequency of encounters as above considered is one of the elements. However, the frequency of encounters may not fully embrace the regularity of encounters. Let us explain this by considering two scenarios, both of which have the same encounter probability when measured by Eq.(4.2). In the first scenario, we assume that the interval $\triangle t_i = t_i - t_{i-1}$, $i = 1, 2, \ldots, n$, is a constant. By contrast, in the second scenario, we assume that the interval is a random variable with a mean of $\overline{\Delta t}$ and a standard deviation of $S_{\triangle t}$. Then, in practice, the first scenario is preferred for information delivery, as it yields a smaller (upto half) average waiting time than the second scenario [84], or it has a higher regularity than the second scenario.

As the frequency of encounters has been considered as a separate (first) factor given in Eq. (4.2),

in this chapter, the regularity of encounters is measured by the formula

$$R = \frac{\overline{\Delta t}}{\overline{\Delta t} + S_{\triangle t}} \tag{4.3}$$

where, when given $\triangle t_i = t_i - t_{i-1}$, $i \in \{1, 2, ..., n\}$, $\overline{\Delta t}$ and $S_{\triangle t}$ are evaluated from the formulas of

$$\overline{\Delta t} \approx \frac{1}{n} \sum_{i=1}^{n} \Delta t_i \tag{4.4}$$

$$S_{\triangle t} \approx \sqrt{\frac{1}{n-1} \sum_{i=1}^{n} (\Delta t_i - \overline{\Delta t})^2} \tag{4.5}$$

Eq.(4.3) shows that the maximum regularity is one, which occurs when Δt_i is a constant. The regularity of encounters decreases, when the standard deviation of Eq.(4.5) increases.

When taking into account of both the frequency and the regularity of encounters, the probability of direct contact between two MNs A and B can be defined as

$$P_{d(A,B)} = P_F \times R \tag{4.6}$$

where P_F and R are given by Eq.(4.2) and Eq.(4.3), respectively. Note that, at the start of the process when there are no encounter records, both the encounter probability P_F and the regularity factor R are initialized to zero.

4.2.1.2 Transitivity Property

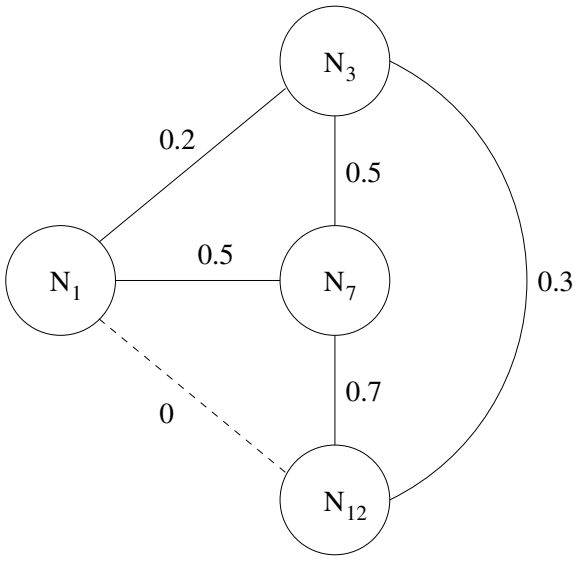

Figure 4.2: An example showing the NL relationship among four MNs.

Apart from the direct connections, the transitivity property of MNs' relationship can also be exploited to improve the performance of information delivery. In a MSN, if there is an intermediate MN, referred to as a forwarding node (FN), having better relationship simultaneously with both a message sender, which is not necessary the SN, and the message's DN, than the direct relationship between the message sender and the DN, it may be more efficient when information is delivered from the message sender to the DN via the FN, instead of directly delivering the information from the message sender to the DN. Straightforwardly, more than one FNs may also be involved to form a route connecting the message sender to the message's DN. In order to decide whether FNs should be employed, a metric called *transitive delivery probability* between two MNs A and B is introduced, which is defined as

$$P_{t(A,B)} = P_{d(A,F_1)} \times P_{d(F_1,F_2)} \times \cdots \times P_{d(F_n,B)} \tag{4.7}$$

where F_i represents the ith FN on the route, and $P_{d(A,B)}$ denotes the probability of direct contact between MNs A and B, as shown in Eq.(4.6).

As an example, Fig.4.2 shows the two-way relationship between any two MNs of N_1, N_3, N_7, and N_{12}. Assume that N_1 has a message destined to N_7, explicitly, this message should be directly sent to node N_7 by N_1. However, when N_1 has a message to N_{12}, it has to first forward this message to either N_3 or N_7, since N_1 does not directly contact N_{12}. Furthermore, N_1 may sometimes need to make a decision to chose between N_3 and N_7. As seen in Fig.4.2, there are four possible routes from N_1 towards N_{12}, which are:

1. Route 1: N_1 via N_3 to N_{12};
2. Route 2: N_1 via N_7 to N_{12};
3. Route 3: N_1 via N_3 and then via N_7 to N_{12};
4. Route 4: N_1 via N_7 and then via N_3 to N_{12}.

According to Eq. (4.7), the transitive delivery probabilities of the four routes can be calculated, which are $P^{(1)}_{t(N_1,N_{12})} = 0.06$, $P^{(2)}_{t(N_1,N_{12})} = 0.35$, $P^{(3)}_{t(N_1,N_{12})} = 0.07$ and $P^{(4)}_{t(N_1,N_{12})} = 0.075$, respectively. Since Route 2 has the highest delivery probability, N_1 prefers to choosing it, in order to deliver the message to N_{12} with high efficiency. Additionally, when N_3 has a message destined to N_1, as seen in Fig.4.2, there are three routes:

1. Route 1: N_3 directly to N_1;
2. Route 2: N_3 via N_7 to N_1;

3. Route 3: N_3 via N_{12} and then via N_7 to N_1.

It can be shown that they have respectively the transitive delivery probabilities $P^{(1)}_{t(N_3,N_1)} = 0.2$, $P^{(2)}_{t(N_3,N_1)} = 0.25$ and $P^{(3)}_{t(N_3,N_1)} = 0.105$. Hence, Route 2 is preferred for delivery of messages from N_3 to N_1, instead of the direct contact of Route 1.

4.2.1.3 Ageing

In general, the delivery probability decreases over time until the next meeting. For this sake, aging effect can be considered in the routing protocols in MSNs. The aging mechanism has been introduced in a number of existing routing techniques, e.g., in the FRESH [85] and SimBetAge [8] protocols. In this chapter, the aging effect is taken into account by updating $P_{d(.,.)}$ of the probability of direct contact. Specifically, when the observation time T in Eq. (4.2) is changed from T_{old} to T_{new} but there are no further encounters between two reference MNs, the probability $P_{d(.,.)}$ of Eq. (4.6) is updated to

$$P_{d(.,.)}(new) = P_{d(.,.)}(old) \times \frac{T_{old}}{T_{new}} \tag{4.8}$$

Note that, unlike $P_{d(.,.)}$, the value of $P_{t(.,.)}$ depends on the $P_{d(.,.)}$ of a number of FNs along a route to a DN. However, our protocol is operated in an egocentric fashion, the update of $P_{(.,.)}$ is only possible, when new encounters occur. Therefore, in our protocol, the aging effect is only directly considered associated with $P_{d(.,.)}$, which, however, implicitly affects $P_{t(.,.)}$ of the transitive delivery probability.

4.2.1.4 Node-Linked Social Contact Probability

Based on the metrics proposed so far, the node-linked social contact probability (N-SCP) between two MNs A and B can be measured by the larger value of $P_{d(A,B)}$ and $P_{t(A,B)}$, expressed as

$$P^{nl}_{(A,B)} = max\{P_{d(A,B)}, P_{t(A,B)}\} \tag{4.9}$$

The N-SCP is used to choose the best route towards the destination, based on the NL relationship, regardless of whether it is a direct link between a message sender and the message destination or it is a multi-hop link via a number of FNs.

4.2.2 Community-Linked Relationship

According to the affiliation concept used in the LABEL [15], BUBBLE [16], social feature enhanced group-based routing [30], and the Community-Aware Opportunistic Routing (CAOR) [86],

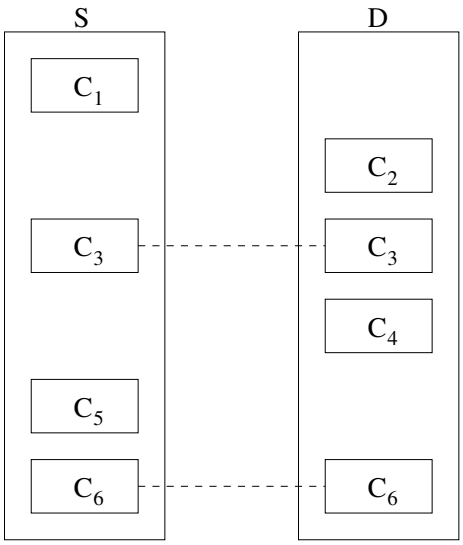

Figure 4.3: An example showing the social relationship between MN S and MN D, where C_3 and C_6 are their mutual PCs.

one type of human behavior is that a person usually prefers to visiting a number of places, depending on her/his social roles. For example, students go to their schools on weekdays, garbage collectors carry out their daily work following fix routes, etc. In general, a person usually has at least one place where s/he often visits. Apart from their homes, people go to work, shopping, school, etc., in different areas. Furthermore, they may have their preferred places, e.g., restaurants, parks, concert halls, clubs, etc., to visit in their leisure time. According to the experiments by [80], nine out of ten of the participants' mobilities can be captured by seventeen mobility patterns. In these patterns, people usually stay within one place or move back and forth between up to six places. Moreover, when two individuals have their preference to visit the same place, the chance of their meeting in that area increases. Therefore, the relationship between two MNs could be reflected through their preferred places, i.e., PCs. This relationship is referred to as the CL relationship. For example, in Fig. 4.3, we illustrate the PC lists of MN S and MN D. While MN S prefers to the communities of C_1, C_3, C_5 and C_6, MN D prefers to the communities of C_2, C_3, C_4 and C_6. They share the communities of C_3 and C_6, which are referred to as their mutual preferences. Assume that node S has a message to be destined to node D. It is most likely that the message is delivered at community C_3 or C_6.

In order to make use of the relationship between two MNs that meet each other in certain communities, similar to the LABEL, the mobility patterns along with the strength of preference of the mobile device owners are listed based on their PCs. Here, the strength of preference is referred to as the community approaching probability P^{ca}, which reflects how often a MN approaches or how long it stays within a given community. Since our routing algorithm is in the egocentric fashion, every MN starts with its own mobility information. Then, the mobility information of different

MNs is exchanged when they encounter, which will be detailed in Section 4.3. Based on the PC lists, a message sender can find the PCs in common and calculates the mutual-community contact probabilities, P^{mcc}, between the message sender and the corresponding destinations. For example, let S represent a message sender holding a number of messages to be destined to the destination MN D. Let C_i represent a mutual PC of both MN S and MN D. Furthermore, let $P^{ca}_{(S,C_i)}$ represent the community approaching probability of MN S to the community C_i. Then, the relationship between MN S and MN D via community C_i can be measured by the probability that MN S and MN D meet at the community C_i, which can be formulated as

$$P^{mcc}_{(S,C_i,D)} = P^{ca}_{(S,C_i)} \cdot P^{ca}_{(D,C_i)} \tag{4.10}$$

Furthermore, as shown in Fig.4.3, it is possible that two MNs have several mutual communities for them to meet. When considering all the mutual communities, we define $P^{cl}_{(S,D)}$ the community-linked social contact probability (C-SCP) between MN S and MN D, which is the probability that MN S and MN D meet in any of their mutual communities. This probability can be evaluated from the formula

$$P^{cl}_{(S,D)} = \sum_{C_i \in \mathcal{C}_{(S,D)}} P^{mcc}_{(S,C_i,D)} \tag{4.11}$$

$$= \sum_{C_i \in \mathcal{C}_{(S,D)}} P^{ca}_{(S,C_i)} \cdot P^{ca}_{(D,C_i)} \tag{4.12}$$

where $\mathcal{C}_{(S,D)}$ denotes the set containing the mutual PCs of MN S and MN D.

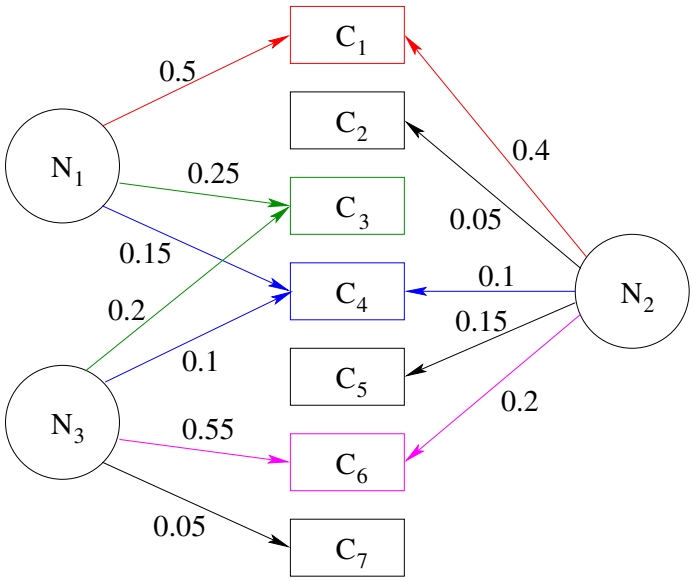

Figure 4.4: An example showing the community approaching probabilities of MNs N_1, N_2 and N_3 towards their PCs.

As an example, Fig.4.4 shows the community approaching probabilities of MNs N_1, N_2 and N_3 towards their PCs. From the figure, we can identify three community-based relationships, which are:

1. Relationship 1: MNs N_1 and N_2 via their mutual communities C_1 and C_4;
2. Relationship 2: MNs N_2 and N_3 via their mutual communities C_4 and C_6;
3. Relationship 3: MNs N_1 and N_3 via their mutual communities C_3 and C_4.

Then, according to Eq. (4.12), the C-SCP between any two of the three MNs can be calculated, which are $P^{cl}_{(N_1,N_2)} = 0.215$, $P^{cl}_{(N_2,N_3)} = 0.12$ and $P^{cl}_{(N_1,N_3)} = 0.065$, respectively. Based on these C-SCP values, we may simplify Fig.4.4 to Fig.4.5, which abstractly shows the social relationships among the three MNs.

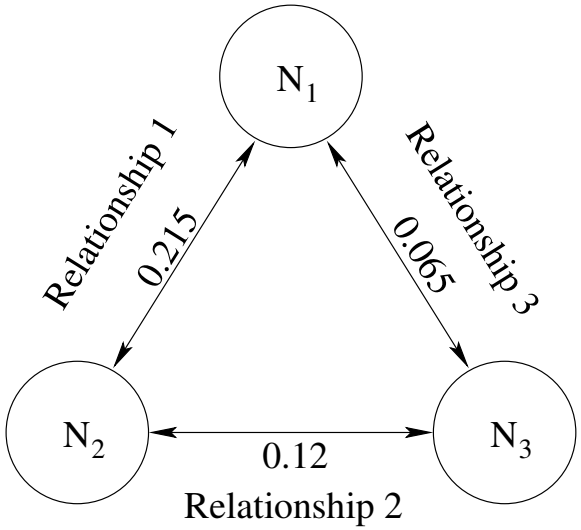

Figure 4.5: A diagram showing the social relationships among MNs N_1, N_2 and N_3 obtained from their mutual PCs.

Let us now assume that N_1 has a message destined to N_2. Explicitly, N_1 should directly deliver this message to N_2 in any case, as the relationship between N_1 and N_2, i.e., Relationship 1, is the strongest one among the three. By contrast, when N_1 has a message to N_3, it will forward the message to N_2, if it meets N_2 before meeting N_3. This is because Relationship 2 is much stronger than Relationship 3. Furthermore, when N_2 has messages to N_1 and N_3, it will choose to deliver the messages directly to them. As shown in Fig.4.5, the relationship between N_2 and N_1 as well as that between N_2 and N_3 are stronger than the relationship between N_1 and N_3. In other words, N_2 has higher chances to encounter both N_1 and N_3 than N_1 encounters N_3. Finally, when N_3 has messages destining to N_1 and N_2, it will give all the messages to either N_1 or N_2, depending on which of them it meets first, since N_1 and N_2 have the strongest relationship.

4.2.3 Social Contact Probability

Above we have defined both the NL relationship and CL relationship, the strength of which is reflected by the N-SCP and C-SCP, as shown in (4.9) and (4.11). Let $P^{nl}_{(S,D)}$ and $P^{cl}_{(S,D)}$ represent the N-SCP and C-SCP from MN S to MN D, respectively. Based on these two probabilities, we can define the social contact probability (SCP) between MN S and MN D as

$$P^{sc}_{(S,D)} = \alpha P^{nl}_{(S,D)} + \beta P^{cl}_{(S,D)} \tag{4.13}$$

where α and β are adjustable weights and $\alpha + \beta = 1$. Specifically, when $\alpha > \beta$, the routing protocol depends more on the NL relationship than on the CL relationship. On the contrary, when $\alpha < \beta$, the route selection emphasizes more on the CL relationship instead of on the NL relationship.

4.3 Social Contact Probability Assisted Routing Protocol

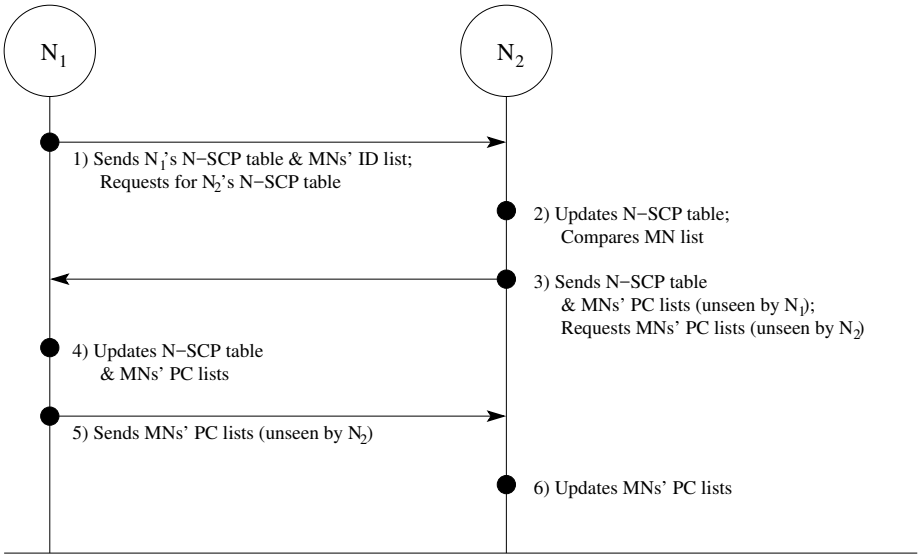

Figure 4.6: A diagram showing the database update procedures, when MNs N_1 and N_2 meet.

Based on the metrics derived in Section 4.2, in this section, we propose a Social Contact Probability assisted Routing (SCPR) protocol, which is operated in two phases. During the first phase, the metrics of delivery probabilities are calculated while MNs' encounter records and PC lists are collected. Specifically, when two MNs meet, an encounter record is added to their encounter history. Then, each MN calculates the probabilities of $P_{d(.,.)}$ towards the other MNs according to Eq.(4.6), while the aging effect is applied to the rest MNs by modifying the corresponding N-SCPs in the N-SCP table, as discussed in Section 4.2.1.3. Then, these two MNs compare and update their databases of the N-SCP tables and PC lists as shown in Fig.4.6, which is detailed as follows.

Step 1 - The process is activated by the MN with a lower identity, such as the first MN, by sending a request for the N-SCP table and the PC lists to the MN with a higher identity, such as the second MN. Simultaneously, the first MN sends the second MN its own N-SCP table as well as the list of the MNs whose PC lists are known to the first MN.

Step 2 - After receiving the request, the N-SCP table and the MN list from the first MN, the second MN first compares and updates its own database. Specifically, based on the information provided by the first MN, the transitive delivery probability ($P_{t(.,.)}$) in the second MN's N-SCP table is recalculated in order to find a better route towards each DN. These updated values are then input to the second MN's N-SCP table, if they are higher than the corresponding existing ones. At the same time, the second MN compares the list of MNs received from the first MN with its own PC lists, and generates a list of MNs containing the MNs that the second MN does not have their PC lists but the first MN has.

Step 3 - The second MN sends the first MN its N-SCP table along with the MNs' PC lists that the first MN does not have. At the same time, it sends the first MN the MN list created in Step 2, and also requests for the MNs' PC lists of those it does not have.

Step 4 - After receiving the N-SCP table and the PC lists from the second MN, the first MN first calculates, compares, and updates the $P_{t(.,.)}$ values in its own N-SCP table, as done at Step 2. Then, it merges the PC lists received from the second MN with its own.

Step 5 - The first MN sends the second MN the PC lists of the MNs requested by the second MN.

Step 6 - Finally, the second MN updates its PC lists by adding the new lists received from the first MN.

Note that, during the updating processes at Step 2 and Step 4, the N-SCP tables of the first and second MNs are updated according to the N-SCP tables received from the second and first MNs, respectively. Let us consider an example, as shown in Fig.4.7 and Table 4.1, where the branch values in Fig.4.7 represent the N-SCPs. Let us assume that N_1 and N_2 meet for the first time. Then, the direct-connection delivery probability ($P_{d(.,.)}$) towards each other is zero as shown in Table 4.1(a) and 4.1(b). After the two MNs encounter, both of them first calculate the $P_{d(.,.)}$ between them, which are shown in the first row of Table 4.1(c) and 4.1(d). Then, they calculate the transitive delivery probabilities ($P_{t(.,.)}$) towards the other MNs via the encounter MN, compare them with the existing values, and update them to the new $P_{t(.,.)}$ values, if the new $P_{t(.,.)}$ values are higher than the corresponding existing ones. Specifically, as shown in Table 4.1(d), which is the updated N-SCP table of N_2. The new $P_{t(.,.)}$ value for N_3 is obtained from the product of $P_{d(.,.)}$ between N_1 and N_3, and N_3's $P_{d(.,.)}$ or $P_{t(.,.)}$, depending on which of them has a higher value.

For example, giving the new $P_{t(.,.)}$ value of 0.216, which is higher than the existing value 0 shown in Table 4.1(b). Hence, the N-SCP value is updated to 0.216, as shown at the cross of the second row and the second column in Table 4.1(d). Similarly, the $P_{t(.,.)}$ value for N_4 is updated to the new value 0.45, as the original value is 0. By contrast, the existing $P_{t(.,.)}$ values for N_5 and N_6 are kept unchanged, as the new values are lower than the corresponding existing ones. Note that, for the sake of simplicity, in this example, the ageing mechanism is ignored after the calculation of $P_{d(.,.)}$.

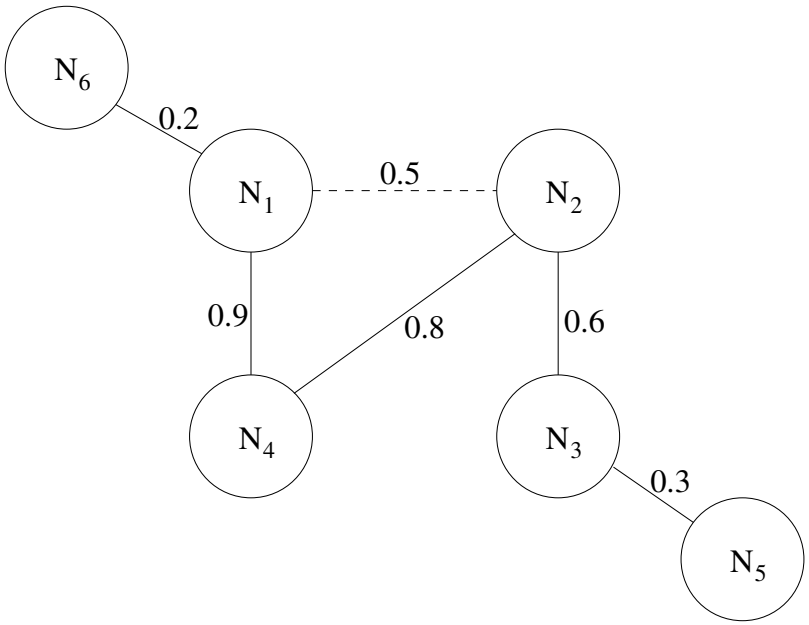

Figure 4.7: An exemplified diagram showing the N-SCPs between MNs.

Note furthermore that, during the third step, the second MN may also request for the PC list of the first MN, when the two MNs meet the first time and when it has not met another MN having the record of the first MN. The second MN may also sends its own PC list to the first MN, if it finds that it is not in the lists received from the first MN. After the information exchange, the MNs recalculate the N-SCPs, C-SCPs, and the SCPs based on the updated N-SCP table and the PC lists, using the formulas provided in Section 4.2.

In the second phase, messages are forwarded from one MN to another MN according to the following rules.

1. When a message sender, which can be a SN or a FN, encounters the DN, messages are certainly directly sent to the DN.

2. When a message sender encounters a MN, which has a stronger relationship with the DN than the sender itself has, messages are forwarded to the MN. In other words, when the SCP of Eq. (4.13) between an encountered MN and the DN is higher than the SCP between the sender itself and the DN, the sender forwards the messages to the encountered MN.

Table 4.1: An example of the N-SCP table update process during an encounter between N_1 and N_2, based on the scenario shown in Fig.4.7. Table (a) and (b) represent the N-SCP tables of N_1 and N_2 before the two MNs meet. Table (c) and (d) show the N-SCP tables of N_1 and N_2 after the update process.

(a)

DN	$P_{d(N_1,.)}$	$P_{t(N_1,.)}$
N_2	0	0.72
N_3	0	0.432
N_4	0.9	0
N_5	0	0.1296
N_6	0.2	0

(b)

DN	$P_{d(N_2,.)}$	$P_{t(N_2,.)}$
N_1	0	0.72
N_3	0.6	0
N_4	0.8	0
N_5	0	0.18
N_6	0	0.144

(c)

DN	$P_{d(N_1,.)}$	$P_{t(N_1,.)}$
N_2	0.5	0.72
N_3	0	0.432
N_4	0.9	0.4
N_5	0	0.1296
N_6	0.2	0.072

(d)

DN	$P_{d(N_2,.)}$	$P_{t(N_2,.)}$
N_1	0.5	0.72
N_3	0.6	0.216
N_4	0.8	0.45
N_5	0	0.18
N_6	0	0.144

In order to explain the operational principles of our SCPR protocol, let us consider a network as shown in Fig.4.8, where the branch values represent the SCPs. Let us assume that N_1 has some messages destined to N_2, N_3 and N_4. Then, when N_1 encounters N_2 before encountering N_3 or N_4, the messages for N_2 are directly delivered by following the first rule. However, according to the second rule, N_1 will not forward N_2 the messages destined to N_3 and N_4, as N_1 itself has a stronger relationship with N_4 than N_2 does, and both N_1 and N_2 have the same relationship strength with N_3. By contrast, when N_1 encounters N_3 before encountering N_2 or N_4, it will then send all the messages to N_3, as the relationships between N_3 and N_2, N_4 are stronger than that between N_1 and N_2, N_4.

4.4 Performance Evaluation

In order to evaluate the performance of our routing technique, we developed our own simulation program based on the PCAM mobility model explained in Chapter 3. In this section, we first explain the simulation scenario and parameter settings used in the simulation. Then, the performance results are provided and discussed.

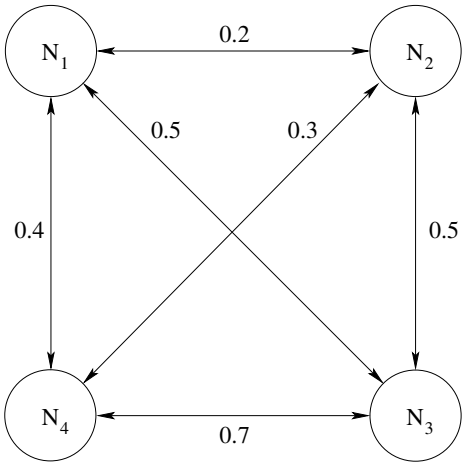

Figure 4.8: An example showing the relationship among four MNs.

4.4.1 Simulation Setup

In our simulations, we consider a MSN with the coverage of 1000 × 1000 square meters (m^2). Within this area, there are 15 communities of each covering an area of 100 × 100 m^2. At the beginning of simulation, the 15 communities are randomly located in the MSN's covered area. Some communities may overlap with each other. In order to create some unpopular areas with low-density of MNs, 50 MNs are randomly distributed inside the areas covered by the communities. Each MN is assigned a random number of communities, which represent its PCs. Then, for each PC, a PC probability is randomly generated with the total probability of 0.9 for each MN.

Referring to the research results shown in [80], we know that approximately 10%, 30% and 20% of the human-dependent MNs usually move within one, two and three places, respectively. Beyond three places, the percentage of a MN traveling towards more locations becomes less and less. Additionally, approximately 10% of MNs' movement patterns can usually not be captured by the preference-based assumption. Based on these observations, in our mobility model, we set the probabilities of 0.125, 0.375 and 0.25 for a MN to have one, two and three PCs. Beyond three PCs, the probability is halved whenever one more PC is involved. In detail, the probability of one MN having four PCs is 0.125, which is half of the probability 0.25 of having three PCs. Similarly, the probability of one MN having five PCs is 0.0625, which is half of the probability 0.125 of having 4 PCs. Similarly, we can have the probabilities for the other cases. After the initial assignments of MNs to the communities, a number of random probabilities are generated for each MN to decide its future movements among the communities.

During our simulations, messages are randomly generated by MNs with a probability of 0.125 and at an interval of $t_{interval}$, meaning that the message generation rate is approximately $0.125/t_{interval}$. In the MSN, a MN can detect its neighbors within a range of r. When a neighbor MN is discovered,

the processes for routing metric update and message transmission, which are described in Section 4.3, are triggered. Specifically, in our experiments, we set the neighbor discovery radius to be $r = 30$ meters (m), while each MN moves in a straight line with a random speed between 0 to 20 meters per second (m/s) and pauses for 10 minutes whenever arriving at a target destination. In summary, the parameters used in our studies are listed in Table 4.2.

Table 4.2: Parameters for simulations.

Parameter	Value	Unit
Simulation area	1000×1000	m^2
Community area	100×100	m^2
Number of communities	15	*communities*
Number of MNs	50	*MNs*
V_{max}	20	*m/s*
r	30	*m*
t_{pause}	600	*s*
$t_{interval}$	60	*s*
T	15	*days*
Probability of message generation	0.125	-

In terms of the SCPR protocol, we conduct the evaluations in three different scenarios determined by the parameters α and β seen in Eq. (4.13). Specifically, the first scenario only uses the NL relationship associated with setting $\alpha = 1$ and $\beta = 0$, which we refer to as the node-linked (N) mode. The second scenario is referred to as the community-linked (C) mode, which corresponds to setting $\alpha = 0$ and $\beta = 1$. Explicitly, this mode represents the SCPR protocol purely using the CL relationship. Finally, the so-called hybrid (H) mode exploits both the NL and CL relationships, associated with setting $\alpha = \beta = 0.5$. Furthermore, we investigate the effect of non-ideal information about MNs behavior on the above-mentioned three modes. In detail, we compare the performance of two sets of simulations for each of the three modes. In the first set of simulations, we assume precise information about the community approaching probabilities, P^{ca}, which are assigned as the initial information of every of the MNs. On the other hand, in the second set of simulations, the values for the community approaching probabilities are randomly increased or decreased up to 50% from their original values. However, in the second set of simulations, the PCs in the PC lists remain the same as in the first set. In comparison with the first set of simulations, the changes made in the second set of simulations are only the values of P^{ca}.

Furthermore, in order to illustrate the achievable performance of our SCPR algorithm in the H mode, we compare it with five existing routing protocols, which are the Epidemic, PRoPHET, SimBet, LABEL, and BUBBLE algorithms. Our experiments are carried out as follows. At the beginning of the experiments, communities, MNs, mobility patterns as well as messages are generated and saved into a file. Then, simulations in the context of our SCPR protocols and the other

five routing protocols are executed in order to generate the performance results. Furthermore, for the sake of accuracy, each simulation is repeated five times. Accordingly, the results drawn in the figures are the averages of the results obtained from the simulations.

Note that, in our experiments, message's transmission time is ignored, while messages' lifetime or time-to-live (TTL) is not considered. We also assume that there is no limit for MNs to store messages. In the Epidemic protocol, the acknowledgment mechanism is ignored and all the copies of a message stored at other MNs are discarded, once it is delivered to its destination.

4.4.2 Performance Results

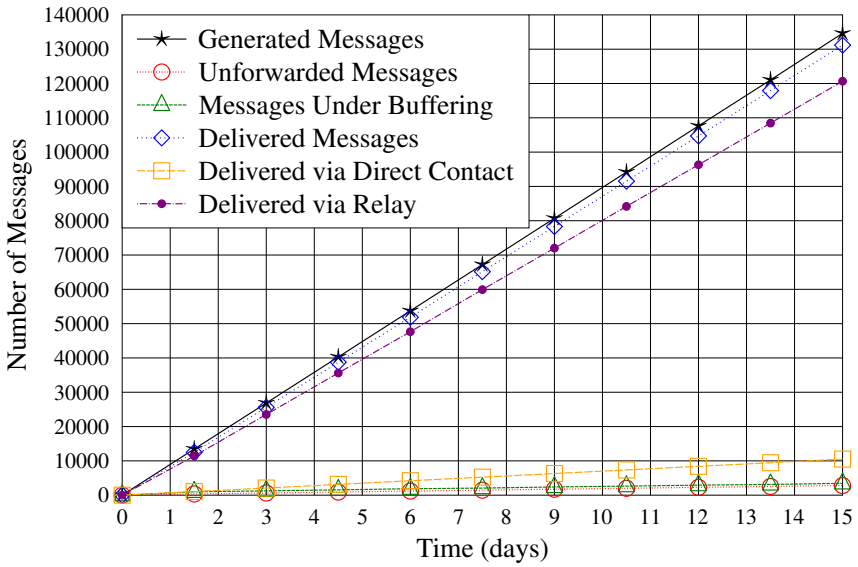

Figure 4.9: States of message delivery via time in a MSN supported by the SCPR protocol.

Fig.4.9 shows the states of message delivery via time in a MSN supported by our SCPR protocol. In the figure, 'Generated Messages' represents the accumulation of the messages generated; 'Unforwarded Messages' represents the messages holding by the original message generator; 'Messages Under Buffering' represents the messages holding by FNs; 'Delivered Messages' represents the total number of messages successfully delivered to their DNs; 'Delivered via Direct Contact' represents the messages delivered from SNs to DNs via direct contacts; and, finally, 'Delivered via Relay' represents the accumulation of the messages delivered with the aid of FNs. As seen in the figure, most of the messages can be successfully delivered to their designated destinations, of which the majority are delivered via FNs, and only a small fraction of messages are delivered by MNs' direct contacts. While there are a small number of undelivered messages, we can observe that most messages forwarded by relay MNs are successfully delivered. This is reflected by the small difference between the number of messages under buffering and the number of unforwarded

messages.

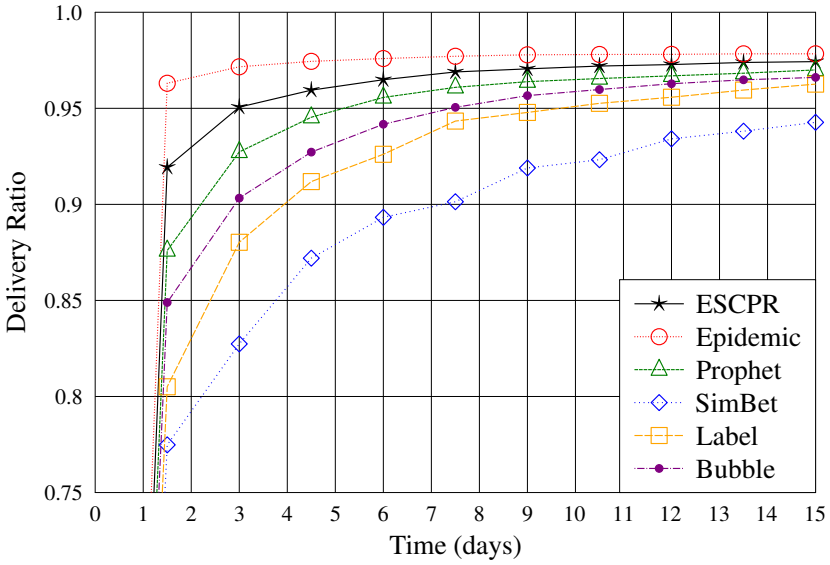

Figure 4.10: Comparison of message delivery ratios of the SCPR and the other five routing protocols.

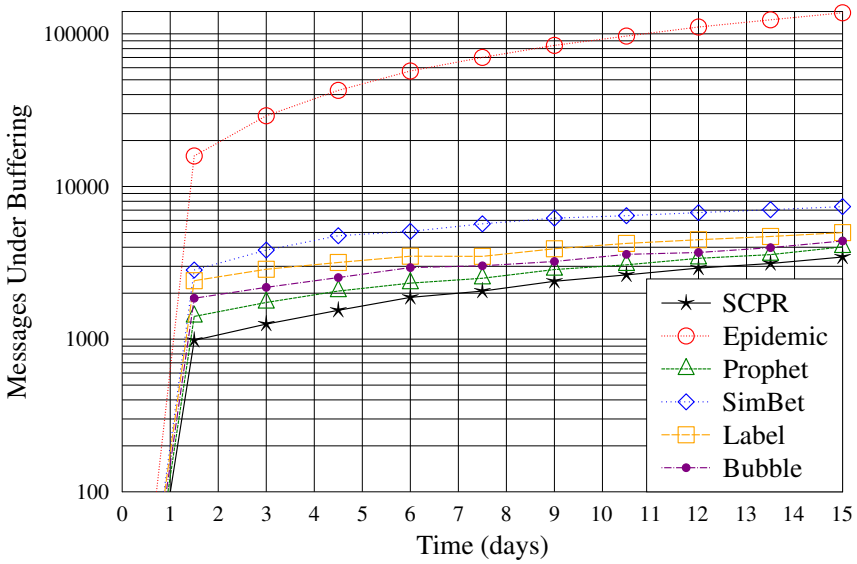

Figure 4.11: Comparison of buffer usages of the SCPR and the other five routing protocols.

In terms of performance comparison, the Epidemic protocol which is a multiple-copy resource-greedy routing protocol always has the best performace comparing to other single-copy approached routing protocols. Accordingly, in this section, we consider the Epidemic protocol as a benchmark, in terms of delivery ratio, end-to-end delay, and number of hops. Fig.4.10 compares the message delivery ratios of our SCPR protocol and the other five routing protocols. The Epidemic protocol has the highest delivery ratio amongst the six considered protocols. However, our SCPR generates

the highest delivery ratio among the five single-copy routing protocols, while the SimBet protocol has the lowest delivery ratio. However, with the increase of simulation time, the Epidemic protocol demands an extreme amount of resources for buffering the message copies, as shown in Fig.4.11. By contrast, the other five single-copy protocols generate a similar number of bufferred messages, which is not only small but also stable.

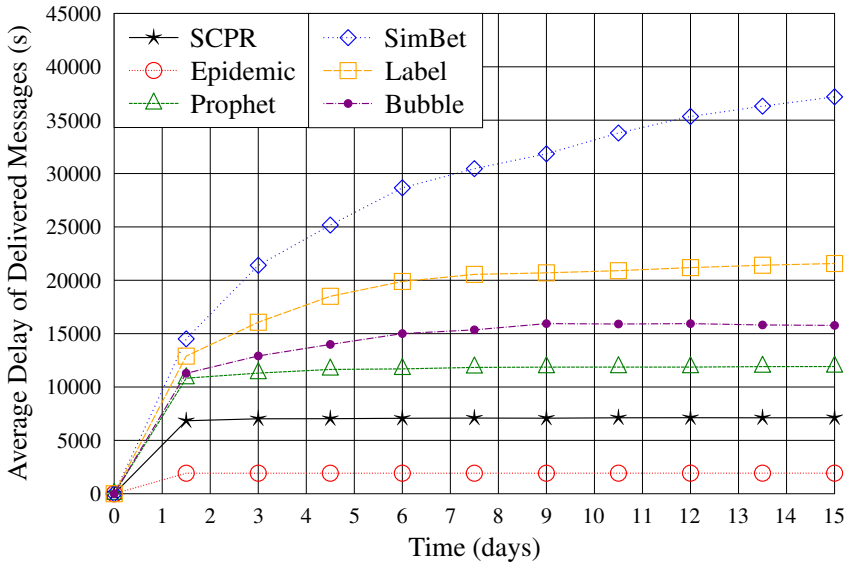

Figure 4.12: Comparison of average delay of the SCPR and the other five routing protocols.

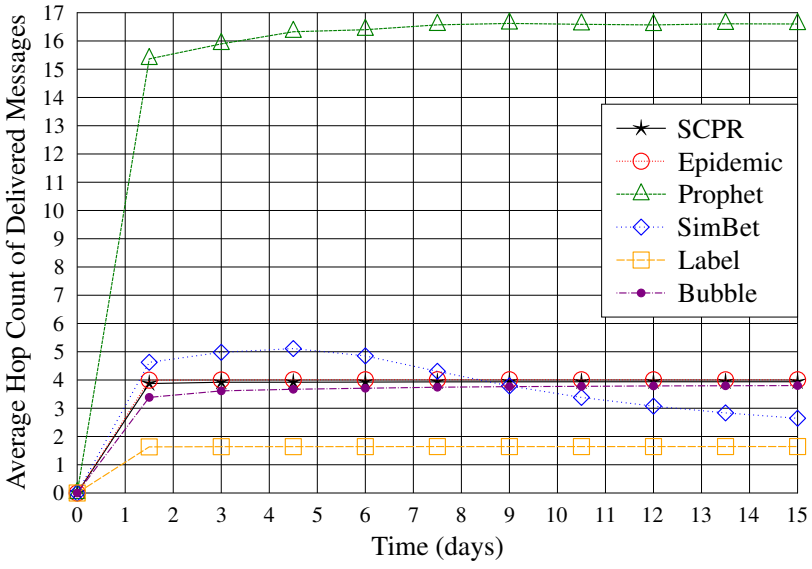

Figure 4.13: Comparison of average number of hops of the SCPR and the other five routing protocols.

Fig.4.12 and Fig.4.13 portray respectively the average delay and the average number of hops used by the delivered messages. Due to using multiple copies at the cost of huge resources for

message buffering, the Epidemic protocol yields the lowest average delay among the six protocols considered. From the results shown in Fig.4.13, we are implied that the MNs operated under the SimBet and LABEL protocols attempt to find direct links for message delivery. As a result, the average message delivery latency of SimBet and LABEL protocol is higher than that of the other four protocols. When comparing our SCPR protocol with the PRoPHET and BUBBLE protocol, we find that they have similar successful delivery ratio. However, as shown in Fig.4.12, our SCPR protocol yields the lowest end-to-end message delivery latency among these three protocols. Moreover, as shown in Fig.4.13, when the PRoPHET algorithm is invoked, more than twice of FNs than that required by our SCPR algorithm are required, in order to deliver the same number of messages. Therefore, for delivery of the same number of messages, the PRoPHET protocol requires about twice of the energy required by the SCPR protocol. As shown in Figs.4.12 and 4.13, our SCPR protocol is capable of attaining the best trade-off between the average delay and the average number of hops for successful message delivery. Its average delay is lower than that of the four single-copy routing protocols, while its required average number of hops for successful message delivery is similar to that of the Epidemic protocol, which is a multiple-copy routing approach.

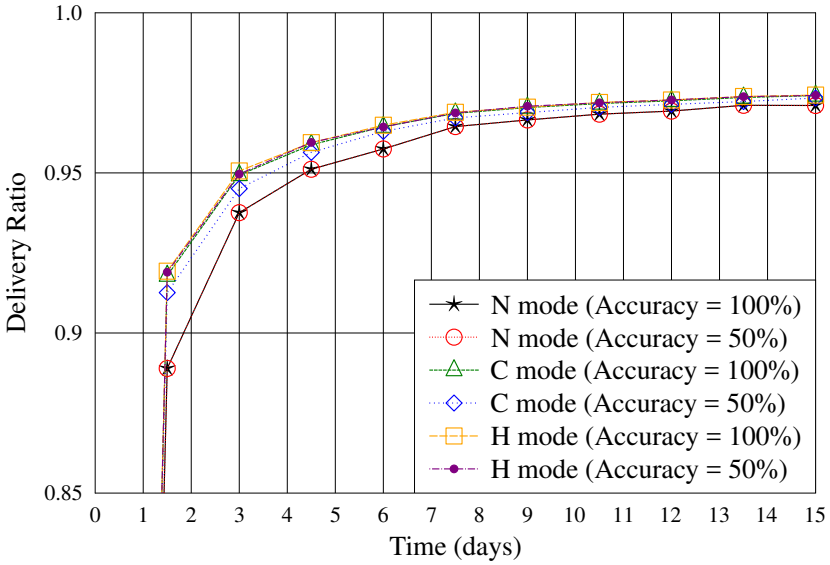

Figure 4.14: Delivery ratios of the SCPR protocol operated under the N, C and H modes, when the information about MNs behavior is ideal or non-ideal.

When the SCPR protocol is operated under the three different modes, namely the N, C and H modes, as described in Section 4.4.1, Fig.4.14 and Fig.4.15 show that the delivery ratios and the amount of message buffering are similar in all the three modes, and when the information about MNs' mobility behavior is ideal or non-ideal. However, the simulation results in these two figures as well as in Fig.4.16 and Fig.4.17 demonstrate that the H mode gives a superior performance over the N and C modes. Specifically, the SCPR protocol under the H mode involves less number of FNs and yields lower average delivery delay than that operated under the N mode. By contrast,

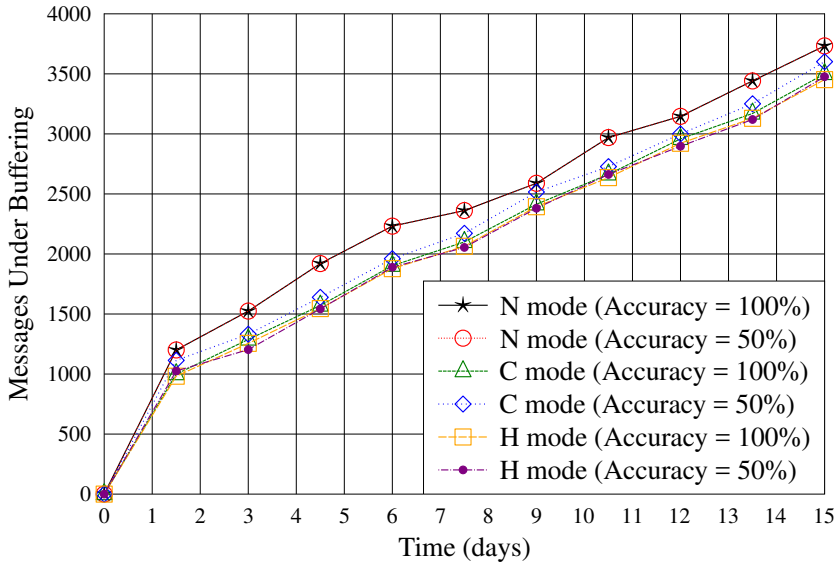

Figure 4.15: Buffer usage in the SCPR protocol operated under the N, C and H modes, when the information about MNs behavior is ideal or non-ideal.

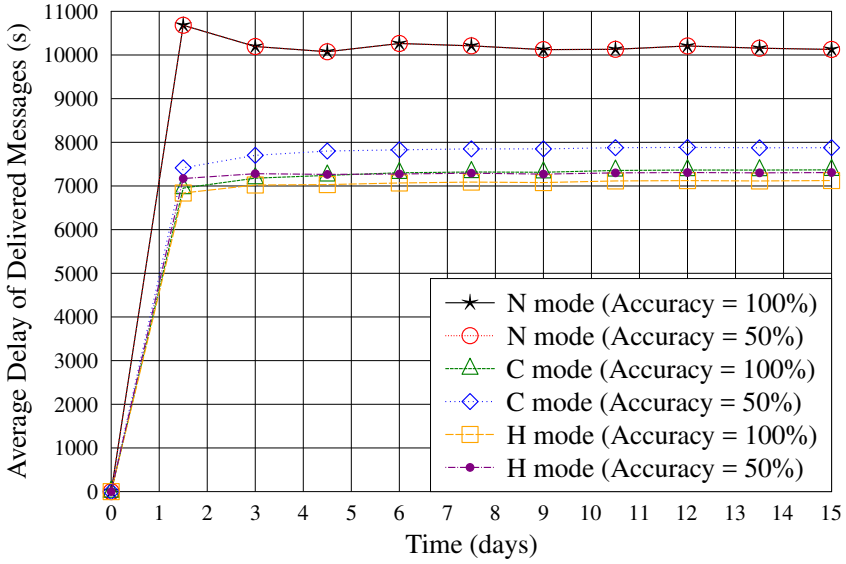

Figure 4.16: Average delay achieved by the SCPR protocol operated under the N, C and H modes, when the information about MNs behavior is ideal or non-ideal.

when comparing the H and C modes, we can see that there is a trade off between the end-to-end delivery latency and the number of MNs required during message transfer. The H mode yields less average delivery delay but involves more hops than the C mode. However, under the C mode, the performance is sensitive to the accuracy of the information about MNs' behavior. When the information about MNs' behavior is reduced from 100% to 50%, the SCPR protocol operated under the C mode is likely to transmit messages via direct contacts, which significantly increases the end-to-end latency, as shown in Fig.4.16 and Fig.4.17. By contrast, when the information about

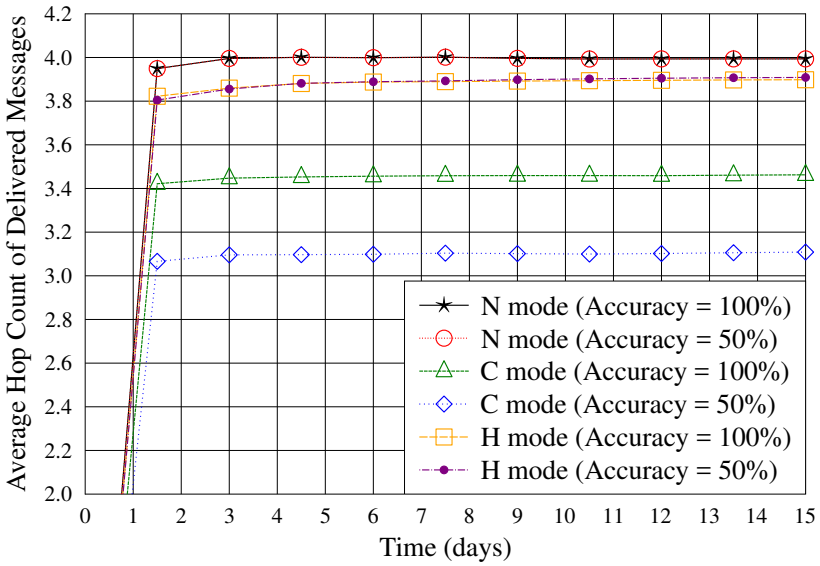

Figure 4.17: Average number of hops of delivered messages in the SCPR protocol operated under the N, C and H modes, when the information about MNs behavior is ideal or non-ideal.

MNs' behavior changes from ideal to non-ideal, the H mode results in a slightly increased average delay, while requiring a similar number of hops. In all the cases, as shown in Figs. 4.14 - 4.17, the performance of the N mode is unaffected by the accuracy of MNs' behavior information. Furthermore, as shown in Fig.4.15, the C mode demands slightly more resources for message buffering than the other modes, when the MNs' behavior information is non-ideal.

4.5 Chapter Summary and Conclusions

In this chapter, we have proposed a SCPR protocol for MSNs, which makes efficient use of the information embedded in the people's social preference. We have proposed the approaches for measuring people's social preference, so that they can be exploited for information delivery in MSNs, both direct contacts and indirect contacts have been integrated. The performance of the proposed SCPR protocol and that of five existing routing protocols for MSNs have been investigated in the context of a proposed and more realistic PCAM mobility model. Furthermore, we have studied the impact of the accuracy of the information about MNs' behavior on the achievable performance of the SCPR protocol. Our studies and performance results show that the SCPR protocol is capable of integrating the merits of the Epidemic, PRoPHET, SimBet, LABEL and BUBBLE protocols, while circumvents their shortcomings of resource-greedy of the Epidemic protocol, and of high message delivery latency of the PRoPHET, SimBet, LABEL and BUBBLE protocols. Furthermore, the SCPR protocol is robust to the inaccuracy of the information about MNs' behavior.

Chapter 5

Energy-Concerned Routing Protocols

The routing protocols designed for mobile social networks (MSNs) have so far mainly focused on maximizing delivery ratio or/and minimizing delay, but rarely considered the energy consumption for message delivery. This chapter addresses the routing protocols for MSNs achieving the trade-off among energy consumption (EC) (or energy-efficiency), delivery ratio (DR) and delay (D), referred to as the EC/DR/D trade-off. We first provide two approaches allowing to design the routing protocols that are capable of attaining desirable EC/DR/D trade-off via controlling the values of the parameters introduced. Then, we extend three existing routing protocols, namely, the social contact probability assisted routing (SCPR), BUBBLE and the PRoPHET protocols, respectively, to the three routing protocols that are able to achieve the EC/DR/D trade-off. Correspondingly, these routing protocols are referred to as the ESCPR, EBUBBLE and the EPRoPHET protocols. Finally, we investigate the performance of these routing protocols based on a community-assisted mobility model as described in Chapter 3, when assuming that messages are either fixed length or the length of messages obeys an exponential distribution retrieved from emails. Our studies show that the proposed approaches are efficient for achieving the desired EC/DR/D trade-off according to practical requirements.

5.1 Introduction

Similar to the other infrastructureless wireless networks, mobile social networks (MSNs) are usually operated based on the battery-powered mobile devices, which are desirable to be energy-efficient, and can last for a relatively long time. Therefore, achieving high energy-efficiency constitutes one of the major challenges in the design of routing algorithms in MSNs. In literature, there are now a range of routing protocols specifically dedicated to MSNs, which include the LA-

BEL [15], BUBBLE [16], PRoPHET [5, 64], SimBet [7], HiBop [9], Social-Greedy Routing [10], etc. However, all these routing protocols have been designed with the main motivation to maximize delivery ratio or/and minimize delivery delay, regardless of the energy consumed for message delivery. By contrast, there are some energy-concerned routing protocols having been proposed for wireless delay-tolerant networks [87–95]. However, these routing protocols do not make use of the social characteristics and the relationship among mobile device carriers. Hence, they are not efficient for employment in MSNs.

In the MSNs operated based on battery powered devices, energy is depleted by a number of processes, including route discovery, route setup, route maintenance, and message transmission [87–89]. Therefore, in order to save battery, it is very important to design the routing protocols for MSNs with high energy-efficiency. In this chapter, as the first attempt, we consider the energy-efficiency issues in the MSN, and motivate to propose the routing protocols for MSNs, which are capable of achieving the trade-off among energy consumption (EC), delivery ratio (DR) and delay (D), referred to as the EC/DR/D trade-off for convenience. Specifically, we motivate to design the routing protocols that are capable of control the EC/DR/D trade-off, so that a good balance among energy consumption, delivery ratio and delay can be attainable in practice. With this motivation, we first analyze the energy consumption in some existing routing protocols for MSNs. From our analysis we find that most of the existing routing protocols for MSNs have the greedy nature. In these protocols, a message carrier, which may be the message's source node (SN) or a forward node (FN), but not the message's destination node (DN), always forwards the message to its first encountered mobile node (MN), provided that the encountered MN has a higher numeric indicator, such as delivery probability, of delivering the message towards the DN than the message carrier itself. In these protocols, a route having many hops may be selected, which may result in a huge energy consumption, but the overall delivery ratio might not be improved much.

Based on the above observations, in this chapter, we propose two types of energy-concerned routing protocols for MSNs. In the first type of protocols, which are referred to as the energy-concerned routing (EnCoR) protocols, we extend three existing routing protocols, namely, our previously proposed social contact probability assisted routing (SCPR) protocol [79], the BUBBLE protocol [16] and the PRoPHET protocol [5, 64], to the corresponding routing protocols achieving the EC/DR/D trade-off. These extended protocols are respectively referred to as the ESCPR, EBUBBLE and the EPRoPHET protocols for convenience of description. As detailed in our forthcoming discourses, in these extended routing protocols, the EC/DR/D trade-off is controlled by a threshold introduced to the route selection process. When a message carrying MN encounters another MN, it forwards the message to the encountered MN, only when the delivery probability from the encountered MN to the DN is higher than that from itself to the DN by at least the threshold. In this way, the ESCPR, EBUBBLE, and the EPRoPHET protocols can effectively control the

trade-off among the consumed energy, delivery ratio and average delay.

In the context of the second type of energy-concerned routing protocols, we propose a so-called energy-efficient social distance routing (ESDR) protocol. For this protocol, we first analyze the effect of message length on the energy consumption during message transmission. Then, we propose a hop estimation method for finding the shortest delivery route based on the social relationship among the MNs. The ESDR protocol makes the routing decisions based on these two metrics as well as the delivery probabilities. By controlling the contribution of these factors, the ESDR can control the EC/DR/D trade-off. Finally, the performance of these routing protocols is investigated by simulations based on the community-based mobility model proposed in Chapter 3. Our studies and performance results show that desirable EC/DR/D trade-off may be attained by appropriately setting the threshold in the EnCoR protocols and the parameters in the ESDR protocol.

The remainder of this chapter is organized as follows. In Section 5.2, we analyze the energy consumption issues in the MSN routing, and identify the problems caused by the existing routing techniques. Section 5.3 considers the EnCoR scheme, and based on which, extends the SCPR, BUBBLE and the PRoPHET protocols to the ESCPR, EBUBBLE and the EPRoPHET protocols. In Section 5.4, we investigate the statistics of some types of messages and address the hop estimation, as well as investigate the effect of these two metrics on the EC/DR/D trade-off. Simulation settings and performance results are provided in Section 5.5. Finally, Section 5.6 summarizes the main conclusions.

5.2 Energy Consumption for Message Transmission

In mobile communications, various approaches, such as those in [87–92, 96–102], have been proposed for prolonging battery's lifetime of mobile devices. Some of them focus on the energy consumed in the processes of route discovery, route setup and route maintenance, while some others emphasize the energy consumption during signal transmission. In MSNs, energy consumption issue has been recognized to be an important challenge, as mobile devices in MSNs often help and cooperate with each other in order to achieve higher efficiency of information delivery over networks. However, considering the routing protocols for MSNs, the BUBBLE [16], SimBet [7], PRoPHET [5, 64], SCPR [79], etc., protocols have all been designed with the objective to find the message delivery routes yielding the highest possible successful delivery probability (or delivery ratio), while the energy consumption during the operations has usually been neglected. As a result, a route that requires extremely high energy consumption might be selected to deliver a message. Furthermore, these routing protocols are usually operated in greedy principle, and a message carrier always forwards the message to its first encountered MN, provided that this encountered MN has

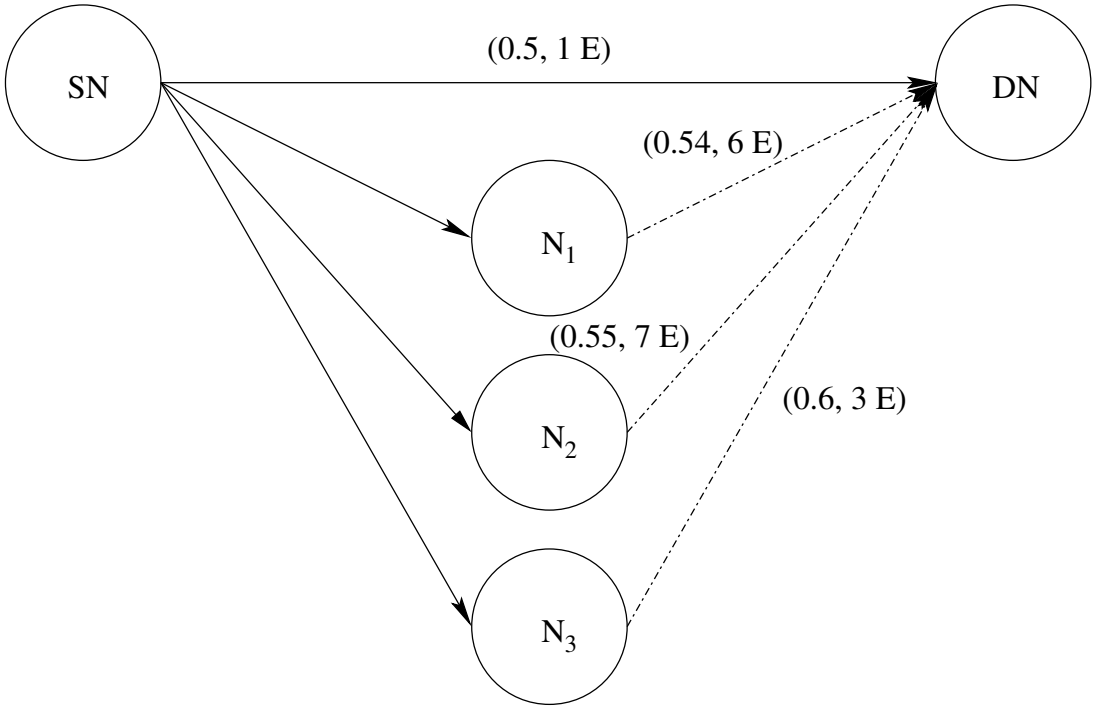

Figure 5.1: Possible routes for message delivery from SN to DN, where (P, E) gives the delivery probability (P) and energy (E) consumed for delivery.

a higher probability than the current message carrier to deliver the message to the DN. However, the routes chosen in this way may not be the efficient ones, when delivery ratio, end-to-end delay and energy consumption are jointly considered. Let us first use an example as shown in Fig.5.1 to demonstrate their trade-off. As shown in Fig.5.1, there are multiple optional routes from SN to DN, which are

1. Route 1 (SN-DN): Direct connection;
2. Route 2 (SN-N_1-DN): Connection via N_1;
3. Route 3 (SN-N_2-DN): Connection via N_2;
4. Route 4 (SN-N_3-DN): Connection via N_3.

Assume that SN first meets N_1 then N_2 and, finally, N_3, before it meets DN. All the above-mentioned routing protocols will select Route 2, since N_1 is first met and the route has a slightly higher delivery probability than SN itself to DN, i.e., Route 1. However, this route may not be the desired one, as both Routes 3 and Route 4 have higher delivery probability than Route 2 and, furthermore, Route 4 consumes significantly lower energy than Route 2. Additionally, when energy-efficiency is the sole objective to achieve, Route 1 is much better than Route 2, as Route 1's delivery

ratio is only slightly lower than that of Route 2, but it requires significantly lower energy for delivery.

The reason behind the above-mentioned is that, in MSNs, routing is done distributively based only on the information, such as delivery probability, usually measured locally via the encounters between MNs. Due to the limited information about the future, some inefficient routes may be used, which consume higher energy, reduce delivery ratio and/or yield increased delay.

In this chapter, we propose the routing protocols for MSNs, which achieve the EC/DR/D trade-off. We consider the average energy consumption per message, representing the energy consumed for successfully delivering a message from its SN to its DN. Hence, the energy consumption includes that required for route discovery, route setup, information transmission, etc. Specifically, when considering the energy consumption during message transmission, according to [93], the energy consumed by a successfully delivered message can be measured by the formula

$$E_P = \sum_{i=1}^{h} E_{n_i,n_{i+1}} \tag{5.1}$$

where h denotes the number of transmissions or the number of hops, n_i are MNs along the route, while $E_{n_i,n_{i+1}}$ represents the energy consumed for delivery a message from the n_ith MN to the n_{i+1}th MN. In principle, the energy required for a transmission is the sum of the energy spent by transmitter, receiver, as well as the forwarding process between the transmitter and receiver. Furthermore, the energy consumed for delivering a message is also depended on the message's length. Assume that $\varepsilon_{u,v}$ and $\omega_{u,v}$ are respectively the energy consumed for transmitting and receiving a message of x bits from MN u to MN v. Then, $E_{u,v}$, for example, in Joules (J) can be evaluated as [87]

$$\begin{aligned} E_{u,v} &= \varepsilon_{u,v} + \omega_{u,v} \\ &= (A_u + \frac{P_{u,v}}{\kappa_u})\frac{x}{r_{u,v}} + \frac{B_v}{r_{u,v}}x \\ &= \frac{1}{r_{u,v}}\left(A_u + B_v + \frac{P_{u,v}}{\kappa_u}\right)x \end{aligned} \tag{5.2}$$

where A_u and B_v are the power required by the transmitter and receiver circuits, respectively, $P_{u,v}$ denotes the transmission power from MN u to MN v, $\kappa_u \in (0,1]$ represents the power efficiency of the amplifier in the transmitter of MN u, and, finally, $r_{u,v}$ is the data rate between MNs u and v. Although Eq. (5.2) may measure the energy consumption with relatively high accuracy, it is cumbersome to use in MSNs. Therefore, for the sake of simplicity, we use the average energy consumption to replace Eq. (5.2). In this case, the average energy consumption for delivery of the

ith message of x_i bits can be expressed as

$$E_i = \sum_{i=1}^{h_i} \gamma x_i = \gamma h_i x_i \tag{5.3}$$

where γ is the average energy consumed per message bit per hop, referred to as the energy consumption factor, which is expressed as

$$\gamma = \mathbb{E}\left[\frac{1}{r_{u,v}}\left(A_u + B_v + \frac{P_{u,v}}{\kappa_u}\right)\right] \tag{5.4}$$

where $\mathbb{E}[\cdot]$ denotes the expectation with respect to MNs u and v. Furthermore, the average energy consumption per message can be evaluated as

$$\overline{E} = \frac{1}{M}\sum_{j=1}^{M} E_j = \frac{\gamma}{M}\sum_{j=1}^{M} h_j x_j \tag{5.5}$$

where M denotes the total number of messages delivered over a MSN.

As shown in Eq.(5.3), the energy consumption of a message is linearly dependent on the message length and the number of hops required to deliver the message from its SN to its DN. Therefore, when the routing protocols are motivated to achieve a good trade-off among the delivery ratio, energy consumption and delay, i.e, the EC/DR/D trade-off, both the length of messages and the number of hops for delivering the messages are required to be reflected in the routing protocols. Therefore, in the following two sections, we consider and compare two scenarios, and design the corresponding routing protocols motivating to achieve a good EC/DR/D trade-off. Specifically, in the first scenario, all messages are assumed the same length. By contrast, the second scenario assumes that message are variable lengths.

5.3 Energy-Concerned Routing in MSNs

In this section, we consider a simple communication scenario, where all messages have the same length and, hence, the energy consumed for transmitting any message over one hop is the same. The assumption of fixed length is satisfied, when messages are actually the fixed length packets that are independently routed. Therefore, according to Eq. (5.3), the energy consumed for delivery of the ith message can be expressed as

$$E_i = e_0 h_i \tag{5.6}$$

where e_0 is the average energy consumption per message per hop. Explicitly, the energy consumed by a message is only dependent on the number of hops.

Straightforwardly, in order to reduce the energy consumption per message, it would be desirable to minimize the number of hops for delivering a message from its SN to its DN. In other words, if energy consumption is the sole objective to minimize, single-hop transmission of messages should be utilized, meaning that a SN transmits a message, only when it directly meets the message's DN. By contrast, when the single-copy routing protocols, such as the SCPR [79], BUBBLE [16], PRoPHET [5, 64], etc., are employed, and when delivery ratio is the sole objective to maximize, a message holding MN, which may be the SN or a FN, will forward the message to any intermediate FN that it encounters, provided that the encountered FN has a higher delivery probability to the DN than the message holding MN. Furthermore, when minimization of delay is the sole objective, multiple-copy routing protocols, such as, the Epidemic [3] protocol, would be desirable, which send a message to any encountered FNs. However and explicitly, the multiple-copy routing protocols are highly energy inefficient, which also require a lot of other resources to operate.

In practice, all the above protocols with one optimization objective are not desirable. Instead, we prefer the routing protocols, which are capable of attaining a 'best' trade-off among energy consumption, delivery ratio and delay, i.e., the 'best' EC/DR/D trade-off. Here, we should note that the 'best' trade-off is dependent on the specific application scenarios in practice. Therefore, when designing the routing protocols for MSNs, we should take the EC/DR/D trade-off into account. In this section, we propose the energy-concerned routing (EnCoR) protocol for achieving the EC/DR/D trade-off.

In our proposed EnCoR, when a MN A holding a message meets a MN B before meeting the message's DN, the decision is made according to the following criteria. Let P_A and P_B be the delivery probabilities from MN A and MN B to the DN, respectively. Let P_{th} be a threshold in probability. Then, in the EnCoR protocol, MN A forwards the message to MN B, only if $P_B - P_A \geq P_{th}$. Otherwise, MN A keeps the message to itself until it meets another MN, which may be the message's DN or another intermediate MN. When it is the message's DN, MN A certainly sends the message to the DN. If it is another MN rather than the message's DN, MN A repeats the above decision-making process when it meets MN B.

The rationality of the EnCoR protocol can be explained as follows. First, when P_B is only slightly larger than P_A, implying that the two MNs have a similar chance to deliver a message to the DN, MN A prefers not to forward the message to MN B for the sake of reducing *energy consumption*. However, when $P_B - P_A \geq P_{th}$, meaning that MN B has an apparently higher chance to deliver a message to the DN than MN A, MN A chooses to forward the message to MN B in favor of the *delivery ratio*. Furthermore, although it is not explicit, the threshold value

also generates impact on the average delivery delay of messages in MSNs, as demonstrated in Section 5.5.

Considering the single-copy routing, our EnCoR protocol can be regarded as a generalized one. It includes the routing protocols that have the sole objective to maximize delivery ratio or that have the sole objective to minimize energy consumption. In more detail, the routing protocols motivated solely to maximize the delivery ratio can be obtained from the EnCoR protocol by setting $P_{th} = 0$. By contrast, the routing protocols with the sole objective to minimize the energy consumption can be obtained from the EnCoR protocol by setting $P_{th} = 1$.

Furthermore, it can be shown that, by introducing the principles of the EnCoR protocol, any *single-copy* routing protocols that forward messages based on delivery probability or the other numerical metrics reflecting the chance of delivery can be readily extended to the corresponding routing protocols achieving the EC/DR/D trade-off. In this chapter, three representative *single-copy* routing protocols for MSNs, namely, the SCPR [79], BUBBLE [16] and the PRoPHET [5, 64], are extended to the corresponding routing protocols achieving the EC/DR/D trade-off. For simplicity of description, these routing protocols are referred to as the ESCPR, EBUBBLE and EPRoPHET protocols, respectively, after their integration with the EnCoR protocol.

5.4 Energy-Efficient Social-Distance Dependent Routing

In the EnCoR protocol considered in the last section, we assumed that all messages are of the same length, resulting in that only the number of hops affects a message's route selection. In practice, message sizes are dependent on the type of services and can be very different. As shown in Section 5.2 and explicitly in (5.3), the length of a message is an important factor of the energy consumed to deliver the message. Instinctively, for a short message, the number of hops may not yield a big impact on the average energy consumption per message. Therefore, a route having a higher delivery probability but more hops may be chosen to deliver the message, in order to achieve a good EC/DR/D trade-off. By contrast, for a long message with every transmission consuming a large amount of energy, the route having fewer hops would be preferred for retaining a good EC/DR/D trade-off. Let us first consider an example as shown in Fig. 5.2 to show the concerned issues.

As shown in Fig. 5.2, there are three possible routes for message delivery from SN to DN.

1. Route 1: Direct connection of SN and DN;
2. Route 2: Connection via N_1, from N_1 to DN there is one hop with the delivery probability of 0.3;

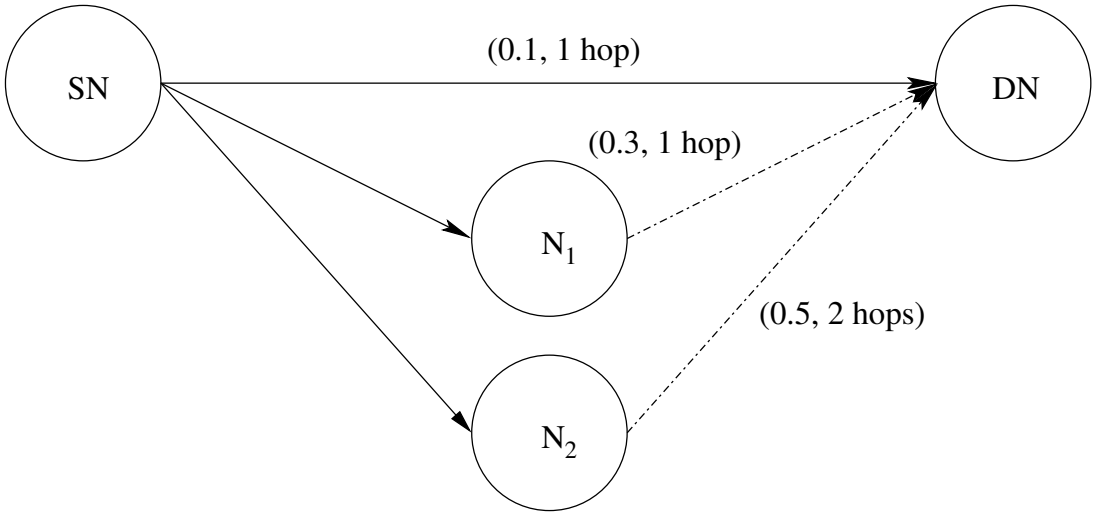

Figure 5.2: Possible routes for message delivery from SN to DN, where (P, H) gives the delivery probability and the number of hops required for delivery.

3. Route 3: Connection via N_2, from N_2 to DN there are two hops with the overall delivery probability of 0.5.

Following our previous discussion, Route 3 having the highest delivery probability may be preferred for delivering short messages, while Route 1 having the lowest number of hops may be desirable for delivering long messages, in order to obtain a good EC/DR/D trade-off. Furthermore, Route 2 may be selected for delivery of the messages of moderate length. In other words, the routes chosen to transmit the messages of different length may be different. Therefore, routing optimization in MSNs should take into account of messages' size, especially, when they are very different, in order to reach a good EC/DR/D trade-off.

According to the above analysis, in this section, we propose another type of energy-concerned routing protocols, which are referred to as the energy-efficient social-distance dependent routing (ESDR) protocols. In the ESDR protocols, the number of messages as well as their size are taken into account in routing optimization, in addition to the number of hops. To serve the purpose, we define an energy cost factor (ECF) for measuring the EC/DR/D trade-off of the routes. Specifically, the ECF of the ith route from a reference MN to the DN is defined as

$$E_{CF}^{(i,\delta)} = \frac{h_{i,\delta} x_{j,\delta}}{L} - \eta P_{i,\delta} \tag{5.7}$$

where $h_{i,\delta}$ denotes the estimated number of hops from MN i to the DN δ, $x_{j,\delta}$ represents the length of the jth message (in bits) destined to DN δ, which is normalized by L denoting the maximum length of the possible messages (in bits), $P_{i,\delta}$ represents the delivery probability of the route from MN i to the DN δ, and, finally, η is a parameter applied to control the EC/DR/D trade-off.

As the route selection of a message sender motivates to minimize the ECF, from (5.7) we can see that, when increasing the value of η, the delivery probability becomes more significant in the ECF, resulting in that the delivery probability is more emphasized than the energy consumption in the ESDR protocols. On the other hand, when reducing the value of η, the first term in (5.7) becomes more dominant. Thus, the corresponding routing protocols put more emphasis on the energy consumption.

In order to reflect the ECF of (5.7) in the routing protocols for MSNs, the delivery probability and the number of hops between any two nodes, as well as the length of messages need to be estimated. First, in MSNs, the delivery probability between any two nodes can be estimated by considering the chance of direct and indirect contacts, with the aid of, such as, distributed information exchange in the SCPR [79]

Second, as shown in the SCPR protocol [79], hop estimation can be obtained from the knowledge gained from MNs' encounter process. Similar to [79], where only delivery ratio is concerned, each MN can build a SCPR's routing table, referred to as SCP table, which includes the direct contact probability been two MNs A and B, expressed as $P_{d(A,B)}$, the transitive delivery probability of $P_{t(A,B)}$ between MNs A and B, and the estimated number of hops from MN A to MN B. As an example, let us consider the MSN shown in Fig. 5.3. Correspondingly, Table 5.1 shows the route table updates, when N_1 and N_2 meet. Specifically, Table 5.1(a) and 5.1(b) show the routing tables of N_1 and N_2 before they meet. They are updated to Tables 5.1(c) and 5.1(d) after their meeting. As seen in Tables 5.1(c) and 5.1(d), the number of hops is determined by the route yielding the highest SCP.

Finally, in terms of the maximum length L of messages, it is obviously depended on the applications or services. In general, messages are not the same length, but may obey certain distribution depended on the specific application. Specifically, for emails, we analyzed two sets of email messages extracted from the individual email inboxes of the University of Southampton during a 39-month period between October 2012 and December 2015. The first set of emails shown in Fig. 5.4(a) consists of 1696 emails, from which we found that the average email length and the standard deviation are approximately 106 and 781 characters, respectively. By contrast, the second set shown in Fig. 5.4(b) contains 2118 email messages, the average length of which is 100 characters and the standard deviation of which is 408 characters. As shown in Figs. 5.4(a) and 5.4(b), both data sets are best fitted to an exponential distribution formulated as

$$f(x) = \alpha e^{-\beta(x-x_0)} \tag{5.8}$$

where x is the email length, while α, β and x_0 are the fitting parameters.

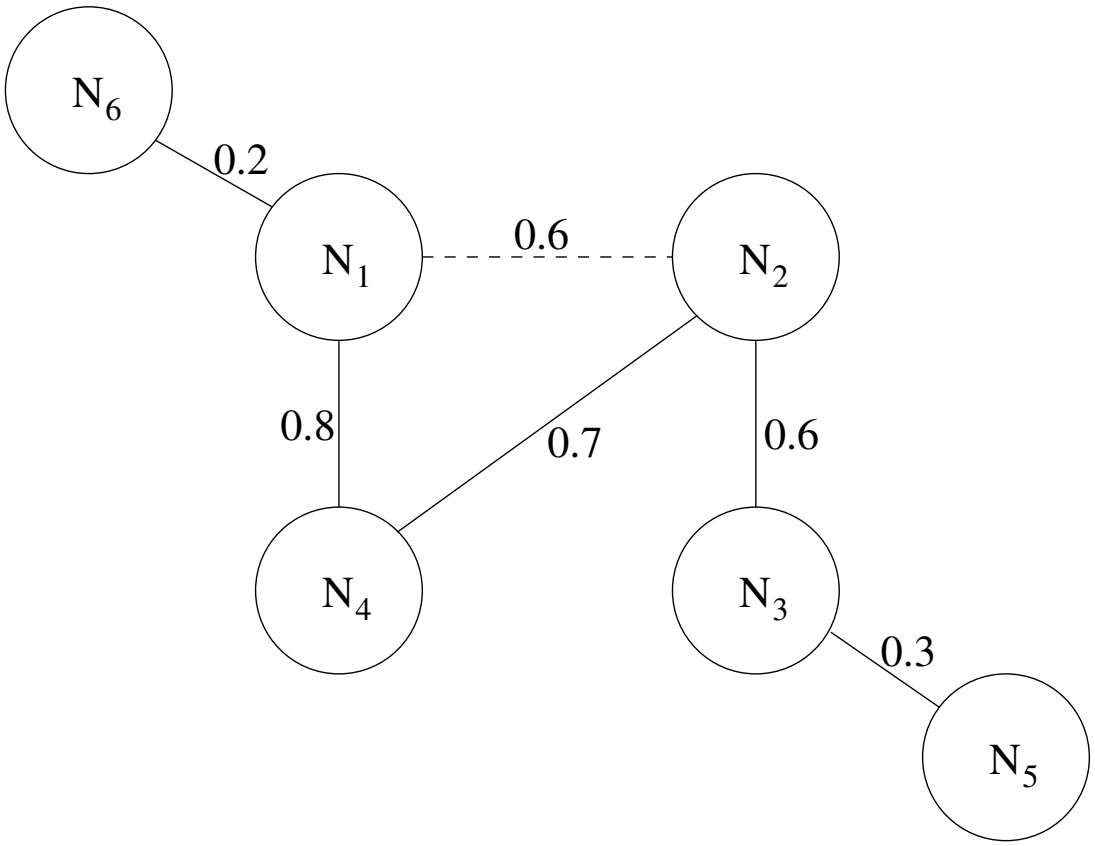

Figure 5.3: An exemplified diagram showing the SCPs between MNs.

In order to find a value for L in (5.7), in this chapter, we consider the one-sided upper bound of message length's distribution, which can be evaluated from the formula [103]

$$L(\lambda) = -\frac{ln(1-\lambda)}{\beta} + x_0 \tag{5.9}$$

where λ is the one-sided upper confidence limit of an exponential distribution, while β and x_0 are provided in (5.8).

With the above preparation, we can now describe the ESDR protocols. In these ESDR protocols, when a MN A carrying a message meets a MN B, MN A then evaluates the ECFs using (5.7), and compares the ECF of the route from MN A to the DN, which is expressed as ECF($A \rightarrow D$), with the ECF of the route from MN A via MN B to the DN, which is expressed as ECF($A \rightarrow B \rightarrow D$). If ECF($A \rightarrow D$) is larger than ECF($A \rightarrow B \rightarrow D$), then, MN A forwards the message to MN B. Otherwise, MN A keeps the message until it meets another intermediate MN or the DN. If the next encountered MN is an intermediate MN, the above process repeats.

As an example, let us consider Fig. 5.2, where three possible routes exist from SN to the DN as stated at the beginning of this section. Let us choose $\lambda = 0.99$, which yields the maximum message length of $L = 84$ Kbytes, when the first data set in Fig. 5.4(a) is considered. Then, when

Table 5.1: An example of the SCP table update process during an encounter between N_1 and N_2, based on the scenario shown in Fig.5.3. Tables a) and b) represent the SCP tables of N_1 and N_2 before the two MNs meet. Tables c) and d) show the SCP tables of N_1 and N_2 after the update process.

(a)

DN	$P_{d(N_1,.)}$	$P_{t(N_1,.)}$	h
N_2	0	0.56	2
N_3	0	0.336	3
N_4	0.8	0	1
N_5	0	0.1008	4
N_6	0.2	0	1

(b)

DN	$P_{d(N_2,.)}$	$P_{t(N_2,.)}$	h
N_1	0	0.56	2
N_3	0.6	0	1
N_4	0.7	0	1
N_5	0	0.18	2
N_6	0	0.112	3

(c)

DN	$P_{d(N_1,.)}$	$P_{t(N_1,.)}$	h
N_2	0.6	0.56	1
N_3	0	0.36	2
N_4	0.8	0.42	1
N_5	0	0.108	3
N_6	0.2	0.0672	1

(d)

DN	$P_{d(N_2,.)}$	$P_{t(N_2,.)}$	h
N_1	0.6	0.56	1
N_3	0.6	0.336	1
N_4	0.7	0.48	1
N_5	0	0.18	2
N_6	0	0.12	2

we set $\eta = 0.5$ in Eq.(5.7), we can obtain three ECFs of the three routes for delivery of a 1-Kbyte email as

1. Route 1: $ECF_1 \approx -0.038$;
2. Route 2: $ECF_2 \approx -0.126$;
3. Route 3: $ECF_3 \approx -0.214$.

Therefore, for a 1-Kbyte message, Route 3 should be chosen by SN, since it has the lowest ECF among the three possible routes. Similarly, for delivery a longer message, such as, a 80-Kbyte message, it can be shown that the ECFs of the three routes are 0.9, 1.75, and 2.61, respectively. Accordingly, Route 1 is the preferred one towards the DN.

5.5 Performance Evaluation

In this section, we evaluate and demonstrate the performance of our proposed energy-efficient routing techniques in conjunction with the SCPR protocol proposed in [79]. We will emphasize the impact of the parameter η in Eq.(5.7) on the energy-efficiency, delivery ratio, and average end-to-end delay. The simulations for the results in this section were conducted based on our community-based mobility model previously proposed in Chapter 3 and in [79, 104].

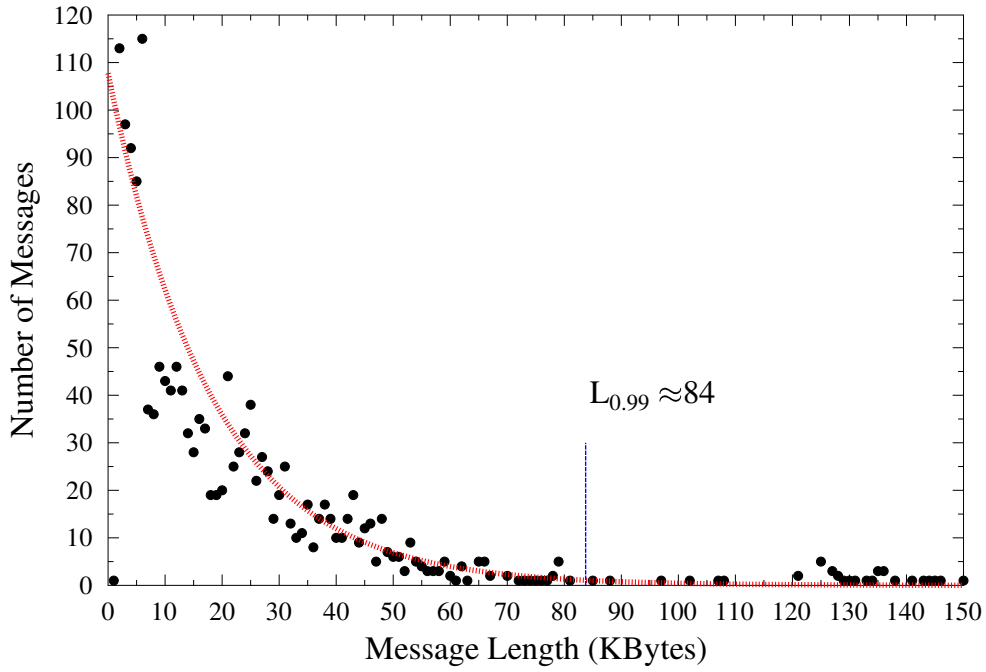

(a)

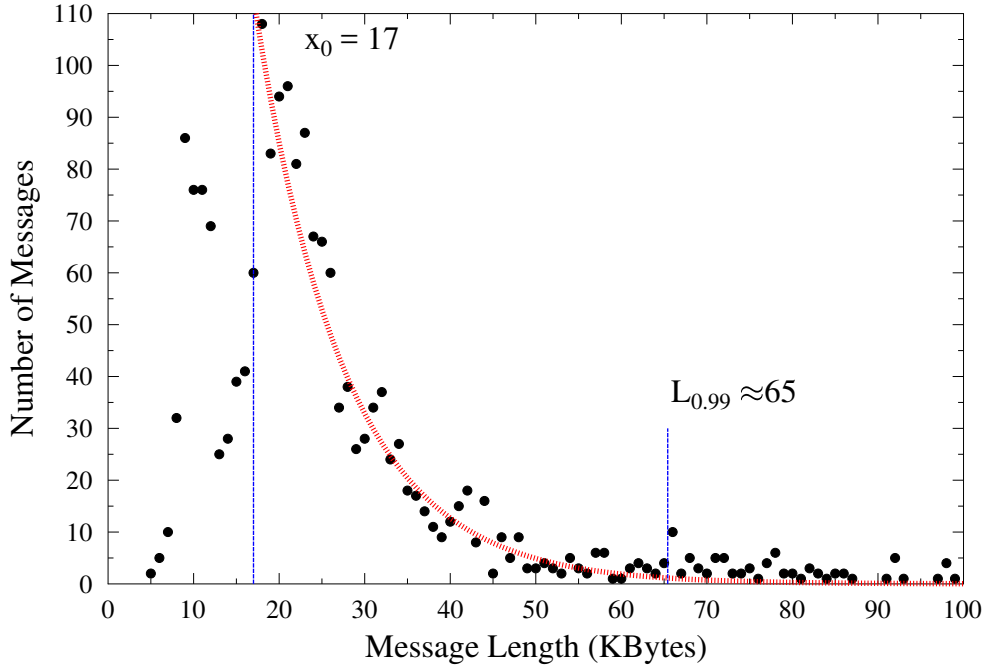

(b)

Figure 5.4: Distribution of the email lengths measuring in bytes. Both data sets are best fitted to the exponential distribution following Eq.(5.8). The parameters of the best fits are, a: $\alpha \approx 107.768, \beta \approx 0.055, x_0 = 0$; b: $\alpha \approx 113.146, \beta \approx 0.095, x_0 = 17$

5.5.1 Simulation Setup

We consider a MSN with the coverage of 1000×1000 square meters (m^2). Within the area, there are 15 communities of each covering an area of 100×100 m^2. At the beginning of simulation, we

assume that the 15 communities are randomly distributed in the considered area. Some communities may overlap with each other, owing to the assumption that one MN may belong to several communities. We assume that there are 150 MNs, which are first randomly distributed, and then randomly move inside the areas covered by the 15 communities according to the considered mobility model. Each MN is assigned a random number, which represents the MN's preferred community (PC).

We set the probabilities of a MN moving within one, two and three communities to be 0.125, 0.375 and 0.25, respectively. Beyond three communities, the probability is halved whenever the MN involves one more community. Following this rule, we can know that the probability of one MN simultaneously included in four communities is 0.125, which is half of the probability 0.25 of one MN belonging to three communities. Similarly, the probability that one MN joins five communities is 0.0625, which is half of the probability 0.125 of one MN belonging to four communities. In this way, we can have the probabilities of the other cases. After the initial assignments of the MNs to communities, each MN moves according to the above assumptions within and across the communities.

In our MSN, for any given MN, firstly, a point within a selected PC is randomly generated, which represents the MN's next destination. Then, the MN travels towards that point with a speed chosen uniformly from $(0, V_{max}]$. After arrival at the destination, the MN pauses for a fixed time t_{pause}. Then, the above process is repeated until one simulation session is completed. During our simulation, messages are randomly generated by MNs at an interval of $t_{interval}$ with their length following an exponential distribution, as shown in Eq.(5.8). In our simulations, the parameters in Eq. (5.8) are chosen to be $\alpha = 105, \beta = 0.05, x_0 = 0$, and $\lambda = 0.99$. Furthermore, in our experiments, messages' lifetime is set to 3 hours, meaning that a message will be deleted from the network, if it is not delivered to its DN within 3 hours. In our MSN, we assume that a MN is capable of detecting its neighbors having the distance upto r meters from it. When a neighbor MN is discovered, the processes for routing metric update and message transmission, as described in Section 5.3, are triggered. In detail, the parameters used in our experiments are chosen as $r = 30\ m$, $V_{max} = 20$ meters per second (m/s), and $t_{pause} = 10$ minutes. Additionally, in order to demonstrate the EC/DR/D trade-off, we assume that the energy consumption factor seen in Eq.(5.4) is reflected by the transmission power with a value of $\gamma \approx 1.7 \times 10^{-5}$, which is a value similar to that used in the experiment of [87].

In summary, the parameters used in our studies are listed in Table 5.2. According to the parameter values shown in Table 5.2, our experiment is then carried out as follows. At the beginning of an experiment, communities, MNs, mobility patterns as well as messages are generated, which are stored in a file. Then, simulations for our ESCPR, EPRoPHET, and EBUBBLE protocols are

Table 5.2: Parameters for simulations

Parameter	Value	Unit
Simulation area	1000×1000	m^2
Community area	100×100	m^2
Number of communities	15	
Number of MNs	150	
V_{max}	20	*m/s*
r	30	*m*
t_{pause}	10	*minutes*
$t_{interval}$	60	*s*
T	30	*days*
Messages' lifetime	3	hours
α	105	
β	0.05	
x_0	0	
λ	0.99	
γ	1.7×10^{-5}	

executed to generate the performance results. Furthermore, in order to attain sufficient accuracy, each simulation is repeated five times to obtain the final average results. Accordingly, the results depicted in the figures represent the average of the results obtained from simulations. Additionally, when steady-state performance is concerned, the results are then obtained from the last 15 days of the 30 day period.

5.5.2 Performance Results

Fig. 5.5 shows the performance of the delivery ratio, average energy consumption per message and the average delay of delivered messages of our ESCPR protocol with different threshold values for P_{th}, when message's lifetime is set to infinity. Fig. 5.6 shows the same performance metrics as Fig. 5.5, when messages' lifetime is set to 3 hours. When comparing Fig. 5.5(a) and Fig. 5.6(a), we can observe that, when message's lifetime is infinity, using different thresholds does not affect the delivery ratio. By contrast, when message's lifetime is limited, a higher threshold of P_{th} yields a lower delivery ratio. This is because, when P_{th} increases, average message delay increases, as shown in Fig. 5.6(a), which results in that some messages having delay longer than 3 hours are deleted and not successfully delivered. As shown in Fig. 5.5(b) and Fig. 5.6(b), explicitly, the energy consumption for both the considered cases decreases, as the threshold P_{th} increases. However, as P_{th} increases, the average delay of the delivered messages also increases, as shown in Figs. 5.5(c) and 5.6(c), although when comparing Figs. 5.5(c) and 5.6(c), the delay in Figs. 5.6(c) with 3-hour message's lifetime is lower than the corresponding delay shown in Fig. 5.5(c) having infinite message lifetime. From Figs. 5.5 and 5.6, we can clearly see that there exists a EC/DR/D

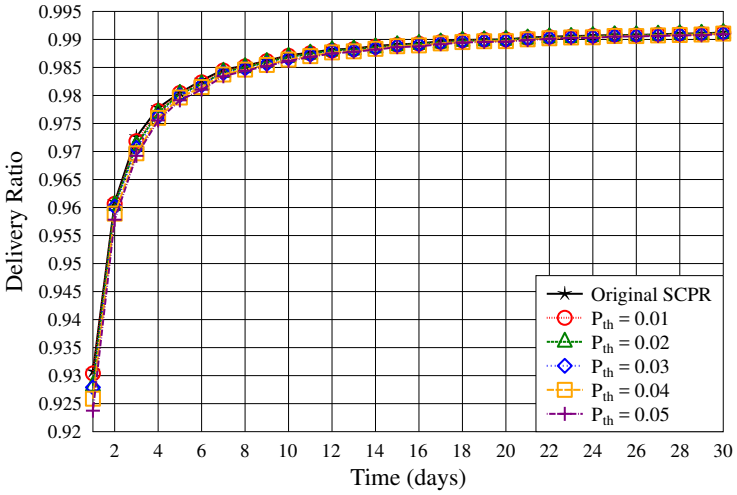

(a) Delivery Ratio

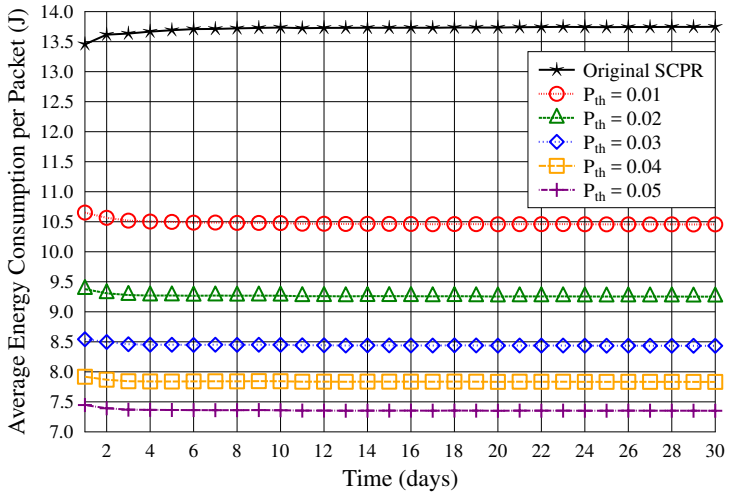

(b) Energy Consumption

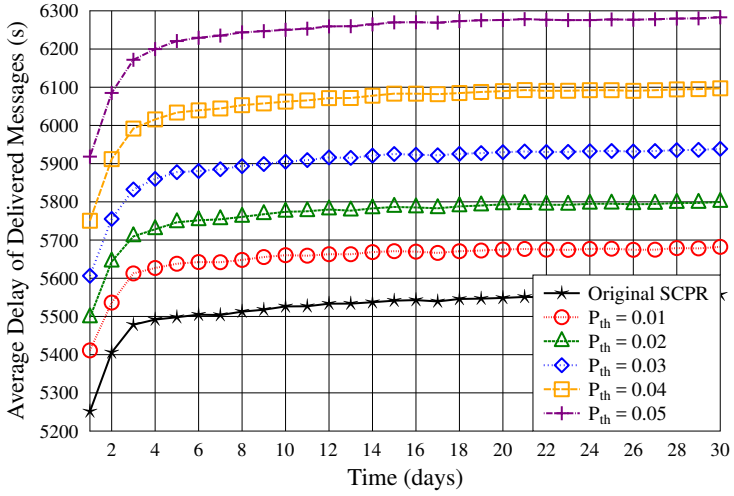

(c) Average Delay

Figure 5.5: Performance of the ESCPR protocol with infinite message lifetime.

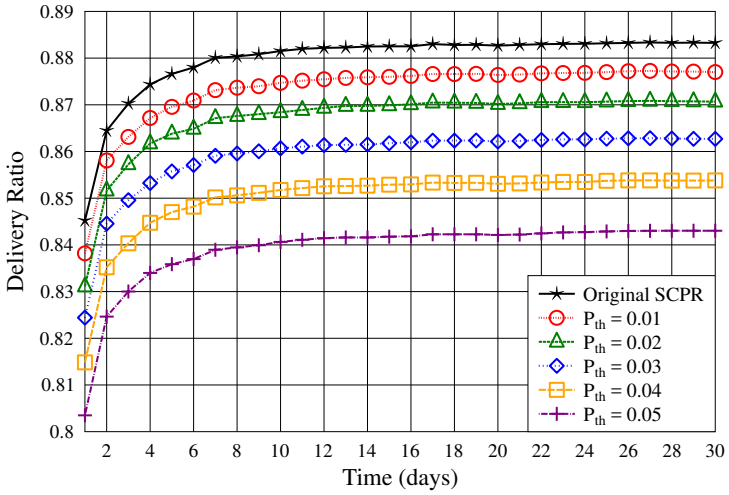

(a) Delivery Ratio

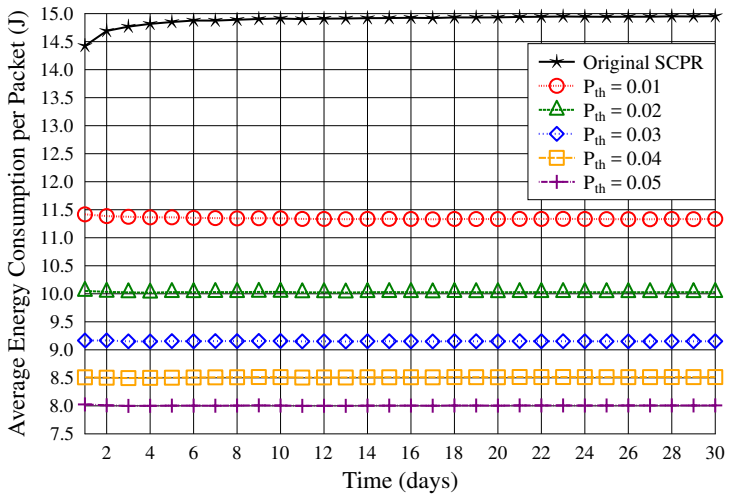

(b) Energy Consumption

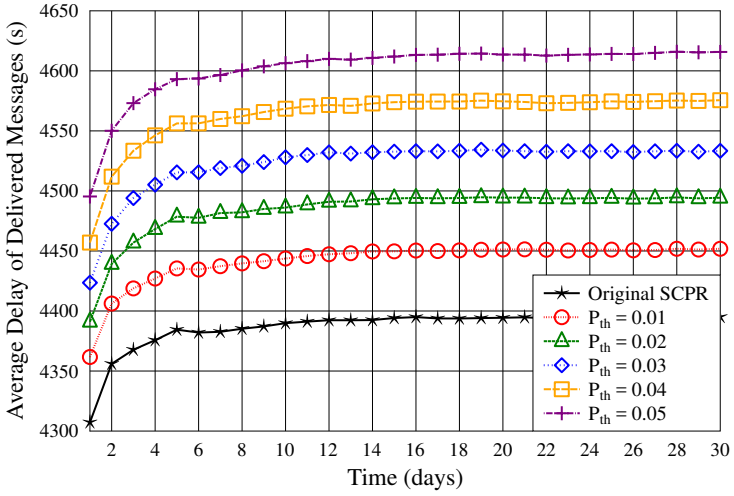

(c) Average Delay

Figure 5.6: Performance of the ESCPR protocol, when message's lifetime is 3 hours.

Table 5.3: Values of global (G) and local (L) P_{th} for Fig.5.8

	Case A		Case B		Case C	
	G-P_{th}	L-P_{th}	G-P_{th}	L-P_{th}	G-P_{th}	L-P_{th}
0	0	0	0	0	0	0
1	0.05	0	0	0.005	0.05	0.005
2	0.1	0	0	0.01	0.1	0.01
3	0.15	0	0	0.015	0.15	0.015
4	0.2	0	0	0.02	0.2	0.02
5	0.25	0	0	0.025	0.25	0.025

trade-off, and in general, delay and delivery ratio may have to be paid for saving energy.

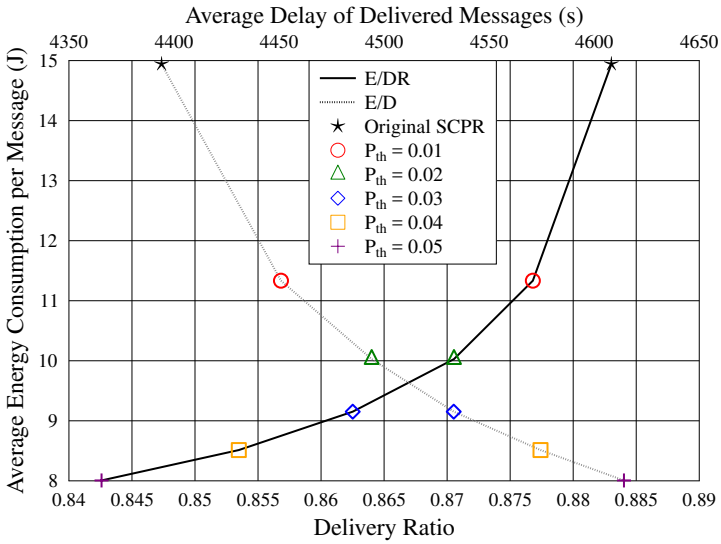

Figure 5.7: Energy consumption versus delivery ratio and average delay for the ESCPR protocol with different thresholds for the EC/DR/D trade-off, when assuming message's lifetime of 3 hours.

Explicitly, the trade-off among the energy consumption, delivery ratio and the delay is shown in Fig.5.7 for the ESCPR protocol with different thresholds of P_{th}, when message's lifetime is assumed to be three hours. Typically, the reduction of energy consumption is paid by longer delay and/or decrease of delivery ratio. As shown in Fig.5.7, interestingly, the energy consumption increases approximately exponentially with the increase of the delivery ratio, while it decreases approximately exponentially with the increase of delay. Note that, in the case that message's lifetime is infinite, as shown in Fig. 5.5, the threshold P_{th} does not affect the delivery ratio noticeably. Correspondingly, trade-off only exists between the average delay and energy consumption.

In Fig.5.8, we study the energy consumption versus the delivery ratio and the average delay performance of the EBUBBLE protocol, when different threshold values are considered. As de-

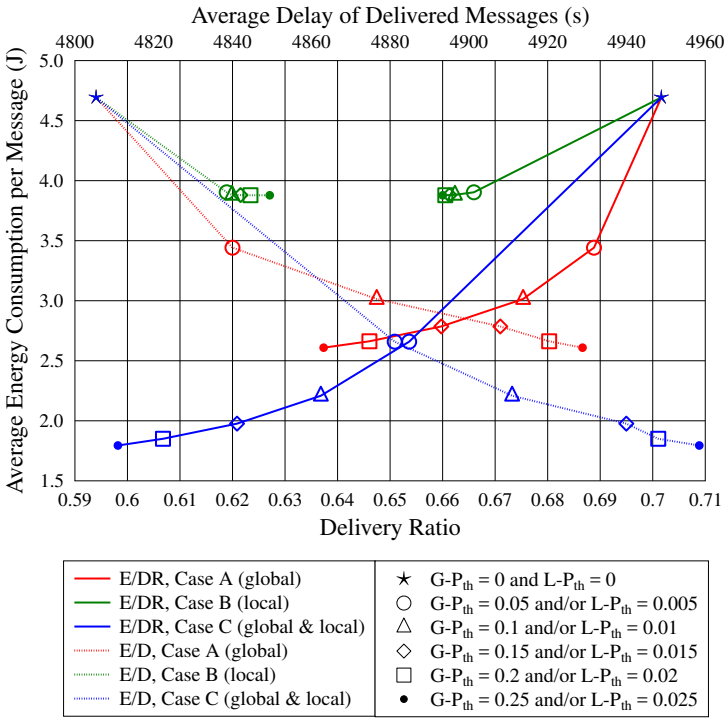

Figure 5.8: Energy consumption versus delivery ratio and average delay for the EBUBBLE protocol operated in Cases A, B and C as defined in Table 5.3.

scribed in Section 5.3, the EBUBBLE protocol is extended from the BUBBLE protocol [16] by introducing our EnCoR algorithm to achieve the EC/DR/D trade-off. Since the BUBBLE protocol uses two types of popularity ranking, namely global ranking and local ranking, in Fig.5.8, we consider three cases as detailed in Table 5.3. Specifically, in Case A, we set the threshold L-$P_{th} = 0$ for the local ranking, while the threshold of G-P_{th} for the global ranking is set to five different values. In contrast, in Case B, the threshold L-P_{th} is set to five different values, while the threshold G-P_{th} is set to 0. Finally, in Case C, both the thresholds L-P_{th} and G-P_{th} are set to the same five different values similar to the above two cases. As shown in Table 5.3, for all the three cases, the thresholds for the local popularity are lower than the corresponding thresholds for the global popularity. This is because in the EBUBBLE protocol, the number of encounters between any two MNs with the same affiliation is usually lower than the number of encounters between any two other MNs that not necessary have the same affiliation. Note that, in Fig.5.8, the topmost points correspond to $P_{th} = 0$. From the results of Fig.5.8 we can see that, in general, the EC/DR/D trade-off presents a similar trend as that of the ESCPR shown in Fig. 5.7. Specifically, when the threshold (either global or local, or both) is increased, the delivery ratio slightly reduces, while the amount of energy consumed per message decreases approximately exponentially. Correspondingly, the EBUBBLE

protocol yields a longer average message delay. Furthermore, Fig.5.8 shows that the best EC/DR/D trade-off may be achieved in Case C. For a given delivery ratio and a given delay, the energy consumption in Case C is lower than that in case A or case B.

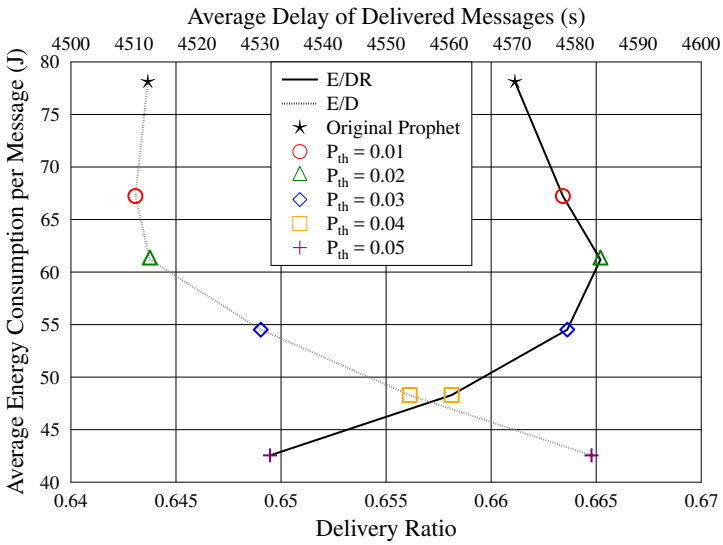

Figure 5.9: Energy consumption versus delivery ratio and average delay for the EPRoPHET protocol with different thresholds for the EC/DR/D trade-off.

Finally, in Fig.5.9, we show the trade-off between the energy consumption and the delivery ratio, and that between the energy consumption and the average delay for the MSNs employing the EPRoPHET protocol. Surprisingly, as seen in Fig.5.9, when the threshold of P_{th} is increased from 0 to about 0.02, the performance of the EPRoPHET protocol may simultaneously improve in terms of the delivery ratio, delay and energy consumption. By contrast, when the threshold of P_{th} is further increased from 0.02 to 0.05, the EC/DR/D trade-off of the EPRoPHET protocol appears the similar characteristics as the ESCPR and the EBUBBLE protocols. The reason for the performance behavior of the EPRoPHET within the threshold range from $P_{th} = 0$ to about $P_{th} = 0.02$ is that the original PRoPHET protocol has a strong greedy characteristic. As mentioned in Section 5.2, this greedy characteristic results in choosing a route that is inefficient in terms of energy consumption, delivery ratio and/or delay.

The results demonstrated so far were obtained under the assumption of fixed message length. Below we consider the cases where message length obeys the PDF of an exponential distribution. As an specific example, Fig. 5.10 shows the performance trade-off of the ESCPR protocol in terms of delivery ratio, average message delay of the delivered messages, average hop count per delivered message, as well as the energy consumption, when various values for the parameter η seen in Eq.(5.7) are used in order to demonstrate the performance trade-off. As shown in Fig. 5.10(a), a

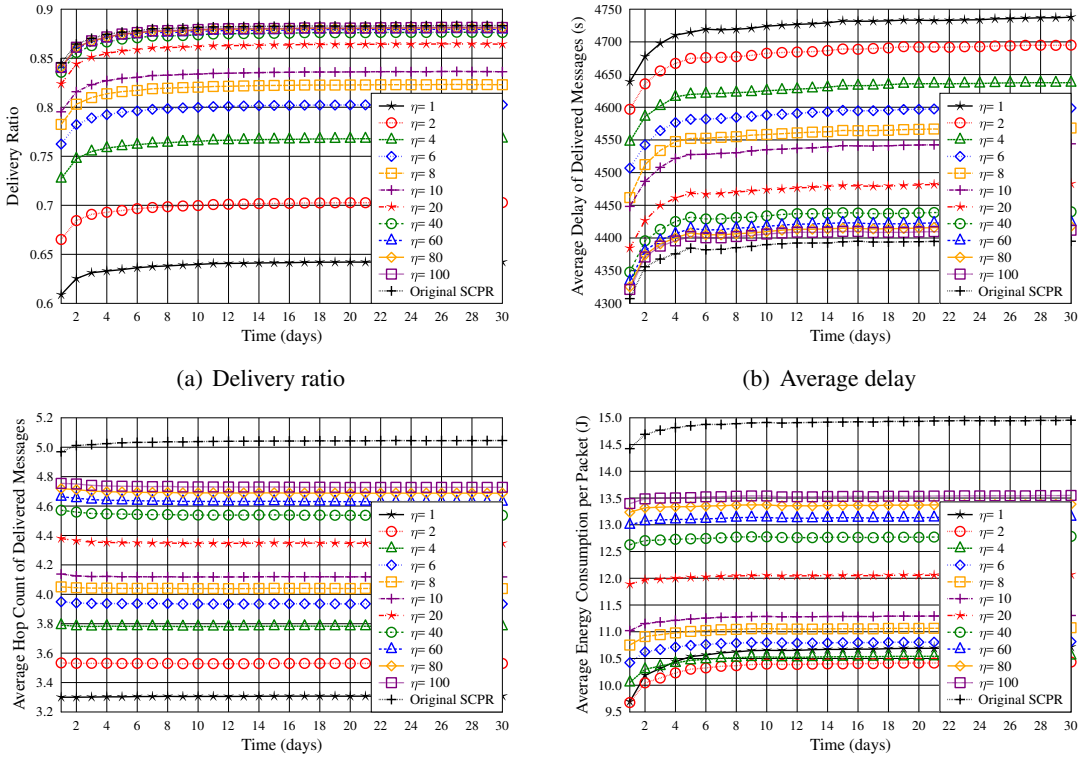

(a) Delivery ratio

(b) Average delay

(c) Hop Count

(d) Energy Consumption

Figure 5.10: Performance of the ESCPR protocol, when message length obeys exponential distribution and message's lifetime is 3 hours.

lower η value yields a lower delivery ratio, as the protocol becomes more desirable for delivering messages using less number of hops, as seen in Fig. 5.10(c). As shown in Fig. 5.10(b), when the η value decreases, the average delay increases. Furthermore, as shown in Fig. 5.10(d), the energy consumption per message decreases, as the value of η in Eq.(5.7) decreases. The reason for the above observation is because the value of η in Eq.(5.7) has a significant impact on route selection. According to the protocol and Eq.(5.7), the route selection depends more on the delivery probability, when the value of η increases. As the result, a route with higher delivery probability is more likely to be selected. Consequently, the delivery ratio and hop count are higher, while the average delay becomes lower. In contrast, when the value of η decreases, the delivery probability in Eq.(5.7) yields less impact, while the energy consumption becomes more dominant. In this case, the ESCPR algorithm gives a higher priority to the routes with lower energy consumption than to the routes with higher delivery probability. Consequently, the delivery ratio and the average number of hops reduce, but the average delay increases. However, as shown in Fig. 5.10(d), when the value of η becomes lower than $\eta = 6$, the energy consumption per delivered message increases due to the increase of message losses, as message's lifetime was limited to 3 hours.

More explicitly, in Fig.5.11, we demonstrate the trade-off among the energy consumption, de-

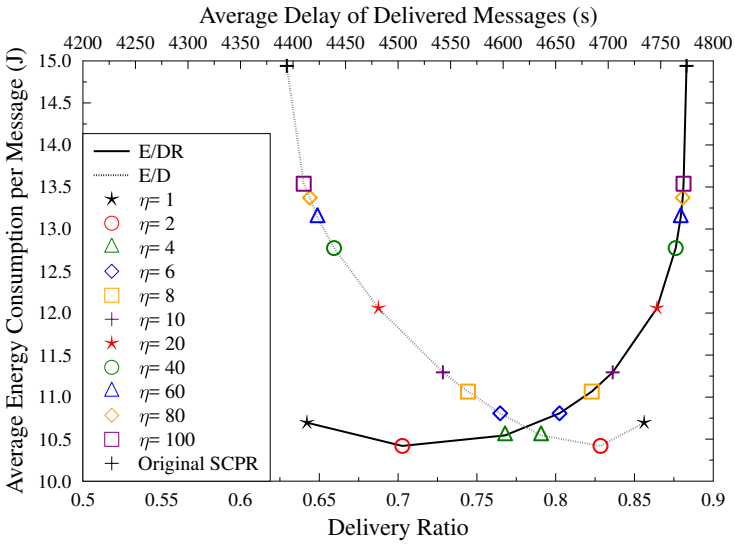

Figure 5.11: EC/DR/D trade-off of the SCPR protocol, when message length obeys exponential distribution and message's lifetime is 3 hours.

livery ratio and the delay. Typically, the reduction of energy consumption results in longer delay and/or decrease of delivery ratio of the ESCPR protocol operated with different value of η, in order to achieve the required E/DR/D trade-off. As shown in Fig. 5.11, again, the energy consumption has an approximately exponentially increasing relationship with the increase of the delivery ratio, and an approximately exponentially decreasing relationship with the increase of the delay. As shown in Fig. 5.11, the above stated relationship continues provided that $\eta > 2$. When $\eta < 2$, the average energy consumption per message becomes higher, while the delivery ratio decreases and the average delay increases. This observation can be explained as follows. According to Eq. (5.7), when the value of η is very low, the route selection is mainly determined be the energy consumption, the routes with low energy consumption are chosen over the routes with high delivery probabilities. In this case, some of the selected routes may not successfully deliver the messages, although they are supposed to consume little energy. Therefore, it wastes energy, due to the unsuccessful message transmission.

In contrast to Fig.5.11, Fig.5.12 shows the energy efficiency versus delivery ratio and average delay performance of the ESCPR protocol. Here, the energy efficiency E_{ff} is evaluated by

$$E_{ff} = \frac{\sum_{i=1}^{N_d} x_i}{\sum_{i=1}^{N} E_i}, \tag{5.10}$$

reflecting the number of information bits transmitted by a unit of energy. In Eq. (5.10), x_i is length in bits of the ith message, E_i is the energy consumed to send the ith message from SN to DN,

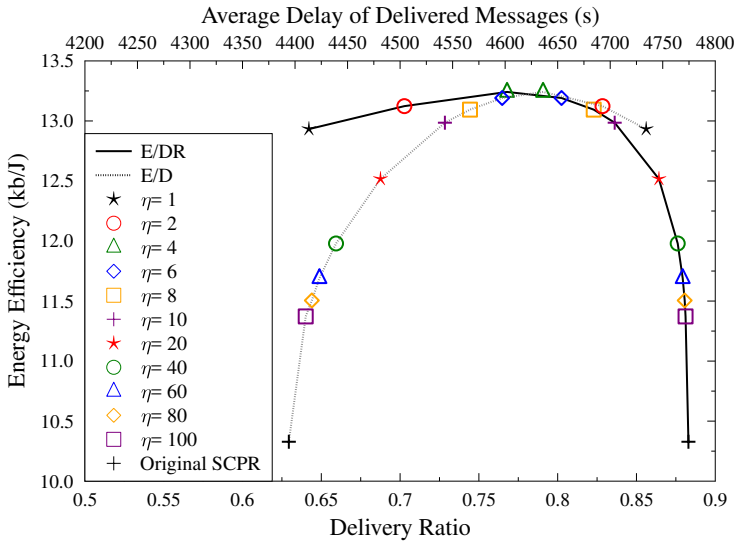

Figure 5.12: Energy-efficiency versus delivery ratio and average delay for the SCPR protocol, when message length obeys exponential distribution and message's lifetime is 3 hours.

N_d is the total number of delivered messages, while N is the total number of messages attempted to deliver. Fig.5.12 shows that, when $\eta < 6$, the energy-efficiency increases nearly linearly with the delivery ratio. By contrast, when $\eta > 6$, the energy efficiency decreases approximately exponentially with the increase of the delivery ratio. In the context of the delay, as seen in Fig. 5.11, the energy efficiency increases approximately exponentially with the increase of the average delay, provided that $\eta > 6$. When $\eta < 6$, the energy efficiency decreases as the delay increases. From Figs. 5.11 and 5.12, we can learn that the value of η should not be too small. Otherwise, the route selection will be mainly determined by energy consumption, without considering the impact of delivery ratio.

5.6 Summary and Conclusions

Two energy-concerned routing protocols, referred to as the energy-concerned routing (EnCoR) and the energy-efficient social distance routing (ESDR) protocols, have been proposed for achieving the EC/DR/D trade-off in the routing for MSNs. Assisted by the approaches, the SCPR, BUBBLE and the PRoPHET protocols have been extended to the ESCPR, EBUBBLE and the EPRoPHET protocols, which are capable of achieving the EC/DR/D trade-off routing in MSNs. The performance of the three routing protocols have been studied by simulation associated with the PCAM model. Our studies and performance results show that all these schemes are capable of attaining the EC/DR/D

trade-off. This is achieved via setting a threshold of delivery probability dependent, so that a message carrier can decide whether the message should be forwarded to another encountered MN or keep to itself. From our studies we can gain the insight that an optimum trade-off, for example, in the sense of maximal energy-efficiency, can be attained by setting the above-mentioned threshold and the desired parameter to their optimum values.

Chapter 6

Conclusions and Future Works

In this chapter, we first provide a summary of the main issues addressed in this thesis as well as the main findings. Then, we discuss the possible future research issues.

6.1 Conclusions

In this thesis, we have investigated some issues in MSNs. Specifically, modelling of mobilities and routing in MSNs have been focused. The main contributions from the research can be summarized as follows.

In Chapter 2, we have provided a comprehensive overview for the mobility models and routing protocols proposed for MANETs, DTNs, OPNETs, and MSNs. It can be shown that MSNs employ the unique characteristics of that MNs' mobilities are determined by the social relationship of the mobile device carriers. Correspondingly, the routing algorithms originally designed for MANETs, even for DTNs, are not efficient for operation in MSNs, and the routing algorithms for MSNs should be designed by taking into account of the social relationship of the MNs in MSNs, in order to improve the efficiency of networking.

Therefore, in Chapter 3, we have proposed two mobility models for MSNs, namely, the PCAM and the RPM models. In a little more detail, our PCAM model has been designed based on the simplicity and randomness of the RWP mobility model with taking into account of the human social behaviors of mutual preferred communities (PCs). By exploiting the fact that people have favorite places to visit, the PCAM model is more practical in comparison to the RWP mobility model, while reserving the RWP model's nature of randomness and simplicity. By contrast, our RPM model has been designed by considering even more perspectives than the PCAM model. Specifically, apart from the human social behavior of mutual PCs, the RPM model also addresses the behaviors of

humans about their daily schedules determined by their roles.

In Chapter 3, the characteristics and performance of the PCAM and RPM models have been investigated. Our studies and simulation results demonstrate that the mobility patterns generated by the PCAM model are closer to the real traces when comparing to the RWP mobility model, while the RPM mobility model fits the best with the real traces than the RWP and PCAM mobility models. In the RPM mobility model, the CCDF of the inter-contact time shows the power law distribution characteristic during the first 12 hours before truncating, which is similar to the characteristics of real mobility traces.

Following the mobility models considered in Chapter 3, then our focus has been on the routing protocols for MSNs. Specifically, we have first proposed and studied the SCPR protocol. In Chapter 4,in this protocol, three social characteristics of MNs have been considered, which are the MN's encountering frequency, regularity, and freshness. From these factors, two message delivery dependent metrics are generated, which are the direct-encounter social contact probability (P_{direct}) and the transitive social contact probability (P_{trans}). The evaluation of P_{direct} is based on both the frequency and the regularity. This is because a higher frequency meeting represents a stronger relationship between two MNs, while a higher regularity gives a higher accuracy in the prediction of the next encounter of the two MNs. By contrast, the freshness of a contact affects the value of P_{direct} by applying the ageing mechanism. In addition to depending on the direct contact for message delivery transitivity reflecting indirect contact can also be used for message delivery, which is counted by the transitive social contact probability, P_{trans}. In our scheme, the value of P_{trans} of a MN is given by the P_{direct} of the encountered MN that has the strongest relationship with a designated destination in the egocentric perspective. When two MNs encounter, each of them calculates an accumulative P_{trans}, which combines the first hop's P_{direct} and the P_{trans} of all the other FNs. Then, a Social Contact Probability (SCP), which indicates the chance of message delivery, is obtained as the higher value between the accumulative P_{trans} and P_{direct}.

As shown in Chapter 4, our SCPR routing protocol has been designed by exploiting the SCP. In this chapter, the performance of the proposed SCPR protocol and that of five existing routing protocols for MSNs have been investigated in the context of a proposed and more realistic PCAM mobility model. Furthermore, we have studied the impact of the accuracy of the information about MNs' behavior on the achievable performance of the SCPR protocol. Our studies and performance results show that the SCPR protocol is capable of integrating the merits of the Epidemic, PRoPHET, SimBet, LABEL and BUBBLE protocols, while circumvents their shortcomings of resource-greedy of the Epidemic protocol, and of high message delivery latency of the PRoPHET, SimBet, LABEL and BUBBLE protocols. Furthermore, the SCPR protocol is robust to the inaccuracy of the information about MNs' behavior.

Following the philosophy of the research in literature, our SCPR routing protocol has also been designed with the motivation to maximize delivery and/or minimize delivery delay. However, in the future wireess networks including MSNs, energy-efficiency constitutes a critical issue that should be considered. Therefore, in Chapter 5, we have addressed the energy-concerned routing in MSNs. Specifically, we have considered the routing protocols for MSNs that are capable of achieving the trade-off among energy consumption (EC), delivery ratio (DR), and delay (D), shortened as the EC/DR/D trade-off. In this chapter, we have proposed two types of energy-concerned routing protocols for MSNs. In the first type of protocols, which are referred to as the energy-concerned routing (EnCoR) protocols, we extend three existing routing protocols, namely, our previously proposed SCPR protocol [79], the BUBBLE protocol [16] and the PRoPHET protocol [5, 64], to the corresponding routing protocols achieving the EC/DR/D trade-off. These extended protocols are respectively referred to as the ESCPR, EBUBBLE and the EPRoPHET protocols for convenience of description. As detailed in Chapter 5, in these extended routing protocols, the EC/DR/D trade-off is controlled by a threshold introduced to the route selection process. When a message carrying MN encounters another MN, it forwards the message to the encountered MN, only when the delivery probability from the encountered MN to the DN is higher than that from itself to the DN by at least the threshold. In this way, the ESCPR, EBUBBLE, and the EPRoPHET protocols can effectively control the trade-off among the consumed energy, delivery ratio and average delay.

In the context of the second type of energy-concerned routing protocols, we have proposed a ESDR protocol. For this protocol, we have first analyzed the effect of message length on the energy consumption during message transmission. Then, we have proposed a hop estimation method for finding the shortest delivery route based on the social relationship among the MNs. The ESDR protocol makes the routing decisions based on these two metrics as well as the delivery probabilities. By controlling the contribution of these factors, the ESDR can control the EC/DR/D trade-off. Finally, the performance of these routing protocols has been investigated by simulations based on our PCAM mobility model. Our studies and performance results show that all these schemes are capable of attaining the EC/DR/D trade-off. This is achieved via setting a threshold of delivery probability dependent, so that a message carrier can decide whether the message should be forwarded to another encountered MN or keep to itself. From our studies we can gain the insight that an optimum trade-off, for example, in the sense of maximal energy-efficiency, can be attained by setting the above-mentioned threshold and the designed parameter to their optimum values.

6.2 Future Works

In this thesis, we have investigated some issues in mobility modelling and routing in MSNs. There are a range of challenges requiring further study, which constitute the future research issues.

Realistic Mobility Models

First, in MSNs, the accuracy of performance evaluation of routing protocols is depended on the realistic level of the mobility models. In this thesis, we have proposed two new mobility models, which can exploit the human social behaviors, including community-bound mobility behavior, role-based schedule, MN's home assignment, and randomness from RWP mobility model. While integrating the merits of random-based mobility models, our proposed mobility models are in general more realistic than most of the existing ones, such as, the RWP mobility model. However, people may have different mobility patterns on different day and time of the day, including, weekdays, weekends, holidays, rush hours during the morning and the evening, day time, and night time. For instances, students usually go to schools on weekdays but stay at home during the weekends, employees travel from home to their offices everyday except weekend and holidays. By taking into account of these facts, we may improve our mobility models, in order to bring them further closer to reality.

Furthermore, we may improve MNs' mobility modelling within and between communities. In [57], apart from having a number of hotspots, similar to communities in our mobility models, it is assumed that MNs may occationally travel to an area outside of the hotspots. In [37], MNs are assumed to be still within home communities, while they move and pause at desks, when they are in their workplaces. Furthermore, in [37], three ways of transportation between communities have been considered, which include walking, traveling by cars and buses, so as to reflect the speeds and selected routes of MNs. In [36], some other statistical features of MNs' mobility and communities are exploited. Specifically, it is suggested that MNs' flight and pause-times have the characteristic of the power law distributions, while the distances between communities on either one or multiple dimensions are also best described by power law distribution. All these features may be integrated into our PCAM and RPM mobility models in order to make them more realistic.

Novel Routing Protocols for MSNs

Based on the mobility models that are capable of modelling closely the real MSNs, it is highly important to design the high-efficiency routing protocols. Depending on the application scenarios and the specific services provided, corresponding routing protocols have to be designed, with the objectives to maximize the message delivery ratio, minimize message delivery delay, minimize the resource consumption, minimize the operational complexity, etc., or their joint or trade-off.

Energy-Efficient Routing and Performance Evaluation

In Chapter 5, we have proposed two types of energy-concerned routing protocols in MSNs. To the best of our knowledge, this was the first attempt to design the energy-efficient routing protocols for MSNs. In literature, the routing protocols for MSNs have mainly been designed to achieve the highest possible delivery ratio or/and lowest possible delivery delay by conceptually taking into

account of the operational resources. By contrast, our EnCoR and ESDR routing protocols have explicitly integrated the energy-consumption, delivery ratio, and delay into the route selection, resulting in the routing protocols, such as, ESCPR, EBUBBLE, and EPRoPHET protocols, that are capable of attaining a EC/DR/D trade-off. However, in addition to the routing protocols achieving the EC/DR/D trade-off, there are many other research issues in the energy-concerned (or energy-efficient) routing. First, even in the routing protocols achieving the EC/DR/D trade-off, we are not clear about how the optimum trade-off is achieved, and what parameters should be engaged for reaching the optimum trade-off. Second, instead of optimising the EC/DR/D trade-off, the routing protocols may be designed to directly maximize the energy-efficiency, which is explained by the number of successfully delivered bits normalised by the energy consumed for delivering these data bits. Third, as discussed in Chapter 5, the message length directly affects the routing performance in terms of energy consumption. We may look further into each different type of messages and the difference in message length for different services. Forth, apart from previous discussion, the transmission range between any two MNs, when a message transmission is started, could affect the energy consumption. Fifth, apart from enegy, we may consider other resouce types, such as bandwidth, which are consumed during a message transmission. Sixth, the performance evaluation and simulation the routing protocols in MSNs also constitute the important research issues. Accordingly, we may replace the PCAM model using in Chapter 4 and 5 with the RPM model or a more realistic mobility model. Furthermore, in the study of the routing protocols for MSNs, model based simulations have been the typical approaches. A very important and highly challenging research area is to find appropriate mathematical tools for the design of routing protocols as well as their performance evaluation.

Bibliography

[1] M. Liu, Y. Yang, and Z. Qin, "A survey of routing protocols and simulations in delay-tolerant networks," in *Proceedings of the 6th International Conference on Wireless Algorithms, Systems, and Applications*, (Berlin, Heidelberg), pp. 243–253, Springer-Verlag, 2011.

[2] Z. Feng and K.-W. Chin, "State-of-the-art routing protocols for delay tolerant networks," *CoRR*, vol. abs/1210.0965, 2012.

[3] A. Vahdat and D. Becker, "Epidemic routing for partially-connected ad hoc networks," tech. rep., Duke University, 2000.

[4] A. Chaintreau, P. Hui, J. Crowcroft, C. Diot, R. Gass, and J. Scott, "Pocket switched networks: real-world mobility and its consequences for opportunistic forwarding," tech. rep., University of Cambridge, 2005.

[5] A. Lindgren, A. Doria, and O. Schelén, "Probabilistic routing in intermittently connected networks," *ACM SIGMOBILE Mobile Computing and Communications Review*, vol. 7, pp. 19–20, July 2003.

[6] S. Milgram, "The small-world problem," *Psychology Today*, vol. 1, pp. 61–67, May 1967.

[7] E. M. Daly and M. Haahr, "Social network analysis for routing in disconnected delay-tolerant MANETs," in *Proceedings of the 8th ACM International Symposium on Mobile ad hoc Networking and Computing*, (New York, NY, USA), pp. 32–40, ACM, 2007.

[8] J. A. Bitsch Link, N. Viol, A. Goliath, and K. Wehrle, "SimBetAge: utilizing temporal changes in social networks for pocket switched networks," in *Proceedings of the 1st ACM Workshop on User-provided Networking: Challenges and Opportunities*, (New York, NY, USA), pp. 13–18, ACM, 2009.

[9] C. Boldrini, M. Conti, and A. Passarella, "Exploiting users' social relations to forward data in opportunistic networks: the HiBOp solution," *Pervasive and Mobile Computing*, vol. 4, no. 5, pp. 633–657, 2008.

[10] K. Jahanbakhsh, G. C. Shoja, and V. King, "Social-greedy: a socially-based greedy routing algorithm for delay tolerant networks," in *Proceedings of the 2nd International Workshop on Mobile Opportunistic Networking*, (New York, NY, USA), pp. 159–162, ACM, 2010.

[11] I. A. Hemadeh and L. L. Yang, "Popularity-aided routing protocol for mobile social networks," in *2014 IEEE 79th Vehicular Technology Conference (VTC Spring)*, pp. 1–5, May 2014.

[12] H. Wu, H. Tang, and L. Dong, *A novel routing protocol based on mobile social networks and internet of vehicles*, pp. 1–10. Cham: Springer International Publishing, 2014.

[13] A. Mtibaa, M. May, C. Diot, and M. Ammar, "Peoplerank: social opportunistic forwarding," in *INFOCOM, 2010 Proceedings IEEE*, pp. 1–5, March 2010.

[14] F. Nazir, J. Ma, and A. Seneviratne, "Time critical content delivery using predictable patterns in mobile social networks," in *Computational Science and Engineering, 2009. CSE '09. International Conference on*, vol. 4, pp. 1066–1073, Aug 2009.

[15] P. Hui and J. Crowcroft, "How small labels create big improvements," in *Proceedings of the 5th IEEE International Conference on Pervasive Computing and Communications Workshops*, (Washington, DC, USA), pp. 65–70, IEEE Computer Society, 2007.

[16] P. Hui, J. Crowcroft, and E. Yoneki, "Bubble rap: social-based forwarding in delay tolerant networks," in *Proceedings of the 9th ACM International Symposium on Mobile ad hoc Networking and Computing*, (New York, NY, USA), pp. 241–250, ACM, 2008.

[17] F. Bai and A. Helmy, *Wireless ad hoc and sensor networks*, ch. A Survey of Mobility Modeling and Analysis in Wireless Adhoc Networks. Kluwer Academic Publishers, June 2004.

[18] C. P. Mayer, *Hybrid routing in delay tolerant networks*. KIT Scientific Publishing, 2011.

[19] D. Brockmann, L. Hufnagel, and T. Geisel, "The scaling laws of human travel," *Nature*, vol. 439, pp. 462–465, jan 2006.

[20] M. C. Gonzalez, C. A. Hidalgo, and A.-L. Barabasi, "Understanding individual human mobility patterns," *Nature*, vol. 453, pp. 779–782, Jun 2008.

[21] I. Rhee, M. Shin, S. Hong, K. Lee, and S. Chong, "On the levy-walk nature of human mobility," in *IEEE 27th Conference on Computer Communications (InfoCom 2008)*, pp. 1597–1605, April 2008.

[22] M. Kim, D. Kotz, and S. Kim, "Extracting a mobility model from real user traces," in *Proceedings of 25th IEEE International Conference on Computer Communications (InfoCom 2006)*, pp. 1–13, April 2006.

[23] P. Hui, A. Chaintreau, J. Scott, R. Gass, J. Crowcroft, and C. Diot, "Pocket switched networks and human mobility in conference environments," in *Proceedings of the ACM SIGCOMM*, pp. 244–251, 2005.

[24] A. Chaintreau, P. Hui, J. Crowcroft, C. Diot, R. Gass, and J. Scott, "Impact of human mobility on opportunistic forwarding algorithms," *IEEE Transactions on Mobile Computing*, vol. 6, pp. 606–620, June 2007.

[25] T. Karagiannis, J. Le Boudec, and M. Vojnovic, "Power law and exponential decay of intercontact times between mobile devices," *IEEE Transactions on Mobile Computing*, vol. 9, pp. 1377–1390, Oct 2010.

[26] K. Lee, S. Hong, S. J. Kim, I. Rhee, and S. Chong, "Demystifying levy walk patterns in human walks," tech. rep., CSC, NCSU, 2008.

[27] J. Broch, D. A. Maltz, D. B. Johnson, Y.-C. Hu, and J. Jetcheva, "A performance comparison of multi-hop wireless ad hoc network routing protocols," in *Proceedings of the 4th Annual ACM/IEEE International Conference on Mobile Computing and Networking*, (New York, NY, USA), pp. 85–97, ACM, 1998.

[28] E. Bulut and B. Szymanski, "Exploiting friendship relations for efficient routing in mobile social networks," *IEEE Transactions on Parallel and Distributed Systems*, vol. 23, no. 12, pp. 2254–2265, 2012.

[29] X. Xie, Y. Zhang, C. Dai, and M. Song, "Social relationship enhanced predicable routing in opportunistic network," in *Proceedings of the 7th International Conference on Mobile ad-hoc and Sensor Networks (MSN 2011*, pp. 268–275, Dec 2011.

[30] F. Li, C. Zhang, Z. Gao, L. Zhao, and Y. Wang, "Social feature enhanced group-based routing for wireless delay tolerant networks," in *Proceedings of 8th International Conference on Mobile ad-hoc and Sensor Networks (MSN 2012)*, pp. 68–74, Dec 2012.

[31] D. Rothfus, C. Dunning, and X. Chen, "Social-similarity-based routing algorithm in delay tolerant networks," in *IEEE International Conference on Communications (ICC 2013)*, pp. 1862–1866, June 2013.

[32] H.-C. Jang and P.-H. Lee, "Social aware assisted transmission in manet," in *Proceedings of the 7th International Conference on Innovative Mobile and Internet Services in Ubiquitous Computing (IMIS 2013)*, pp. 342–347, July 2013.

[33] L. Gao, M. Li, A. Bonti, W. Zhou, and S. Yu, "Multidimensional routing protocol in human-associated delay-tolerant networks," *IEEE Transactions on Mobile Computing*, vol. 12, pp. 2132–2144, Nov 2013.

[34] A. Mei and J. Stefa, "Swim: a simple model to generate small mobile worlds," in *IEEE InfoCom 2009*, pp. 2106–2113, April 2009.

[35] S. Kosta, A. Mei, and J. Stefa, "Small world in motion (swim): modeling communities in ad-hoc mobile networking," in *Sensor Mesh and ad hoc Communications and Networks (SeCoN) 2010, 7th Annual IEEE Conference on Communications Society*, pp. 1–9, June 2010.

[36] K. Lee, S. Hong, S. J. Kim, I. Rhee, and S. Chong, "Slaw: a new mobility model for human walks," in *IEEE InfoCom 2009*, pp. 855–863, April 2009.

[37] F. Ekman, A. Keränen, J. Karvo, and J. Ott, "Working day movement model," in *Proceedings of the 1st ACM SIGMOBILE Workshop on Mobility Models*, (New York, NY, USA), pp. 33–40, ACM, 2008.

[38] J. Scott, R. Gass, J. Crowcroft, P. Hui, C. Diot, and A. Chaintreau, "Crawdad data set cambridge/haggle (v. 2006-01-31)." Downloaded from http://crawdad.org/cambridge/haggle/, Jan. 2006.

[39] J. Leguay, A. Lindgren, and T. Friedman, "Crawdad data set upmc/content (v. 2006-11-17)." Downloaded from http://crawdad.org/upmc/content/, Nov. 2006.

[40] C. Bettstetter, G. Resta, and P. Santi, "The node distribution of the random waypoint mobility model for wireless ad hoc networks," *IEEE Transactions on Mobile Computing*, vol. 2, pp. 257 – 269, july-sept. 2003.

[41] C. Bettstetter, H. Hartenstein, and X. Pérez-Costa, "Stochastic properties of the random waypoint mobility model," *Wireless Networks*, vol. 10, pp. 555–567, Sept. 2004.

[42] I. Rubin and C. W. Choi, "Impact of the location area structure on the performance of signaling channels in wireless cellular networks," *IEEE Communications Magazine*, vol. 35, pp. 108–115, Feb 1997.

[43] V. A. Davies, "Evaluating mobility models within an ad hoc network," Master's thesis, Colorado School of Mines, 2000.

[44] T. Camp, J. Boleng, and V. Davies, "A survey of mobility models for ad hoc network research," *Wireless Communications & Mobile Computing (WCMC): Special Issue on Mobile ad hoc Networking: Research, Trends and Applications*, vol. 2, pp. 483–502, 2002.

[45] E. Royer, P. Melliar-Smith, and L. Moser, "An analysis of the optimum node density for ad hoc mobile networks," in *IEEE International Conference on Communications*, vol. 3, pp. 857–861, 2001.

[46] B. Liang and Z. Haas, "Predictive distance-based mobility management for PCS networks," in *Proceedings of the 18th Annual Joint Conference of the IEEE Computer and Communications Societies*, vol. 3, pp. 1377–1384, mar 1999.

[47] C. Bettstetter, "Smooth is better than sharp: a random mobility model for simulation of wireless networks," in *Proceedings of the 4th ACM International Workshop on Modeling, Analysis and Simulation of Wireless and Mobile Systems*, (New York, NY, USA), pp. 19–27, ACM, 2001.

[48] C. Bettstetter, "Mobility modeling in wireless networks: categorization, smooth movement, and border effects," *ACM SIGMOBILE Mobile Computing and Communications Review*, vol. 5, pp. 55–66, July 2001.

[49] J. Ariyakhajorn, P. Wannawilai, and C. Sathitwiriyawong, "A comparative study of random waypoint and gauss-markov mobility models in the performance evaluation of MANET," in *International Symposium on Communications and Information Technologies*, pp. 894–899, 18 2006-sept. 20 2006.

[50] X. Hong, M. Gerla, G. Pei, and C.-C. Chiang, "A group mobility model for ad hoc wireless networks," in *Proceedings of the 2nd ACM International Workshop on Modeling, Analysis and Simulation of Wireless and Mobile Systems*, (New York, NY, USA), pp. 53–60, ACM, 1999.

[51] G. Jayakumar and G. Ganapathi, "Reference point group mobility and random waypoint models in performance evaluation of manet routing protocols," *Journal of Computer Systems, Networks, and Communications*, vol. 2008, pp. 13:1–13:10, Jan. 2008.

[52] M. Sánchez and P. Manzoni, "Anejos: a java based simulator for ad hoc networks," *Future Generation Computer Systems*, vol. 17, no. 5, pp. 573–583, 2001.

[53] P. Johansson, T. Larsson, N. Hedman, B. Mielczarek, and M. Degermark, "Scenario-based performance analysis of routing protocols for mobile ad-hoc networks," in *Proceedings of the 5th Annual ACM/IEEE International Conference on Mobile Computing and Networking*, (New York, NY, USA), pp. 195–206, ACM, 1999.

[54] H. Babaei, M. Fathi, and M. Romoozi, "Obstacle mobility model based on activity area in ad hoc networks," in *International Conference on Computational Science and Its Applications*

(ICCSA '07) (O. Gervasi and M. Gavrilova, eds.), vol. 4706, pp. 804–817, Springer Berlin Heidelberg, 2007.

[55] J. Tian, J. Hahner, C. Becker, I. Stepanov, and K. Rothermel, "Graph-based mobility model for mobile ad hoc network simulation," in *Proceedings of 35th Annual Simulation Symposium*, pp. 337–344, april 2002.

[56] M. Abdulla and R. Simon, "Characteristics of common mobility models for opportunistic networks," in *Proceedings of the 2nd ACM Workshop on Performance Monitoring and Measurement of Heterogeneous Wireless and Wired Networks*, (New York, NY, USA), pp. 105–109, ACM, 2007.

[57] M. Abdulla and R. Simon, "A simulation study of common mobility models for opportunistic networks," in *Simulation Symposium, 2008. ANSS 2008. 41st Annual*, pp. 43–50, April 2008.

[58] H. Ashtiani, H. M. Pour, and M. Nikpour, "A survey of MANET routing protocols in large scale and ordinary networks," *Global Journal of Computer Science and Technology*, vol. 10, pp. 14–27, Oct. 2010.

[59] H. Bakht, "Survey of routing protocols for mobile ad hoc network," *International Journal of Information and Communication Technology Research*, vol. 1, Oct. 2011.

[60] C. E. Perkins and P. Bhagwat, "Highly dynamic destination-sequenced distance-vector routing (dsdv) for mobile computers," in *Proceedings of the Conference on Communications Architectures, Protocols and Applications*, pp. 234–244, 1994.

[61] D. B. Johnson and D. A. Maltz, "Dynamic source routing in ad hoc wireless Networks," in *Mobile Computing*, pp. 153–181, Kluwer Academic Publishers, 1996.

[62] C. Perkins and E. Royer, "Ad-hoc on-demand distance vector routing," in *Proceedings of the 2nd IEEE Workshop on Mobile Computing Systems and Applications*, pp. 90–100, feb 1999.

[63] P. Jacquet, "Optimized link state routing protocol (olsr)." RFC 3626, Febuary 2003.

[64] A. Lindgren, A. Doria, E. Davies, and S. Grasic, "Probabilistic routing protocol for intermittently connected networks," 8 2012. RFC 6693.

[65] S. Jain, M. Demmer, R. Patra, and K. Fall, "Using redundancy to cope with failures in a delay tolerant network," in *in Proceedings of ACM SIGCOMM*, pp. 109–120, Online]. Available: http://dx.doi.org/10.1145/1080091.1080106, 2005.

[66] Z. Li, L. Sun, and E. C. Ifeachor, "Adaptive multi-copy routing for intermittently connected mobile ad hoc networks," in *in IEEE GLOBECOM '06*, 2006.

[67] J. Burgess, B. Gallagher, D. Jensen, and B. N. Levine, "Maxprop: Routing for vehicle-based disruption-tolerant networks," in *In Proc. IEEE INFOCOM*, 2006.

[68] J. Wu, S. Yang, and F. Dai, "Logarithmic store-carry-forward routing mobile ad hoc networks," *IEEE Transactions on Parallel and Distributed Systems*, vol. 18, no. 6, pp. 429–439, 2007.

[69] M. P. Wittie, K. A. Harras, K. C. Almeroth, and E. M. Belding, "On the implications of routing metric staleness in delay tolerant networks," *Comput. Commun.*, vol. 32, pp. 1699–1709, Oct. 2009.

[70] J. Niu, X. Zhou, K. Wang, and J. Ma, "A data transmission scheme for community-based opportunistic networks," in *Proceedings of the 5th International Conference on Wireless Communications, Networking and Mobile Computing*, WiCOM'09, (Piscataway, NJ, USA), pp. 3009–3013, IEEE Press, 2009.

[71] Q. Li, S. Zhu, and G. Cao, "Routing in socially selfish delay tolerant networks," in *Proceedings of the 29th Conference on Information Communications*, INFOCOM'10, (Piscataway, NJ, USA), pp. 857–865, IEEE Press, 2010.

[72] R. Jathar and A. Gupta, "Probabilistic routing using contact sequencing in delay tolerant networks," in *Proceedings of the 2Nd International Conference on COMmunication Systems and NETworks*, COMSNETS'10, (Piscataway, NJ, USA), pp. 138–147, IEEE Press, 2010.

[73] N. Li and S. K. Das, "A trust-based framework for data forwarding in opportunistic networks," *Ad Hoc Netw.*, vol. 11, pp. 1497–1509, June 2013.

[74] I. A. Hemadeh, "Routing protocol for mobile social networks," Master's thesis, University of Southampton, Sept. 2012.

[75] M. Musolesi and C. Mascolo, "Designing mobility models based on social network theory," *SIGMOBILE Mob. Comput. Commun. Rev.*, vol. 11, pp. 59–70, July 2007.

[76] C. Bettstetter and O. Krause, "On border effects in modeling and simulation of wireless ad hoc networks," in *Proc. 3rd IEEE International Conference on Mobile and Wireless Communication Networks (MWCMN)*, 2001.

[77] D. M. Blough, G. Resta, and P. Santi, "A statistical analysis of the long-run node spatial distribution in mobile ad hoc networks," in *Proceedings of the 5th ACM International Workshop on Modeling Analysis and Simulation of Wireless and Mobile Systems*, MSWiM '02, (New York, NY, USA), pp. 30–37, ACM, 2002.

[78] E. M. Royer, P. M. Melliar-Smith, and L. E. Moser, "An analysis of the optimum node density for ad hoc mobile networks," in *In proceedings of the IEEE international conference on communications*, pp. 857–861, 2001.

[79] P. Pholpabu and L.-L. Yang, "Social contact probability assisted routing protocol for mobile social networks," in *IEEE 79th Vehicular Technology Conference (VTC Spring) 2014*, pp. 1–5, May 2014.

[80] C. M. Schneider, V. Belik, T. Couronné, Z. Smoreda, and M. C. González, "Unraveling daily human mobility motifs," *Journal of the Royal Society Interface*, vol. 10, May 2013.

[81] B. B. Mandelbrot, *The fractal geometry of nature*. W.H.Freeman and Company, New York, 1977.

[82] N. Vastardis and K. Yang, "The importance of social tie detection in socially-aware opportunistic routing," in *Proceedings of the 4th Computer Science and Electronic Engineering Conference (CEEC 2012)*, pp. 133–138, Sept 2012.

[83] N. Vastardis and K. Yang, "Multi-phase socially-aware routing in distributed mobile social networks," in *Proceedings of the 9th International Wireless Communications and Mobile Computing Conference (IWCMC 2013)*, pp. 1353–1358, July 2013.

[84] D. Bertsekas and R. Gallager, *Data networks*. Englewood Cliffs, N.J. : Prentice Hall, 2nd ed., 1992.

[85] H. Dubois-ferriere, M. Grossglauser, and M. Vetterli, "Age matters: efficient route discovery in mobile ad hoc networks using encounter ages," in *Proceedings of the 4th ACM International Symposium on Mobile Ad Hoc Networking &Amp; Computing*, pp. 257–266, 2003.

[86] M. Xiao, J. Wu, and L. Huang, "Community-aware opportunistic routing in mobile social networks," *IEEE Transactions on Computers*, vol. 63, pp. 1682–1695, July 2014.

[87] J. Vazifehdan, R. Prasad, and I. Niemegeers, "energy-efficient reliable routing considering residual energy in wireless ad hoc networks," *IEEE Transactions on Mobile Computing*, vol. 13, pp. 434–447, Feb 2014.

[88] J. Zhu and X. Wang, "Model and protocol for energy-efficient routing over mobile ad hoc networks," *IEEE Transactions on Mobile Computing*, vol. 10, pp. 1546–1557, Nov 2011.

[89] J. Zhu and X. Wang, "Peer: a progressive energy efficient routing protocol for wireless ad hoc networks," in *Proceedings in 24th Annual Joint Conference of the IEEE Computer and Communications Societies (IEEE InfoCom 2005)*, vol. 3, pp. 1887–1896, March 2005.

[90] S. Yin and X. Lin, "Multipath minimum energy routing in ad hoc network," in *IEEE International Conference on Communications 2005 (ICC 2005).*, vol. 5, pp. 3182–3186, May 2005.

[91] M. Younus, A. Minhas, M. Javed, and A. Naseer, "Eear: efficient energy aware routing in wireless sensor networks," in *Proceedings of the 7th International Conference on ICT and Knowledge Engineering 2009*, pp. 57–62, Dec 2009.

[92] C. Chilipirea, A. Petre, and C. Dobre, "Energy-aware social-based routing in opportunistic networks," in *27th International Conference on Advanced Information Networking and Applications Workshops (WAINA 2013)*, pp. 791–796, March 2013.

[93] Shivashankar, H. Suresh, G. Varaprasad, and G. Jayanthi, "Designing energy routing protocol with power consumption optimization in manet," *IEEE Transactions on Emerging Topics in Computing*, vol. 2, pp. 192–197, June 2014.

[94] S. Bing, L. Yang, L. Zhenbo, and C. Jiapin, "An ant-based on-demand energy routing protocol for ad hoc wireless networks," in *International Conference on Wireless Communications, Networking and Mobile Computing, 2007 (WiCom 2007).*, pp. 1516–1519, Sept. 2007.

[95] A. Mohajerzadeh, M. Yaghmaee, and Z. Eskandari, "Tree based energy efficient and congestion aware routing protocol for wireless sensor networks," in *Proceedings of the 11th IEEE Singapore International Conference on Communication Systems 2008 (ICCS 2008)*, pp. 1707–1711, nov 2008.

[96] P.-J. Wan, G. Calinescu, X.-Y. Li, and O. Frieder, "Minimum-energy broadcast routing in static ad hoc wireless networks," in *Proceedings of 20th Annual Joint Conference of the IEEE Computer and Communications Societies*, vol. 2, pp. 1162–1171, 2001.

[97] H. Wang, L. Zhang, D. Zhou, and C. Wang, "A distributed energy-efficient routing scheme in ad hoc networks," in *Proceedings of the 4th International Conference on Computer and Information Technology 2004 (CIT '04)*, pp. 646–651, Sept 2004.

[98] J. Zhu, C. Qiao, and X. Wang, "A comprehensive minimum energy routing scheme for wireless ad hoc networks," in *23rd Annual Joint Conference of the IEEE Computer and Communications Societies (InfoCom 2004)*, vol. 2, pp. 1437–1445, March 2004.

[99] X. Jin, W. Cai, and Y. Zhang, "A red based minimum energy routing algorithm for wireless ad-hoc networks," in *Proceedings on International Conference on Wireless Communications, Networking and Mobile Computing 2005*, vol. 2, pp. 757–761, Sept 2005.

[100] J. Chen, L. Jia, X. Liu, G. Noubir, and R. Sundaram, "Minimum energy accumulative routing in wireless networks," in *Proceedings of 24th Annual Joint Conference of the IEEE Computer and Communications Societies*, vol. 3, pp. 1875–1886, March 2005.

[101] X. Liu, H. Hou, H. Yu, and H. Hu, "Lebr: a localized energy balancing routing algorithm in wireless sensor networks," in *International Conference on Communication Technology 2006 (ICCT '06)*, pp. 1–4, Nov 2006.

[102] S. Chen, M. Huang, Y. Li, Y. Zhu, and Y. Wang, "Energy-balanced cooperative routing in multihop wireless ad hoc networks," in *IEEE International Conference on Communications (icc) 2012*, pp. 307–311, June 2012.

[103] M. Hazewinkel, *Encyclopaedia of mathematics: monge - ampère equation - rings and algebras*. Encyclopaedia of Mathematics, Springer US, 2013.

[104] P. Pholpabu and L.-L. Yang, "A mutual-community-aware routing protocol for mobile social networks," in *IEEE Global Communications Conference (GlobeCom) 2014*, pp. 2917–2922, Dec 2014.